



UNIL | Université de Lausanne

Unicentre

CH-1015 Lausanne

<http://serval.unil.ch>

Year : 2020

EFFECT OF ELECTROCONVULSIVE THERAPY FOR MAJOR DEPRESSION ON BRAIN VOLUME AND MICROSTRUCTURAL PROPERTIES

Gyger Lucien

Gyger Lucien, 2020, EFFECT OF ELECTROCONVULSIVE THERAPY FOR MAJOR DEPRESSION ON BRAIN VOLUME AND MICROSTRUCTURAL PROPERTIES

Originally published at : Thesis, University of Lausanne

Posted at the University of Lausanne Open Archive <http://serval.unil.ch>

Document URN : urn:nbn:ch:serval-BIB_6A6F72AD95F69

Droits d'auteur

L'Université de Lausanne attire expressément l'attention des utilisateurs sur le fait que tous les documents publiés dans l'Archive SERVAL sont protégés par le droit d'auteur, conformément à la loi fédérale sur le droit d'auteur et les droits voisins (LDA). A ce titre, il est indispensable d'obtenir le consentement préalable de l'auteur et/ou de l'éditeur avant toute utilisation d'une oeuvre ou d'une partie d'une oeuvre ne relevant pas d'une utilisation à des fins personnelles au sens de la LDA (art. 19, al. 1 lettre a). A défaut, tout contrevenant s'expose aux sanctions prévues par cette loi. Nous déclinons toute responsabilité en la matière.

Copyright

The University of Lausanne expressly draws the attention of users to the fact that all documents published in the SERVAL Archive are protected by copyright in accordance with federal law on copyright and similar rights (LDA). Accordingly it is indispensable to obtain prior consent from the author and/or publisher before any use of a work or part of a work for purposes other than personal use within the meaning of LDA (art. 19, para. 1 letter a). Failure to do so will expose offenders to the sanctions laid down by this law. We accept no liability in this respect.



UNIL | Université de Lausanne

Faculté de biologie
et de médecine

Département de Neurosciences Cliniques

**EFFECT OF ELECTROCONVULSIVE THERAPY FOR MAJOR
DEPRESSION ON BRAIN VOLUME AND
MICROSTRUCTURAL PROPERTIES**

Thèse de doctorat en Neurosciences

présentée à la

Faculté de Biologie et de Médecine
de l'Université de Lausanne

par

LUCIEN GYGER

Neuroscientifique diplômé de l'Université de Genève, Suisse

Jury

Prof. Jean-Pierre Hornung, Président

Prof. Bogdan Draganski, Directeur

Prof. Patrik Vuilleumier, Expert

Prof. Indira Tendolkar, Expert

Lausanne 2020

**Programme doctoral interuniversitaire en Neurosciences
des Universités de Lausanne et Genève**



Imprimatur

Vu le rapport présenté par le jury d'examen, composé de

Président·e	Monsieur	Prof.	Jean-Pierre	Hornung
Directeur·trice de thèse	Monsieur	Prof.	Bogdan	Draganski
Expert·e·s	Madame	Prof.	Indira	Tendolkar
	Monsieur	Prof.	Patrik	Vuilleumier

le Conseil de Faculté autorise l'impression de la thèse de

Monsieur Lucien Gyger

Maîtrise en Neurosciences Université de Genève

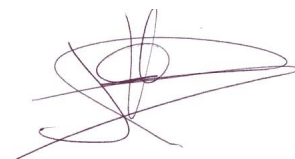
intitulée

**EFFECT OF ELECTROCONVULSIVE THERAPY
FOR MAJOR DEPRESSION ON BRAIN VOLUME
AND MICROSTRUCTURAL PROPERTIES**

Lausanne, le 6 mars 2020

pour Le Doyen
de la Faculté de Biologie et de Médecine

Prof. Jean-Pierre Hornung



Acknowledgements

First of all, I would like to express my gratitude to my supervisor, Prof. Bogdan Draganski, for his teaching, help and most of all for his patience.

I would like also to thank all the senior researchers from my lab, Dr Ferath Kherif, Dr Cristina Ramponi, Prof. Antoine Lutti and Dr Marzia De Lucia, for their help throughout my thesis.

I am grateful to Dr Jean-Frédéric Mall and Emina Nicollier for opening the doors of the ECT unit of the psychiatric hospital of Cery and help recruiting patients.

My special gratitude goes to all patients that took bravely part in this study and without whom my thesis would not have been possible.

I am particularly grateful to the President of the Jury, Prof. Jean-Pierre Hornung, and honoured to have as experts Prof. Indira Tendolkar and Prof. Patrik Vuilleumier who agreed to evaluate my thesis work.

A special thanks to Marcel Gyger, Christian Pfeiffer and Michael Pereira for reading, commenting and editing my thesis.

Many thanks to all my colleagues for their help, their advices, their expertise, in particular to, Gretel Sanabria-Diaz, Lester Melie-Garcia, Giulia Di Domenicantonio, Christine Kieffer, David Riedo, Estelle Dupuis, Javier Barranco-Garcia and Lydia Horwath.

Renaud Marquis, Sandrine Mueller and Anne Ruef are mentioned with gratitude for having introduced me to the field at the beginning of my research.

Lab life is not only intellectual work but also social interactions. I would like to thank, Claudia Modenato, Florent Gaillard, Mirco Nasuti, Manuel Spühler, Thierry Phénix, Dave Slater, Sandra Martin-Brevet, Leyla Loued-Khenissi, Adriano Bernini, Zsuzsanna Püspöki, Kate Gaberova. Maya Jastrzębowska, Wiktor Olszowy, Adeliya Latipova, Peilei Tan and Olga Trofimova for their warmth, enthusiasm and organization of so many nice extra-laboratory events; a special thanks to Elham Barzegaram and Christian Pfeiffer for all the nice climbing we did together.

To my family and to all my friends who helped me one way to the other since my childhood.

A special thanks to Anya Ampuero and Laïka.

This work is dedicated to the memory of my mother, Claudette.

Abstract

Major depressive disorder (MDD) affects worldwide more than 300 million individuals and is the second contributor to the Years Lived with Disability (DALY). Despite a large therapeutic arsenal, significant number of patients does not recover sufficiently swift from a depressive episode and suffer for a prolonged period of time. For these patients, electroconvulsive therapy (ECT) is the most efficient somatic treatment though its precise mechanism of action is still unknown. Pre-clinical studies indicate that neuroplasticity, and in particular neurogenesis in the hippocampus (HP), are possibly related to the treatment effect. This notion is also supported by human studies that consistently demonstrate hippocampal volume increases in patients undergoing ECT.

In the first part of my project, I sought answering the question whether the observed grey matter (GM) volume increase related to ECT are differentially distributed along HPs longitudinal axis with a predominant effect on the anterior “limbic” portion of the HP. To this aim, 9 MDD patients treated with ECT were scanned before and after ECT. According to our hypothesis, we found a strong spatial effect of ECT induced GM volume change along the main HP axis indicating that the anterior part of the HP is more strongly affected by ECT. Individuals’ clinical outcome was associated with volume changes in the anterior and not in the posterior HP. This study shows that the effect of ECT is not uniform but depends on the position along the longitudinal axis of the HP and indicates the importance of the anterior HP for the mechanism of action of ECT.

In the second part of my project, I tried to address some potential bias in current computational anatomy studies that have limited the straightforward neurobiological interpretation of the observed ECT induced brain changes. Indeed, volume estimation based on T1-weighted contrast is not only influenced by macrostructural changes of brain anatomy but is also influenced by microstructural properties of the brain tissue (the water, myelin and iron content). Therefore, we used advanced MRI acquisition in a new sample of 9 patients to perform a quantitative investigation of the contribution of GM volume, water, myelin and iron to the plasticity occurring during a treatment of ECT. We observed increase of GM volume in the HP and in the anterior cingulate without notable change in microstructural properties. We also found that a widespread pattern of regions including the medial prefrontal cortex, the bilateral HP, the bilateral striatum, and the precuneus were associated with clinical outcome. Interestingly, in the medial PFC we found a large contribution of water and myelin content but no contribution of GM volume, which means that classical morphometric studies would be blind to this association. My findings indicate the potential of quantitative MRI to enhance our understanding of the biological processes underlying the therapeutic effects of ECT in MDD patients.

Résumé

La dépression majeure affecte 300 millions d'individus et est le deuxième contributeur aux nombres d'années de vie corrigées de l'incapacité (DALY) au niveau mondial. Malgré un grand arsenal thérapeutique, un nombre important de patients ne répondent pas suffisamment aux traitements et souffrent pour une période prolongée. Pour ces patients, l'électroconvulsivothérapie (ECT) est le meilleur traitement dans cette situation bien que son mécanisme d'action soit mal compris. Des études pré-cliniques indiquent que la neuroplasticité, et en particulier la neurogenèse dans l'hippocampe (HP), sont des éléments clés du mécanisme d'action de l'ECT. Cette hypothèse est aussi supportée par des études cliniques qui ont démontré de manière consistante que le volume de l'HP est augmenté chez les patients recevant de l'ECT.

Dans la première partie de ma recherche, j'ai cherché à répondre à la question de savoir si l'augmentation de volume de matière grise causé par l'ECT est distribuée de manière différentielle le long de l'axe longitudinal de l'HP, avec l'hypothèse que l'effet est prédominant sur la partie antérieure ou « limbique » de l'HP. Dans ce but, 9 patients traités par ECT ont été scannés avant et après l'ECT. En accord avec notre hypothèse, nous avons trouvé une forte dépendance spatiale du changement de volume lié à l'ECT par rapport à la position le long de l'axe longitudinal de l'HP, la partie antérieure de l'HP étant la plus susceptible aux effets de l'ECT. De plus, nous avons trouvé que l'état clinique était associé avec la plasticité dans la partie antérieure mais pas postérieure de l'HP. Cette étude met en avant le fait que l'effet de l'ECT n'est pas uniforme mais dépend de la position le long de l'axe longitudinal de l'HP. Ceci indique le rôle tout particulier de l'hippocampe antérieur dans le mécanisme d'action de l'ECT.

Dans la seconde partie de mon projet, j'ai tenté d'adresser certains biais potentiels dans les études actuelles d'anatomie computationnelle qui limitent l'interprétation neurobiologique des changements de volume observés après un traitement d'ECT. En effet, les contrastes pondérés en T1 sont aussi influencés par les propriétés microstructurelles du tissu cérébral (le contenu en eau, myéline et fer). Par conséquent, nous avons utilisé des acquisitions d'imagerie par résonance magnétique (IRM) avancées dans un nouvel échantillon de 9 patients afin de faire une investigation quantitative de la contribution de la matière grise, de l'eau, de la myéline et du fer à la plasticité qui a lieu lors d'un traitement d'ECT. Nous avons observé une augmentation de la matière grise dans l'HP et le cortex cingulaire antérieur sans changement notable au niveau des propriétés microstructurelles. Nous avons aussi trouvé qu'un large nombre de régions incluant le cortex préfrontal médial, les HP, le striatum ventral et le précuneus était associé avec le changement d'état clinique. Dans le cortex préfrontal médial, il y avait une grande contribution de l'eau et de la myéline sans contribution notable de la matière grise, ce qui signifie que les études morphométriques classiques n'auraient pas détecté cette association. Ceci indique le potentiel de l'IRM quantitatif afin de mieux comprendre les processus associés aux bénéfices thérapeutiques de l'ECT sur la dépression.

List of abbreviations

Amy	Amygdala
Ant	Anterior
BD	Bipolar Disorder
DARTEL	Diffeomorphic Anatomical Registration using Exponentiated Lie algebra
DSM	Diagnostic and Statistical Manual of Mental Disorder
EC	Entorhinal cortex
ECT	Electroconvulsive therapy
FWE	Family-wise error
FWHM	Full-width-at-half-maximum
GLM	General Linear Model
GM(V)	Grey matter (volume)
HAMD	Hamilton Depression Rating Scale
HC	Healthy controls
HP	Hippocampus
L	Left
MADRS	Montgomery-Asberg Depression Rating Scale
MDD	Major depressive disorder
MNI	Montreal Neurological Institute
MPM	Multi-parameters map
MPRAGE	Magnetization Prepared Rapid Gradient Echo
MRI	Magnetic resonance imaging
MT	Magnetization Transfer
PCA	Principal Component Analysis
PFC	Prefrontal Cortex
Post	Posterior
PD	Proton Density
qMRI	Quantitative MRI
R	Right
R1	Relaxation time R1
R2*	Relaxation time R2*
RF	Radio Frequency
ROI	Region of interest
SD	Standard deviation
SSCP	Sum of Square and Cross Product matrix
T1	Relaxation time T1
T2	Relaxation time T2
TE	echo time
TR	repetition time
TRD	Treatment Resistant Depression

Table of contents

1. INTRODUCTION	12
1.1. Major depressive disorder	12
1.2. Treatment resistant depression	13
1.3. Integrated model of depression	14
1.3.1. <i>Cognitive model of depression and neural correlates</i>	14
1.3.1.1. <i>Cognitive model</i>	14
1.3.1.2. <i>Functional neural correlate of the cognitive model</i>	15
1.3.2. <i>Computational anatomy findings in MDD</i>	17
1.3.3. <i>Role of hippocampal neurogenesis in MDD</i>	18
1.4. ECT	19
1.4.1. <i>History of ECT</i>	19
1.4.2. <i>Modified ECT</i>	21
1.4.3. <i>Contemporary use of ECT</i>	22
1.4.4. <i>ECT efficacy</i>	22
1.4.5. <i>Side effect of ECT</i>	22
1.4.6. <i>ECT mechanism of action</i>	23
1.4.6.1. <i>ECT effect on the anterior hippocampus</i>	24
1.4.6.2. <i>Tissue micro-structure changes underlying ECT-induced plasticity</i>	25
2. GOALS OF THE THESIS AND HYPOTHESIS	27
2.1. Study 1: Differential effect of ECT on grey matter volume along the hippocampal longitudinal axis	27
2.2. Study 2: Quantitative MRI study of the effect of ECT on brain structure	27
3. STUDY 1: DIFFERENTIAL EFFECT OF ECT ON GM VOLUME INCREASE IN THE HIPPOCAMPUS ALONG ITS LONGITUDINAL AXIS	31
3.1. Material and methods	31
3.1.1. <i>Participants</i>	31
3.1.2. <i>MRI data acquisition and preprocessing</i>	31
3.1.3. <i>Definition of hippocampal main spatial axes</i>	33
3.1.4. <i>Statistical analysis</i>	33
3.2. Results	36
3.2.2. <i>Main effect of ECT</i>	37
3.2.3. <i>Correlation with symptoms improvement</i>	42
3.3. Summary study 1	47
4. STUDY 2: QUANTITATIVE MRI STUDY OF THE EFFECT OF ECT ON BRAIN STRUCTURE	48
4.1. Material and methods	48
4.1.1. <i>Procedure</i>	48
4.1.1.1. <i>Ethical statement</i>	48

4.1.1.2. Participants.....	48
4.1.1.3. Study design	48
4.1.1.4. ECT procedure.....	49
4.1.2. Data acquisition and pre-processing	50
4.1.2.1. Clinical phenotype	50
4.1.2.2. MRI data acquisition.....	50
4.1.2.3. MRI data preprocessing.....	51
4.1.2.3.1. Maps creation	51
4.1.2.3.2. Longitudinal data alignment (Figure 8, steps 2 and 3)	52
4.1.2.3.4. Standardization.....	53
4.1.2.4. Statistical analysis	53
4.2. Results.....	63
4.2.1. Depression severity	63
4.2.1.1. Quantitative assessment.	63
4.2.1.2. Qualitative assessment.....	63
4.2.2. Neuroimaging	64
4.2.2.1. Effect of ECT.....	64
4.2.2.2. Association with change of depression severity	66
4.3. Summary study 2.....	68
5. DISCUSSION	70
5.1. Study 1	70
5.1.1. ECT effect on the anterior hippocampus.....	70
5.1.2. Association with clinical outcome.....	71
5.1.3. Limitations and strength of the study.....	72
5.1.4. Conclusion study 1	73
5.2. Study 2	73
5.2.1. Effect of an ECT series: “true” volume change in limbic and cognitive control areas.....	74
5.2.1.1. Absence of change of water content in the hippocampus.....	74
5.2.2. Long-term effect of ECT	75
5.2.3. Association with clinical outcome.....	76
5.2.4. Limitations and strengths of the study	79
5.2.5. Conclusion study 2	81
6. GENERAL CONCLUSION	82
7. REFERENCES	84
8. APPENDICES.....	98
8.1.1. Appendix 1	98
8.1.2. Appendix 2	98
8.1.3. Appendix 3	99
8.1.4. Appendix 4	100

List of figures

Study 1

Figure 1: Graphical representation of the principal component analysis of right and left hippocampus coordinates corresponding to Montreal Neurological Institute standardised space.

Figure 2: Effect of electroconvulsive on grey matter volume on the entire brain (A) and in the left and right hippocampus (B).

Figure 3: Spatial regression analysis of the relationship between rate of change of grey matter volume and position along the longitudinal axis of the hippocampus.

Figure 4: Three-way interaction between group, side and sub-region of the confirmatory analysis using discrete data.

Figure 5: Scatterplots of symptom improvement assessed with the Hamilton Depression Rating Scale (HAMD) versus grey matter volume at baseline.

Figure 6. Scatterplots of symptom improvement assessed with the HAMD versus grey matter volume rate of change.

Study 2

Figure 7: Timeline of study

Figure 8: Overview of the pre-processing pipeline.

Figure 9: Design matrix.

Figure 10: Overview multivariate General Linear Model.

Figure 11: A. Evolution of depressive symptoms as measured by the Montgomery-Asberg Depression Rating Scale (MADRS).

Figure 12: Statistical map for multivariate analysis of the difference between t_0 and t_2 .

Figure 13: Statistical map for multivariate analysis of the difference between t_0 and t_3 .

Figure 14: Statistical map for multivariate association between MRI measurements and change of depression severity.

Figure 15: Statistical map for multivariate association with change of depression severity between t_0 and t_3 .

List of tables

Table 1: Socio-demographic and clinical characteristics of the sample in study 1.

Table 2: Beta coefficients of the generalized least square model testing the relation between grey matter volume rate of change and position along the main spatial axis of the hippocampus.

Table 3: Contrasts between beta-coefficients of the generalized least square model testing the relation between grey matter volume rate of change and the position along the main spatial axis of the hippocampus.

Table 4: ANOVA table of the confirmatory discrete analysis.

Table 5: Post-hoc tests of the three-way interaction of the confirmatory analysis of discrete data.

Table 6: Relationship between GMV at baseline and symptom improvement assessed with the HAMD between baseline and 3 months.

Table 7: Relationship between the GMV at baseline and symptom improvement assessed with the HAMD between baseline and 3 months.

Table 8: Relationship between the GMV change and symptom improvement assessed with the HAMD between baseline and 3 months.

Table 9: Group differences in the relationship between GMV change and symptom improvement assessed with the HAMD between baseline and 3 months.

1. Introduction

1.1. Major depressive disorder

Major depressive disorder (MDD) has worldwide a yearly prevalence of 6% and a lifetime prevalence around 15% (Kessler et al., 2003). It is currently estimated that MDD is the 2nd contributor to the number of days lived with disability both in developed and developing countries (Vos et al., 2016). In addition to its direct negative consequences, MDD is associated with physical health issues such as higher rate of diabetes, heart disease, ischemic stroke, hypertension, obesity, cancer, cognitive impairment and dementia (Lépine & Briley, 2011; Penninx, Milaneschi, Lamers, & Vogelzangs, 2013). Overall, MDD increases the risk of mortality of 60 to 80% and contributes to 10% to all causes of mortality (Cuijpers et al., 2014; Walker, McGee, & Druss, 2015).

MDD is a clinical entity defined by observable and self-reported signs or symptoms. According to the latest version of the Diagnostic and Statistical Manual of Mental Disorders (American Psychiatric Association, 2013), at least 5 of the following symptoms have to be present during the same 2-week period (and at least 1 of the symptoms must be depressed mood or diminished interest/pleasure) to diagnose a major depressive episode:

- Depressed mood
- Diminished interest or loss of pleasure in almost all activities (anhedonia)
- Significant weight change (5%) or change in appetite
- Change in sleep: Insomnia or hypersomnia
- Change in activity: Psychomotor agitation or retardation

- Fatigue or loss of energy
- Guilt/worthlessness: Feelings of worthlessness or excessive or inappropriate guilt
- Concentration: diminished ability to think or concentrate, or more indecisiveness
- Suicidality: Thoughts of death or suicide, or has suicide plan

MDD is almost twice more prevalent in women than in men (Bromet et al., 2011; Seedat et al., 2009). The typical age of onset of the disorder is during the period between late adolescence and 40s (Eaton et al., 2014). The median duration of a depressive episode is approximately 90 days and 50% of patients recover during the 3 first months, 63% in 6 months and 76% within 12 months (Spijker, Graaf, Bijl, & Beekman, 2002). However, 20% of patients have not recovered after 2 years.

1.2. Treatment resistant depression

The typical first-line treatment for MDD recommended by the American Psychiatric Association are pharmacological treatment with antidepressants and psychotherapy (Armstrong, 2011). Concerning pharmacological therapy, only 36.8% of patients suffering of MDD respond to a first treatment, and 30.6%, 13.7% and 13% of patients respond to a second, third and fourth treatment step respectively, leading to an overall cumulative remission rate of 67% (Rush et al., 2006). This means that a major part of the patients' population does not respond and develop a treatment resistant depression (TRD). TRD is usually defined as an absence of response to at least two antidepressant trials (Conway, George, & Sackeim, 2017). According to this definition it is estimated that around 30% of patients will develop TRD (Fabbri et al., 2018). As TRD involves considerable socio-economic burden (McCrone et al., 2018),

there is pressing need to develop new therapeutic strategies so that these patients can swiftly recover from the ongoing depressive episode.

Currently, the treatment of choice for patient with TRD is the electroconvulsive therapy (ECT) (Kellner et al., 2012). Indeed, ECT can achieve 70% of response, which is defined as a reduction of > 50% of symptoms severity in individual with TRD. This response rate is higher than the results obtained with pharmacological treatment with antidepressants (Folkerts et al., 1997). Since the neurophysiology and impact of ECT on the brain are not well understood, it is of utmost importance to investigate the underlying neurobiological process. This opens a window of opportunity to improving current application modes and to stratifying patients that will benefit from established or novel ECT application regimens.

1.3. Integrated model of depression

1.3.1. Cognitive model of depression and neural correlates

1.3.1.1. Cognitive model

Beyond the description that constitutes the DSM-based diagnosis of MDD, we denote the integrative theory of depression, known under “unified model of depression” by Beck (Beck & Bredemeier, 2016). This framework is mainly centred on the cognitive mechanism underlying the clinical presentation of depressive disorders. But it also integrates many other sources of information especially regarding the neurobiological mechanisms involved in MDD (for reviews see Beck, 2008; Beck & Bredemeier, 2016). It is also the scientific basis of the cognitive-behavioural therapy - established and scientifically validated psychological intervention for MDD (Gartlehner et al., 2017). According to the proponents of this theory, MDD is thought to be primarily caused and maintained by the dysregulation of cognitive

processes (Disner, Beevers, Haigh, & Beck, 2011). Due to finite resource for processing the vast amount of information in our environment, an individual has to select which information to process and which one to neglect. One mechanism that drives this selection is the emotional content of stimuli. Attention is preferentially directed towards emotional stimuli as compared to neutral stimuli, because it is thought to be the signal that the stimulus is relevant for the individual (Brosch, Scherer, Grandjean, & Sander, 2013). However, when this process is systematically biased towards negative stimuli, it can become maladaptive and leads to reinforcement of negatively biased interpretations about the self, about the environment (social and non-social) and about the future (also called the Beck's cognitive triad, see (Beck, 1979)). The "depressogenic" beliefs are thought to play a pivotal role in the establishment and perpetuation of a depressive episode. In addition, rumination – a maladaptive and recurrent thought pattern about the causes and consequences of negative emotion – is thought to enhance the "depressogenic" dysfunctional negative beliefs leading to the perpetuation and recurrence of depressive episode (Nolen-hoeksema, 2000).

1.3.1.2. Functional neural correlate of the cognitive model

Since its first formulation, the cognitive model of depression has received large support from experimental research in cognitive psychology and has also played a central role in the integration of findings coming from different levels of analysis (for reviews see (Beck, 2008; Beck & Bredemeier, 2016; Disner, Beevers, Haigh, & Beck, 2011; McClintock et al., 2014)). Especially, functional neuroimaging research has provided evidence of neural substrate for the excessive tendency to process negative stimuli and avoid positive stimuli. MDD patients tend to selectively more attend to negative stimuli as compared to control subjects (Kellough, Beevers, Ellis, & Wells, 2008; Peckham, McHugh, & Otto, 2010). This tendency to allocate more attention to negative stimuli is thought to arise from top-down deficit related to hypoactivity

in the ventrolateral prefrontal cortex (vlPFC) an area important for selecting stimuli (Beevers, Clasen, Stice, & Schnyer, 2010; Fales et al., 2008), and from reduced activity in the dorsolateral PFC and rostral anterior cingulate cortex, two areas crucial to disengage attention from negative stimuli (Bush, Luu, & Posner, 2000; Shafritz, Collins, & Blumberg, 2006). In addition to attentional deficit resulting in preferential engagement of attentional process towards negative stimuli, MDD patients also show a preferential processing of negative information once a stimulus has been perceived, which then results in a negativity bias in interpreting perceived information (Mathews & Macleod, 2005).

The processing of emotional information has been demonstrated to robustly activate the amygdala (Costafreda, Brammer, David, & Fu, 2008; Phelps & LeDoux, 2005). When comparing MDD patients with healthy controls, studies report more intense and long-lasting amygdala activation in response to negative stimuli in MDD patients. These amygdala effects are not present for positive stimuli (Drevets, 2001; Siegle, Steinhauer, Thase, Stenger, & Carter, 2002). It has been shown that amygdala activity is under the regulation of the left dorsolateral PFC. These two structures appear to have anticorrelated pattern of activity (Costafreda et al., 2008; Davidson, 2000; Fales et al., 2008; Siegle et al., 2002). Therefore, as dorsolateral PFC activity is lower in MDD patients, it can be inferred that amygdala activity is higher in MDD patients partly due to a reduction of top-down control of negative emotions from higher order brain structure.

MDD patients not only preferentially process negative stimuli, they also show decreased response to positive affect and reward (Herzallah et al., 2013; Huys, Pizzagalli, Bogdan, & Dayan, 2013; Pizzagalli, Iosifescu, Hallett, Ratner, & Fava, 2008). In normal conditions, the reward signal in the ventral striatum is generated by interactions between the vlPFC and the nucleus accumbens (Del Arco & Mora, 2008; Wager, Davidson, Hughes, Lindquist, & Ochsner,

2008). Supporting this notion, neuroimaging studies reported decreased ventral striatum activity in MDD patients during the experience of positive affect (Epstein et al., 2006; Heller et al., 2009). In summary, the tendency of MDD patients to process preferentially negative emotions and to be less sensitive to positive emotions arise from dysfunction in brain circuits including increased activity in the limbic system and decrease of activity in the cognitive control and reward systems.

In addition to the cognitive bias at stake in depression, rumination is also a central manifestation of MDD. This process is reflected in neural circuits by an increased activity of brain region of the default mode network, a system involved in self-referential processes (Whitfield-Gabrieli & Ford, 2012).

1.3.2. Computational anatomy findings in MDD

Computational anatomy studies analyse magnetic resonance imaging (MRI) data in brain space to allow for inferences on morphometry features associated with a variable and/or category of interest. This classical approach has been quite unsuccessful to provide consistent neural substrate of MDD due to insufficient sample size, heterogeneity of the disorder and a complex pattern of interaction between clinical presentation and brain structure (Schmaal et al., 2016). However, recent multi-site highly powered computational anatomy studies have provided strong evidence of structural abnormalities in MDD. Two studies from the ENIGMA-MDD consortium (Schmaal et al., 2017, 2016) demonstrated that cortical and subcortical lower volumes are found in MDD patients in the hippocampus, in the PFC, in the anterior and posterior cingulate cortices, in the insula and temporal lobes when compared with healthy controls. Moreover, a severe history of depression is negatively related to hippocampal volume (Zaremba et al., 2018).

1.3.3. Role of hippocampal neurogenesis in MDD

Although the existence of neurogenesis in the adult human brain was debated following recently published negative findings (Sorrells et al. 2018), it is generally accepted that new neurons are continuously generated throughout the life in the dentate gyrus of the human hippocampus (Boldrini et al., 2018; Eriksson et al., 1998; Moreno-jiménez et al., 2019; Spalding et al., 2013). It is estimated that approximately 700 new neurons are added each day in the dentate gyrus (Spalding et al., 2013). Pre-clinical studies of MDD have demonstrated that pharmacological treatment with antidepressants stimulate neurogenesis in the dentate gyrus of the hippocampus (Malberg, Eisch, Nestler, & Duman, 2000; Perera et al., 2007), and that experimental ablation of neurogenesis blocks the effect of these treatments (Santarelli, 2003). However, the artificial inhibition of neurogenesis in pre-clinical model of MDD does not induce depressive-like behaviour (Tanti & Belzung, 2013). These observations can be interpreted in the context of a recent study showing that hippocampal neurogenesis confers resilience to stress (Anacker et al., 2018). As stress is a major trigger factor of MDD (Pine, Cohen, Johnson, & Brook, 2002), these findings suggest that abnormal neurogenesis plays a crucial role in the pathophysiology of depression, although its dysfunction in a non-challenging environment is not sufficient to cause MDD.

In humans, the neurogenic theory of MDD is corroborated by post-mortem findings of a lower number of neurons in the dentate gyrus of MDD individuals as compared to healthy controls (HC) (Boldrini et al., 2013) and of higher number of neural progenitor cells in the dentate gyrus of MDD patients treated with antidepressant as compared to untreated patient and HC (Boldrini et al., 2009). Moreover, paralleling the finding from pre-clinical model, resilience to MDD is associated with larger volume of the dentate gyrus in a post-mortem study (Boldrini et al., 2019b).

1.4. ECT

Electroconvulsive therapy is a treatment of choice in patients with TRD (Kellner et al., 2012). Indeed, ECT can achieve 70% of response (define as a reduction of > 50% of symptoms severity) in individual with TRD, a response rate higher than with pharmacological antidepressants (Folkerts et al., 1997). Therefore, it is of utmost importance to better understand the neurobiological basis of the effect of ECT to foster the development of new therapeutic strategies that can achieve response or remission in the class of patients that do not respond to usual pharmacological treatments.

1.4.1. History of ECT

In 1927, the Nobel Prize in Medicine was awarded to Julius Wagner-Jauregg for the development of treatment of psychosis by inducing fever (Tsay, 2013). He would successfully improve the symptoms of his patients affected by dementia paralytica or progressive paralysis caused by advanced Neurosyphilis by inoculating the parasite of malaria (Wagner-Jauregg, 1887). This discovery showed that psychiatric disorders could have a biological origin (Grözinger, Conca, Nickl-Jockschat, & Di Pauli, 2013; Tsay, 2013). Inspired by the work of Wagner-Jauregg, the French psychologist Constance Pascal published in 1926 "Treatment of mental illnesses by shocks" where she sustains that a new mental equilibrium could be obtain by shock therapies (Barbier, Serra, Loas, & Breathnach, 1999; Grözinger et al., 2013). Furthermore, the literature in the 19th century highlighted an association between epilepsy and psychiatric illnesses. It was observed that psychiatric symptoms could suddenly replace seizures in epileptic disorders and thus designated as epileptic equivalents (Krishnamoorthy & Trimble, 1999). On this basis, Hans Heinrich Landolt conducted EEG experiments on psychotic and epileptic subjects. He observed an antagonism between epilepsy and

schizophrenia (Krishnamoorthy & Trimble, 1999; Landolt, 1958). László Joseph Meduna observed a clinical improvement of psychosis in the post-ictal period of epileptic patients. He performed a histological study on epileptics and schizophrenics human brains showing a higher density of glial cells in epileptic brains than in schizophrenic brains. Thus, he hypothesised that schizophrenia could be cured by convulsive therapies (Grözinger et al., 2013; Landolt, 1958; Wright & Bruce, 1990). The earliest shock treatment, developed in 1933 by Sakel was the insulin coma therapy. The treatment consisted in the induction of a hypoglycaemic coma by injecting insulin. The convulsions happened in 10-30% of the cases and were considered as a side-effect of this therapy. However, severe complications such as brain damage and death could result from the insulin coma therapy (Grözinger et al., 2013; Sabbatini, 1997; Tsay, 2013; Wright & Bruce, 1990). Based upon his observations, Meduna developed a convulsive therapy using Metrazol or Cardiazol for schizophrenia. Although this therapy showed some success, it provoked a feeling of imminent death just before the onset of convulsion which was hardly tolerated by the patients. Moreover, this treatment led to post-ictal psychomotor agitation, was dangerous causing spine fractures in 42 % of the patients and expensive (Grözinger et al., 2013; Landolt, 1958; Sabbatini, 1997; Wright & Bruce, 1990). As part of the larger set of these “shock therapy”, ECT was introduced by the Italian neurologist and psychiatrist Ugo Cerletti and his student Lucio Bini. In the first trials on dogs, the electrodes were placed in the mouth and in the anus, which caused deadly arrhythmias in about half the animals. Bini determined that the cause stands in the passage of the electrical current through the heart. The subsequent bitemporal placement of electrodes enable a safe execution of the therapy. ECT was administered to a schizophrenic patient for the first time in the Clinic for Nervous and Mental Disorders in Rome in April 1938. Soon after this first

successful trial on human, it started to be applied to other psychiatric disorders among which major depression (Aruta, 2011; Endler, 1988; Metastasio & Dodwell, 2013; Tsay, 2013).

It has been proven that epilepsy is not protective against psychiatric disorder but that artificially-induced seizures lead to spectacular clinical improvement in depression. Nowadays, none of these therapies are practiced with the exception of ECT. It has proven to be the most efficient, the better tolerated and the less costly method (The UK ECT Review Group, 2003).

1.4.2. Modified ECT

The most common adverse effect due to ECT in its early form was injuries related to muscular convulsion, such as spinal compression fractures. In order to prevent these complications, a new highly controlled procedure, known as modified ECT, has been developed. A brief general anaesthesia without intubation is achieved with a short-acting anaesthetic and neuromuscular blocking agent prior the administration of an electric current (Wang, Milne, Rooney, & Saha, 2014). Preoxygenation strategies inducing hyperoxia and hypocapnia improved the efficiency of ECT by increasing the intensity and the duration of the epileptic seizure. If needed, short-acting beta blocker can be administrated to counterbalance the sympathetic activation caused by the seizure (Zhao, Jiang, & Zhang, 2016). The stimulation performed as first intention unilaterally in the non-dominant hemisphere and the standard titration of the epileptogenic activity enable to make the ECT technique safer (Conus et al., 2013). This is the standard procedure used nowadays in most of the countries practicing ECT.

1.4.3. Contemporary use of ECT

Although it is also used in treatment-resistant schizophrenia, ECT is primarily indicated for treatment-resistant form of depressive disorders and for extremely severe and urgent form of depression with life-threatening risk (The UK ECT Review Group, 2003). Moreover, ECT is an appropriate rapid solution for severe psychiatric situations with presence of stupor, delusional symptoms, serious psychomotor retardation, or hallucinations (Jain & Singh, 2010). Finally, it can be used as second intention in prolonged or severe mania, treatment resistant catatonia, neuroleptic malignant syndrome, schizoaffective disorder, vegetative dysregulation postpartum psychosis and psychosis in the first trimester of pregnancy (Jain & Singh, 2010; Kennedy et al., 2009).

1.4.4. ECT efficacy

ECT is the best treatment currently available with more than 50% of response in treatment-resistant patients and more than 70% in patients with non-resistant depression. The efficacy of ECT is confirmed by two meta-analyses that reported a superior effect of real- vs sham-ECT and state-of-the-art pharmacological treatment (Kho, van Vreeswijk, Simpson, & Zwinderman, 2003; The UK ECT Review Group, 2003).

1.4.5. Side effect of ECT

The most common somatic side effects of ECT are cardiocirculatory. Therefore, every patient that has a suspicion of cardiovascular risk factor is examined by a cardiologist to decide if the treatment can be done. Nonetheless, ECT-related mortality rate (2.1 per 100'000) is lower than mortality rate of general anaesthesia in relation to surgical procedure (3.4 per 100'000) (Tørring, Sanghani, Petrides, Kellner, & Østergaard, 2017).

The immediate side effect of ECT is post-ictal confusion lasting maximum few hours. But the most serious side effect of ECT is retrograde and anterograde amnesia, however it is transient and no deficit is present after 6 months (Nuninga et al., 2018).

1.4.6. ECT mechanism of action

Animal models using electroconvulsive shocks (ECS), the pre-clinical model of ECT, bring empirical evidence supporting the role of ECT in neurogenesis (Ueno et al., 2019), gliogenesis (Jansson, Wennström, Johanson, & Tingström, 2009), synaptogenesis (C. Zhao, Warner-Schmidt, Duman, & Gage, 2012) and angiogenesis (Hellsten et al., 2005). Given the “neurogenic” hypothesis for depression (Miller & Hen, 2015) and the evidence for seizure-associated increase in production and survival of new-born neurons in the hippocampus (Madsen et al., 2000; Ueno et al., 2019), one current assumption is that the effects of ECT are due to seizure-induced increment of adult neurogenesis. A steadily growing number of computational anatomy brain MRI studies, meta- and mega-analyses confirmed this notion by demonstrating ECT-induced increases in hippocampus volume. These volume changes are thought to represent the effects of increased adult neurogenesis (Dukart et al., 2014; Gbyl & Videbech, 2018; Oltedal et al., 2018; Takamiya et al., 2018; Tendolkar et al., 2013). Taking advantage of more reliable atlas information on hippocampus subfields and optimal image resolution at ultra-high 7T field strength, a recent study showed ECT effects confined to the dentate gyrus (DG) known for its particular role in neurogenesis (Nuninga et al., 2019). These findings are at odds with previous reports showing effects in other hippocampal subfields (Cao et al., 2018). These contradictory results can be explained by methodological differences in MRI data acquisition and processing prior to statistical analysis.

1.4.6.1. ECT effect on the anterior hippocampus

In the last few years we have witnessed interest in studying the hippocampal longitudinal axis that complement the traditional focus on its transversal axis with cyto-architecturally well-defined boundaries between subfields, linked to distinct neurobiological functions. A simplistic view attributes memory and spatial navigation to the posterior hippocampus, whilst the anterior parts are associated with limbic functions (Fanselow & Dong, 2010). More recent studies suggested gradual change of function along the longitudinal or anteroposterior axis rather than sharply defined borders (Strange, Witter, Lein, & Moser, 2014). The assumption of a gradient along the hippocampal longitudinal axis is supported by evidence of corresponding patterns at gene expression (Vogel, La, & Grothe, 2019), cellular (Brun et al., 2008) and network level (Dalton, McCormick, & Maguire, 2018) (for comprehensive review see (Strange et al., 2014)).

Up to date, besides descriptive reports on ECT-related changes localised in the anterior hippocampus (Bai et al., 2019; Joshi et al., 2016; Leaver et al., 2019), there are no publications that explicitly tested for differential ECT-induced effects along the hippocampal longitudinal axis. There are several lines of evidence from animal models and human studies showing that the impact of adult neurogenesis on depression depends on a gradient along the hippocampal longitudinal axis. Targeted ablation of neurogenesis in the dorsal hippocampus of mice corresponding to posterior hippocampus in humans affects spatial memory, whereas lesion in the ventral, i.e. in humans anterior portion abolishes antidepressant effects (Wu & Hen, 2014). Post mortem studies show that major depressive disorder patients have reduced granule neurons and neural progenitor cells in the anterior but not posterior hippocampal DG (Boldrini et al., 2019a, 2013). Along the same lines, antidepressants increase selectively the number of

neural progenitor cells in the anterior but not posterior hippocampus (Boldrini et al., 2012, 2009).

1.4.6.2. Tissue micro-structure changes underlying ECT-induced plasticity

In humans, there is mounting evidence from single cohort studies, meta- and mega-analyses of magnetic resonance imaging (MRI) data that ECT is strongly associated with hippocampus volume changes (Dukart et al., 2014; Gbyl & Videbech, 2018; Takamiya et al., 2018) and with more scarce evidence that ECT is associated with cortical alterations (Ousdal et al., 2019). Despite the attribution of ECT effects to the hippocampal dentate gyrus and neurogenesis (Takamiya et al., 2018), there is still no compelling evidence about the processes underlying the observed anatomy changes.

Novel multi-parameter mapping MRI protocols indicative for myelin, free water and iron content allow for quantification of brain tissue microstructure properties whilst avoiding misinterpretation of the observed volume changes (Lorio et al., 2014). Particularly in the context of longitudinal assessment, these techniques provide higher precision given their quantitative character with much lower test-retest (Gracien et al., 2019) and inter-scanner variability than the workhorse of computational anatomy - T1-weighted imaging (Weiskopf et al., 2013). The benefit of using multi-contrast parameter mapping converges on the investigation of the measurable contributions of myelin, iron and tissue free water above and beyond morphometry estimates (Lorio et al., 2014) that can be further linked to the observed ECT-related changes in clinical phenotype.

Given the lack of empirical evidence about the very nature of ECT effects on the human brain, the question about hippocampal oedema associated with prolonged seizure activity as cause for the observed hippocampus volume changes remains unanswered (Kim et al., 2001; Righini,

Pierpaoli, Alger, & Di Chiro, 1994; Szabo et al., 2005). Previous studies reported increased T1-relaxation time in the acute phase after ECT that can be interpreted as related to changes in water content (Mander et al., 1987; Scott, Douglas, Whitfield, & Kendell, 1990). The observed increased signal in T1-relaxation time is also impacted by changes in paramagnetic ion concentration and protein content (Akber, 1996). Along the same lines, the reported absence of ECT-associated T2-relaxation changes does not exclude oedema (Kunigiri, Jayakumar, Janakiramaiah, & Gangadhar, 2007). Studies using diffusion-weighted Imaging brought some evidence against the assumption of ECT-induced hippocampal oedema showing reduction of mean diffusivity (Jorgensen et al., 2016) and no change in the clinically used index of apparent diffusion coefficient (Szabo et al., 2007). Given that diffusion-derived indices are not an absolute measure of water content, the previous results do not enable to draw conclusions about the hypothesis that ECT related hippocampus volume increase is explained by a post-ECT oedema. Proton density estimates remain the best measurement of water content in brain tissue (Tofts, 2004).

2. Goals of the thesis and hypothesis

2.1. Study 1: Differential effect of ECT on grey matter volume along the hippocampal longitudinal axis

Considering the fact that the anterior hippocampus is involved in functions that are typically altered in depression (Fanselow & Dong, 2010), (Boldrini et al., 2013) and recent reports showing ECT effects located in this part of the brain (Bai et al., 2019; Joshi et al., 2016; Leaver et al., 2019), we hypothesized that ECT has differential topological effects along the hippocampal longitudinal axis. The main goal of the first part of my thesis project is the investigation of the effects of ECT along the longitudinal hippocampal axis. To this end, we analysed MRI data acquired before and after ECT treatment using computational anatomy framework for longitudinal data that we combined with a spatial analysis looking for structural changes along the hippocampal principal axes. Aiming to avoid the interpretational ambiguity of previous longitudinal studies with respect to effects on brain anatomy related to symptom improvement due to ECT vs symptom improvement due to pharmacological intervention, we also included in our analysis patients receiving only pharmacological treatment in addition to healthy controls.

2.2. Study 2: Quantitative MRI study of the effect of ECT on brain structure

The effect of ECT on GM volume in the hippocampus, but also to a lesser extent in other subcortical and cortical structures, has been well documented in several studies (Ousdal et al., 2019; Takamiya et al., 2018). However, all these studies use T1-weighted imaging to assess local GM volume changes across the brain. Volume estimations derived from this type of contrast are not only influenced by volume per se but also by changes in tissue microstructural

properties such as change in water, myelin and iron contents, the main constituent of cerebral tissue (Lorio et al., 2016). Nonetheless, novel techniques of quantitative MRI (qMRI) allow to quantitatively assess the contribution of these factors to the MRI contrast. Recently developed qMRI protocols provide estimations of water content using Proton Density (PD), macromolecular content (of which myelin is the largest contributor) using Magnetization Transfer (MT), longitudinal relaxation time $R1 (= 1/T1)$, a measure influenced mainly by myelin but also by iron content), and effective transverse relaxation time $R2^* (=1/T2^*)$, a measure of iron content; for a review see (Weiskopf, Mohammadi, Lutti, & Callaghan, 2015)). These new types of MRI maps give more straightforward measurements of microstructural properties of brain tissue and can potentially provide a better understanding of the biological processes underlying structural plasticity (Draganski et al., 2011). Moreover, these measurements are promising candidates for biomarkers for mood disorders as their inter-scanner variability is much lower than with T1-weighted imaging (Weiskopf et al., 2013).

This study addresses three neurobiological questions and one methodological question. The first question is whether the volumetric changes caused by ECT are due to a reorganisation of grey matter or to an oedema reflecting inflammation and neuronal death. Indeed, such a process is found in status epilepticus (Kim et al., 2001; Righini et al., 1994; Szabo et al., 2005) along with long-term hippocampal sclerosis in mesial temporal lobe epilepsy (Thom, 2014). Therefore, one might hypothesize that similar alterations could be observed in patients treated by ECT. Mander et al. (1987) and Scott et al. (1990) observed in two early nuclear magnetic resonance studies an increased T1 relaxation time in brains of patients immediately after ECT, a finding that could be interpreted as an increase of water content. However, as stated before, T1 relaxation time is related to water content but it is additionally influenced by other factors such as paramagnetic ion concentration, and protein content (Akber, 1996).

Therefore, it could be argued that the measurements used in these two early studies lacked specificity and one could therefore challenge the hypothesis that ECT leads to a cortical reorganisation. Moreover, these two studies reported, at the time, results with very poor spatial resolution due to technical limitations (the signal was averaged over the whole hemispheres in both studies). A more recent study by Kunigiri et al. (2007) did not find changes in T2 relaxation and could not rule out the hypothesis of an ECT-induced oedema, because T2 relaxation time is a composite measure not exclusively linked to water content (Tofts, 2004). More recently, studies using Diffusion Weighted Imaging have brought some evidence against the hypothesis of ECT-induced oedema in the hippocampus by showing a reduction of Mean Diffusivity (Jorgensen et al., 2016) and no change in Apparent Diffusion Coefficient (Szabo et al., 2007). However, diffusion-derived measures do not give an absolute measure of water content but of how water can diffuse in the cerebral tissue. Thus, these metrics are influenced by the proportion of water in intra- vs extracellular compartments even if the total amount of water is constant. In our study we use a more stable metric of tissue water content, namely Proton Density (Tofts, 2004).

The second question of this study is the whole-brain investigation of tissue microstructure property changes along ECT treatment using the various measures derived from qMRI: PD, MT, R1 and R2*. By using multiple MRI measurements that are quantitative and more closely linked to the properties of the brain tissue, we expect greater sensitivity and specificity to detect plasticity process related to ECT, thus getting a more accurate description of the effects of ECT on the brain.

The third question was to explore how changes of GM volume and tissue microstructural properties is related to clinical outcome. Again, using more specific measurements, we aim to better delineate the anatomical regions important for the recovery from MDD following ECT.

The last question was related to the choice and implementation of the appropriate statistical model used to analyse our data. Indeed, longitudinal multi-contrast neuroimaging studies involve data acquisitions at several time points, using multiple imaging sequences during each scanning session. Two sources of dependency between observations have to be considered in the statistical model: First, multiple contrasts are acquired from the same patient during each scanning session, and, second, repeated measurements over time are collected from each patient. One frequently-used approach to multi-contrast data analysis is modelling each contrast separately, i.e. to fit one univariate General Linear Model (GLM) for each contrast (see for example (Stefani et al., 2019)). However, this methodology can increase the type I error rate and does not model the relationship between dependent variables (Fox, 2015). The use of multivariate statistics allows to assess how a combination of dependent variables reflect an effect of interest, and thus provides more information than the univariate GLM approach (McFarquhar et al., 2016). The recent implementation of the multivariate General Linear Model (GLM) for neuroimaging data proposed by (McFarquhar et al., 2016) facilitates the modelling of either multi-contrast datasets, or repeated measures datasets but cannot be applied to datasets that have both characteristics. In this study, we propose a more general implementation of the multivariate GLM that combine the multiple dependent variables and repeated measurement approaches.

In summary, this longitudinal study proposes to investigate neural plasticity induced by ECT using quantitative MRI, to test if change of water content occurs in the hippocampus alongside the well-established change of GM volume. In addition, we aim at describing at the whole brain level how ECT affects microstructural properties of the brain tissue and how clinical outcome is related to this change. Finally, the last aim of the study is to implement a multivariate approach to model our multi-contrast and repeatedly measured data.

3. Study 1: Differential effect of ECT on GM volume increase in the hippocampus along its longitudinal axis

3.1. Material and methods

3.1.1. Participants

We analysed data from 22 patients with major depressive disorder (MDD), 11 patients with bipolar disorder (BD) and 30 healthy controls (HC) that took part in an already published study (Dukart et al., 2014). Our sub-sample differs from the previously reported cohort by the exclusion of bipolar patients that are in a current manic episode and the fact that here, we use data from two out of three acquisition time points - baseline [M0] and 3 months [M3], which allowed us to include additional study participants. Patients' pharmacological treatment consisting of antidepressants, lithium, mood stabilizers, atypical and typical antipsychotics was continued for the whole study duration following best clinical practice criteria. Following the logic of clinical decision-making, pharmaco-resistant patients were treated with right unilateral ECT in due course of hospitalization with three ECT sessions per week (N = 9; 5 MDD/4 BD). Symptom severity was assessed with the 17-item Hamilton Depression Rating Scale (HAM-D, score 0 - 50). A detailed description of the sub-sample and between-group comparisons are reported in Table 1.

3.1.2. MRI data acquisition and preprocessing

Structural MRI data were acquired on a 1.5T Magnetom VISION (Siemens) scanner with a vacuum-moulded head holder (Vac-Pac™, Olympic Medical) to reduce motion. For each session we obtained two consecutive T1-weighted images in sagittal mode using a 3D

magnetization prepared rapid gradient echo (MPRAGE) sequence (TR = 11.4 ms, TE = 4.4 ms, field of view = 269 mm, flip angle = 30°, 154 contiguous slices, voxel-size: 1.05 × 1.05 × 1.05mm, slab 161 mm, matrix size = 256 × 256). We calculated the average of both acquisitions to achieve a higher signal-to-noise ratio. For data processing we used SPM12 (Statistical Parametric Mapping software: www.fil.ion.ucl.ac.uk/spm, Wellcome Trust Centre for Neuroimaging, UCL London, UK) running under Matlab R2017a. Aiming at higher anatomical precision across time points, we used the longitudinal diffeomorphic registration toolbox that maps individual time point data to a mid-way average (Ashburner & Ridgway, 2013; Ziegler, Ridgway, Blakemore, Ashburner, & Penny, 2017). We then automatically classify brains' grey matter, white matter, cerebro-spinal fluid and non-brain tissue in the framework of SPM12s "unified segmentation" approach using enhanced tissue priors (Lorio et al., 2016) and estimate spatial registration parameters to the standardized Montreal Neurological Institute space. We then create maps of grey matter volume (GMV) rate of change by multiplying the subject specific Jacobian determinants estimated in the first step with the corresponding GMV map obtained from the mid-way average. The unit of the GMV map is the amount of relative change per year, i.e. for a given rate of change of 0.5 a voxel of 1 mm³ increases to a value of 1.5 mm³ after one year.

For the region-of-interest (ROI) analysis of hippocampal GMV rate of change we used the definition of hippocampus borders in the Neuromorphometrics atlas in SPM12 derived from the "MICCAI 2012 Grand Challenge and Workshop on Multi-Atlas Labeling" (www.masi.vuse.vanderbilt.edu/workshop2012/index.php). As input for statistical analysis we extracted the eigenvariate of the GMV rate of change in the anterior and posterior part of the left and right hippocampus (Chen & Etkin, 2013; Satpute, Mumford, Naliboff, & Poldrack, 2012) (anterior y= -10 to -21mm, mid y= -21 to -32 mm and posterior y= -32 to -43 mm). After

excluding the hippocampus mid-portion, we used the anterior and posterior ROI values for a 3-way interaction analysis between GROUP x HEMISPHERE x SUBREGION and for correlation with symptom severity scores.

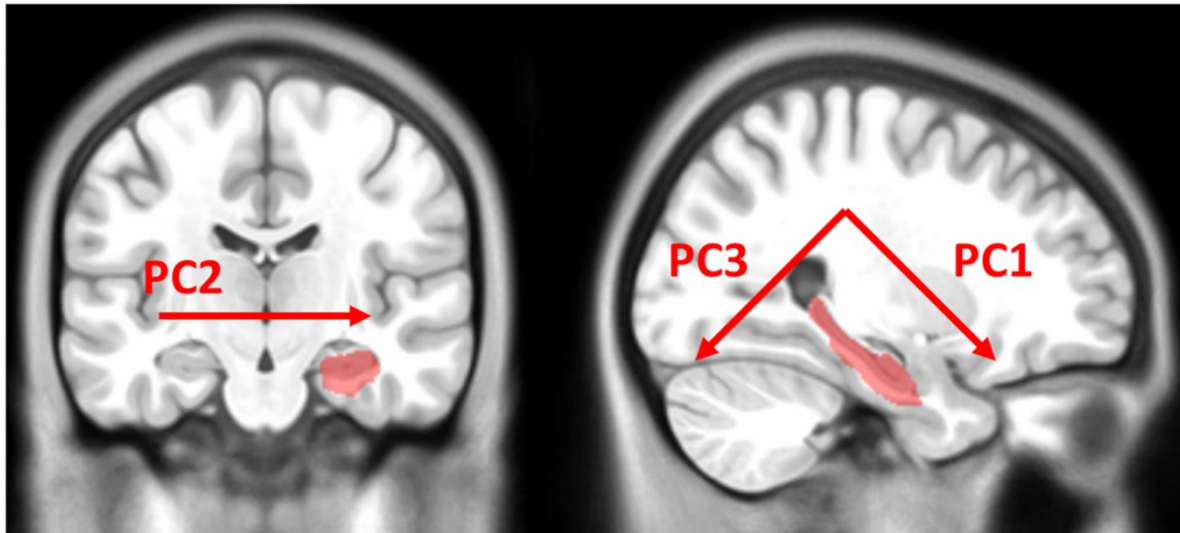
3.1.3. Definition of hippocampal main spatial axes

For data-driven representation of the hippocampal main spatial axes we extracted the MNI coordinates of each hippocampal voxel within the structure defined by the Neuromorphometrics atlas. We then performed a Principal Component Analysis – PCA, on the x, y and z coordinates and used the 1st principal component as indicator for the longitudinal hippocampal axis to then test for differential ECT effects along the spatial gradients (see Figure 1).

3.1.4. Statistical analysis

For statistical whole-brain analysis of the ECT effects we created a one-way analysis-of-variance (ANOVA) design with three groups - MDD, BD and HC, including ECT and pharmacological treatment as dummy variables, additional to regressors for age and gender.

For ROI topographical analysis with search volume restricted to the hippocampus we used a linear mixed model with factors GROUP [ECT, no-ECT and HC], HEMISPHERE [left and right] and AXIS [three PCA components indicative for the three main spatial axes]. To adjust for the spatial autocorrelation between voxels we specify a 3-dimensional spherical correlation structure of the error term using the generalized least squares approach. The correlation structure was estimated for each level of the interaction GROUP x HEMISPHERE (six correlation structures). Following the model estimation, we extracted the residuals β of the relationship between mean GMV rate of change and PC1 for each level of the GROUP x



For right hippocampus:
PC1 corresponds to a superior+posterior / anterior+inferior axis
PC2 to a left / right axis
PC3 to a superior+anterior / inferior+posterior axis

HP	MNI	PC1 rotation	PC2	PC3
Right	X	0.06	-0.99	0.01
	Y	0.77	0.04	0.65
	Z	-0.64	-0.05	0.76
Left	X	0.05	0.99	0.09
	Y	-0.77	-0.02	0.64
	Z	0.64	-0.1	0.76

Figure 1: Principal component analysis of right (R) and left (L) hippocampus coordinates corresponding to Montreal Neurological Institute (MNI) standardised space. Red arrows represent the main axes estimation resulting from the Principal Component Analysis (PCA) for the right hippocampus.

HEMISPHERE interaction (six β estimates). We then performed two series of post-hoc tests:

- i. each β was tested for significant difference from zero;
- ii. estimation of the following differential contrasts: 1) $\beta_{ECT/Right}$ vs $\beta_{NoECT/Right}$ 2) $\beta_{ECT/Right}$ vs $\beta_{HC/Right}$ 3) $\beta_{NoECT/Right} - \beta_{HC/Right}$ 4) $\beta_{ECT/Left}$ vs $\beta_{NoECT/Left}$ 5) $\beta_{ECT/Left}$ vs $\beta_{HC/Left}$ and 6) $\beta_{NoECT/Left}$ vs $\beta_{HC/Left}$.

The two families of post-hoc tests were controlled for type I errors using false discovery rate (FDR) correction for multiple comparisons.

To confirm the validity of our results we performed a second ROI analysis using hard-border subdivision of anterior, mid and posterior hippocampus as suggested previously (Chen & Etkin, 2013; Satpute et al., 2012). We estimated a linear mixed model with between-subject fixed-effect GROUP [ECT vs. no-ECT vs. HC] and the within-subject fixed-effect HEMISPHERE [left vs. right], SUBREGION [anterior vs. posterior] after adjusting for the effects of age and gender. To account for the hierarchical nature of our data we specified an individual-specific random intercept with all possible interactions between the factors. The planned post-hoc tests with linear contrasts tested the three-way interaction GROUP x HEMISPHERE x SUBREGION – e.g. left - right difference by anterior - posterior difference by group.

We estimated the association between symptom severity (assessed with the HAMD) and baseline GMV across hippocampal SUBREGION (anterior vs. posterior) and HEMISPHERE (left vs. right) using a linear model testing the interaction with treatment group (ECT vs no- ECT). Using the same approach and design, we correlate the treatment related symptoms severity improvement (assessed with the HAMD) and GMV rate of change. Planned post-hoc tests compared the difference between the slopes of the two treatment groups.

All whole-brain analyses were carried out in the General Linear Model framework of SPM12 using the Random Field Theory after family-wise error (FWE) corrections for multiple comparisons at $p_{FWE} < .05$. For the ROIs analyses we used the R 3.5.2 package nlme (Pinheiro, Bates, DebRoy, Sarkar, & The R Development Core Team, 2013) for fitting generalized least square and linear mixed models and the package emmeans (Russell, 2018) for post-hoc tests. We report ROI analyses results after FDR correction for multiple comparisons.

3.2. Results

3.2.1. Demographic and clinical phenotype

Group	Socio-demographic table		
	<i>ECT</i>	<i>No ECT</i>	<i>Healthy controls</i>
N	9	24	30
Age (mean ± SD)	53.7 ± 11.1	48.9 ± 11.3	48.2 ± 11.1
Female / Male	6F/3M	12F/12M	15F/15M
Education years (mean ± SD)	14.4 ± 2.7	14.8 ± 2.5	15.7 ± 2.2
MDD / BD	5 MDD/4 BD	17 MDD/7 BD	-
Number of depressive episode (mean ± SD)	6.9 ± 5.5	4.3 ± 3.9	-
Disease duration in years (mean ± SD)	15.4 ± 9.3	9.5 ± 10.5	-
Cumulative duration of depressive episode in months (mean ± SD)	32.6 ± 10.6 ^{a(**)}	16.3 ± 12.5 ^{a(**)}	-
Duration current episode in months (mean ± SD)	8.4 ± 7.2	4 ± 3.3	-
Antidepressant (%)	100%	91.7%	-
Lithium (%)	33.3%	0%	-
Mood stabilizer (%)	22.2%	25%	-
Atypical antipsychotic (%)	77.8%	29.2%	-
Typical antipsychotic (%)	0%	0%	-
HAMD at baseline (mean ± SD)	22.9 ± 6.1 ^{b(***)}	24.9 ± 5.4 ^{b(***)}	-
HAMD at 3 month (mean ± SD)	8.9 ± 7.2 ^{b(***)}	9.3 ± 6.7 ^{b(***)}	-
^a significant difference between ECT and no ECT patients group ^b significant difference between baseline and 3 month * = $p < .05$, ** = $p < .01$, *** = $p < .001$			

Table 1: Sociodemographic and clinical characteristics of patients treated with ECT (ECT), pharmacological treatment only (No ECT) and healthy controls. MDD = major depressive disorder, BD = bipolar disorder

There were no differences in age, gender and years of education between groups defined by treatment - ECT (n=9), no-ECT (n=24) and HC (n=30). The ECT and no-ECT groups did not differ in the number of depressive episodes, disease duration and duration of the current episode,

whereas the ECT group had longer cumulative duration of depressive episode compared to the no-ECT group ($p < .01$). Depression severity assessed with the HAMD score did not differ between ECT and no-ECT groups at any time point and both groups showed reduction of depression severity from baseline to 3 months ($p < .001$) (see Table 1).

3.2.2. Main effect of ECT

The whole-brain analysis showed only for the ECT group an increase of GMV rate of change in the right hippocampal complex and amygdala ($p_{FWE} < .05$, $k = 5183$, peak: $x = 30$, $y = -11$, $z = -20$; Figure 2 A).

The analysis for a differential ECT effect along the hippocampal antero-posterior axis demonstrated a linear increase of the GMV rate of change towards the anterior part of the hippocampus bilaterally (right: $\beta = 0.01 \pm 0.002$, $p < .01$; left: $\beta = 0.005 \pm 0.002$, $p < .05$, Figure 3 and Tables 2 and 3) but not for the other interaction analyses ($p > .12$). The comparison of regression coefficients for the right hippocampus confirmed the steeper change in the ECT group compared with the no-ECT (estimate difference = 0.01 ± 0.003 , $p < .01$) and with the HC groups (estimate difference = 0.012 ± 0.003 , $p < .01$). There was no difference between the no-ECT and HC groups (estimate difference = 0.002 ± 0.003 , $p = .53$). In the left hemisphere, we found a trend between ECT and HC (estimate difference = 0.007 ± 0.003 , $p = .056$) in the absence of other significant effects (all $p > .14$) (Figure 3 and Tables 2 and 3).

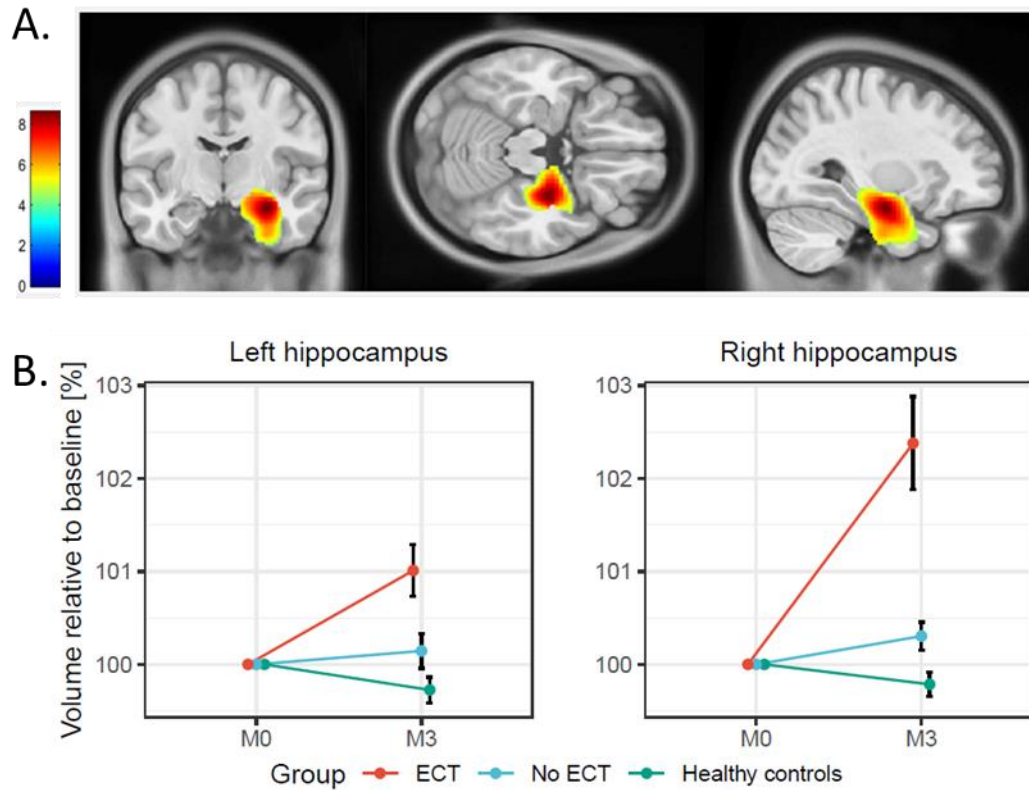


Figure 2: A. Statistical Parametric Map of differential grey matter volume (GMV) rate of change in electro-convulsive therapy (ECT) patients and two control groups (no-ECT and HC) projected on T1-weighted image in standard Montreal Neurological Institute space after pFWE < .05 correction for multiple comparisons across the whole-brain. B. Relative volume change of left (L) and right (R) hippocampus at 3 months (M3) expressed as percentage of baseline (M0). Error bars representing standard errors.

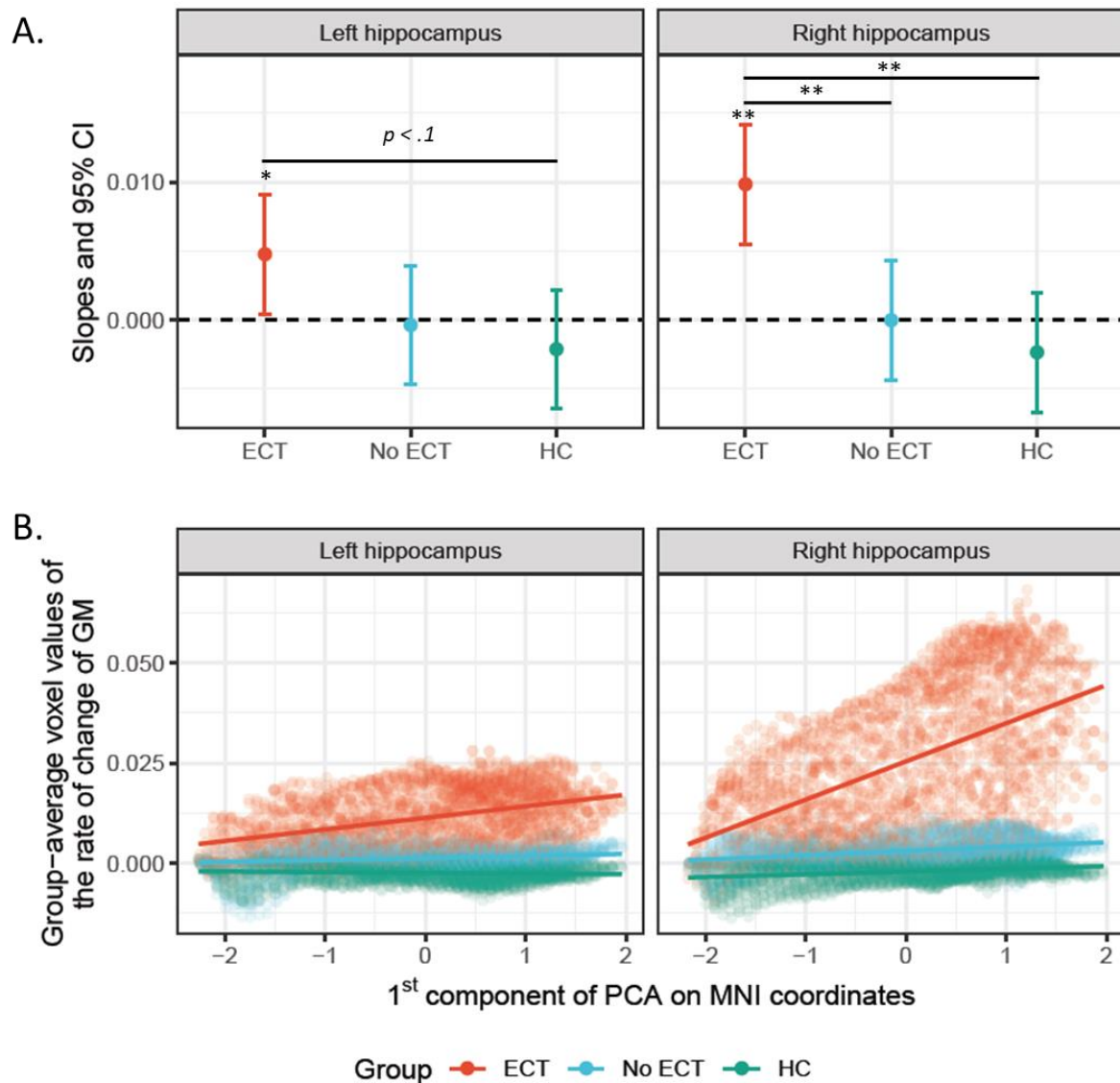


Figure 3: **A.** GROUP \times HEMISPHERE interaction with representation of beta coefficients (with 95% CI) across GROUP (ECT - red, no-ECT - blue and HC - green) after correction for multiple comparisons (* $p_{FDR} < .05$, ** $p_{FDR} < .01$). **B.** Correlation plot between voxel-wise GMV rate of change in left and right hippocampus and gradient along the main spatial axis of the hippocampus (1st principal component) across GROUP (ECT, no-ECT and HC). On the x-axis, negative value indicates voxels closer to posterior and positive value voxels closer to anterior hippocampal sub-region.

	Group	β estimate	SE	df	lower 95% CI	upper 95% CI	T-ratio	p-value
R hippo- campus	ECT	0.0099	0.0021	21.51	0.0055	0.0142	4.70	0.000
	NoECT	0.0000	0.0021	21.51	-0.0044	0.0043	-0.01	0.991
	HC	-0.0024	0.0021	21.51	-0.0067	0.0020	-1.12	0.274
L hippo- campus	ECT	0.0048	0.0021	21.51	0.0004	0.0091	2.29	0.032
	NoECT	-0.0004	0.0021	21.51	-0.0047	0.0040	-0.18	0.859
	HC	-0.0021	0.0021	21.51	-0.0065	0.0022	-1.02	0.319

Table 2: Beta coefficients of the generalized least square model testing the relation between grey matter volume rate of change and position along the main spatial axis of the hippocampus defined as the 1st principal component of a Principal Component Analysis (PCA) performed on the MNI coordinates of the right (R) and left (L) hippocampus.

	β contrast	SE	df	T-ratio	p-value
$\beta_{ECT/Right} - \beta_{NoECT/Right}$	0.0099	0.0030	21.51	3.33	0.009
$\beta_{ECT/Right} - \beta_{HC/Right}$	0.0122	0.0030	21.51	4.12	0.003
$\beta_{NoECT/Right} - \beta_{HC/Right}$	0.0023	0.0030	21.51	0.79	0.528
$\beta_{ECT/Left} - \beta_{NoECT/Left}$	0.0051	0.0029	21.51	1.75	0.143
$\beta_{ECT/Left} - \beta_{HC/Left}$	0.0069	0.0029	21.51	2.34	0.058
$\beta_{NoECT/Left} - \beta_{HC/Left}$	0.0018	0.0029	21.51	0.59	0.558

Table 3: Contrast between beta coefficients of the generalized least square model testing the relation between grey matter volume rate of change and the position along the main spatial axis of the hippocampus.

The confirmatory analysis using a hard-border hippocampus subdivision showed a significant three-way GROUP x HEMISPHERE x SUBREGION interaction ($F(2, 180) = 4, p < .05$). The post-hoc tests revealed that the steeper GMV rate of change in the right anterior hippocampus was specific to the ECT when compared to the no-ECT group (estimate difference = 0.013 +/- 0.005,

p < .05) or to the HC group (estimate difference = 0.012 +/- 0.005, p < .05). There was no difference between the no-ECT and HC group (estimate difference = -0.001 +/- 0.003, p = .77) (Figure 4 and Tables 4 and 5).

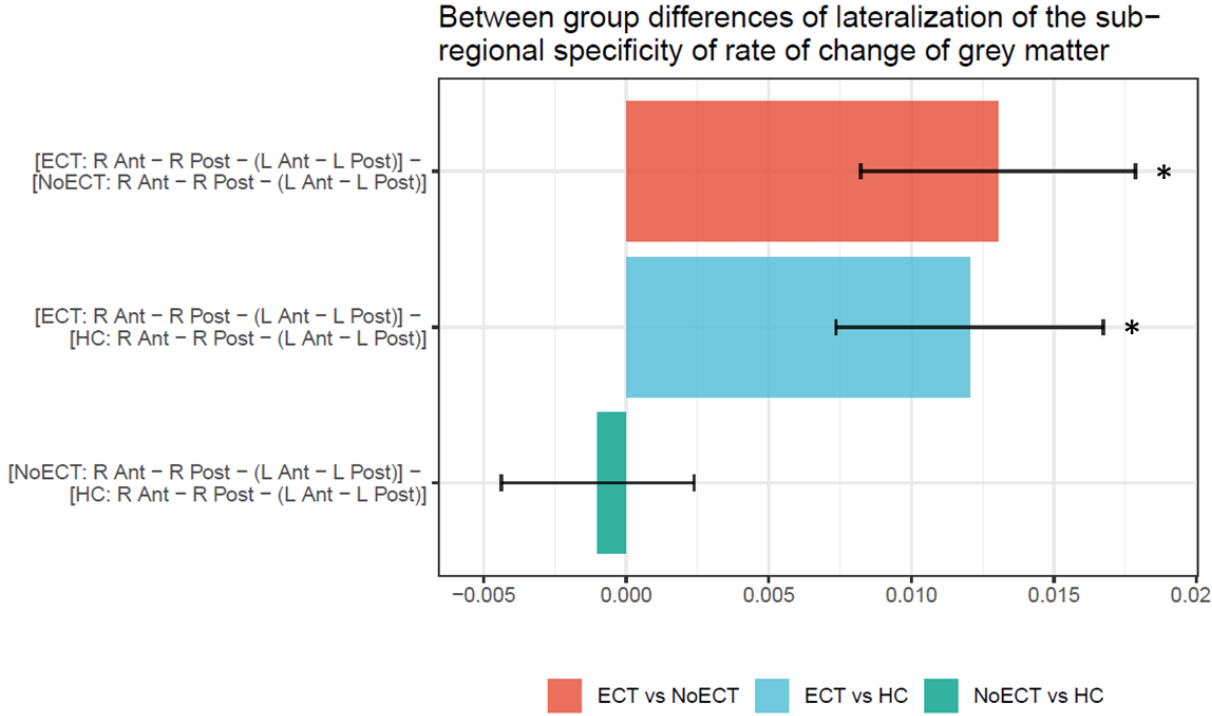


Figure 4: Three-way interaction between group, side and sub-region. Each contrast is testing the between group difference of the R vs L within group difference in GMV rate of change within a sub-region. Star indicates contrasts significantly different from zero (p < .05 corrected for multiple comparison using FDR).

	numDF	denDF	F-value	p-value
(Intercept)	1	180	2.46	0.119
Group	2	58	21.37	0.000
Subregion	1	180	9.02	0.003
Hemisphere	1	180	7.90	0.005
Age	1	58	0.47	0.494
Gender	1	58	8.96	0.004
Group x Subregion	2	180	14.81	0.000
Group x Side	2	180	10.60	0.000
Subregion x Side	1	180	6.03	0.015
Group x Subregion x Side	2	180	4.00	0.020

Table 4: ANOVA table of the confirmatory analysis

Contrast	Estimate	SE	df	T-ratio	p-value
[ECT: R Ant - R Post - (L Ant - L Post)] - [NoECT: R Ant - R Post - (L Ant - L Post)]	0.0130	0.0048	180	2.71	0.016
[ECT: R Ant - R Post - (L Ant - L Post)] - [HC: R Ant - R Post - (L Ant - L Post)]	0.0121	0.0047	180	2.57	0.016
[NoECT: R Ant - R Post - (L Ant - L Post)] - [HC: R Ant - R Post - (L Ant - L Post)]	-0.0010	0.0034	180	-0.29	0.768

Table 5: Post-hoc tests of the three-way interaction of the confirmatory analysis

3.2.3. Correlation with symptoms improvement

We observed a positive correlation between the volume of the anterior hippocampus at baseline and symptoms change only for the ECT group (right anterior hippocampus: estimate = 118.4 +/- 37.3, $p < .01$; left anterior hippocampus: estimate = 96.5 +/- 46.9, $p < .05$, Figure 5, Tables 6 and 7). The comparison of slopes between the ECT and no-ECT group in the anterior

hippocampus showed a significantly steeper slope in the ECT compared to non-ECT group for the right (estimate difference = 103 +/- 43, $p < .05$) and a trend for the left hemisphere (estimate difference = 95 +/- 55.3, $p = .096$).

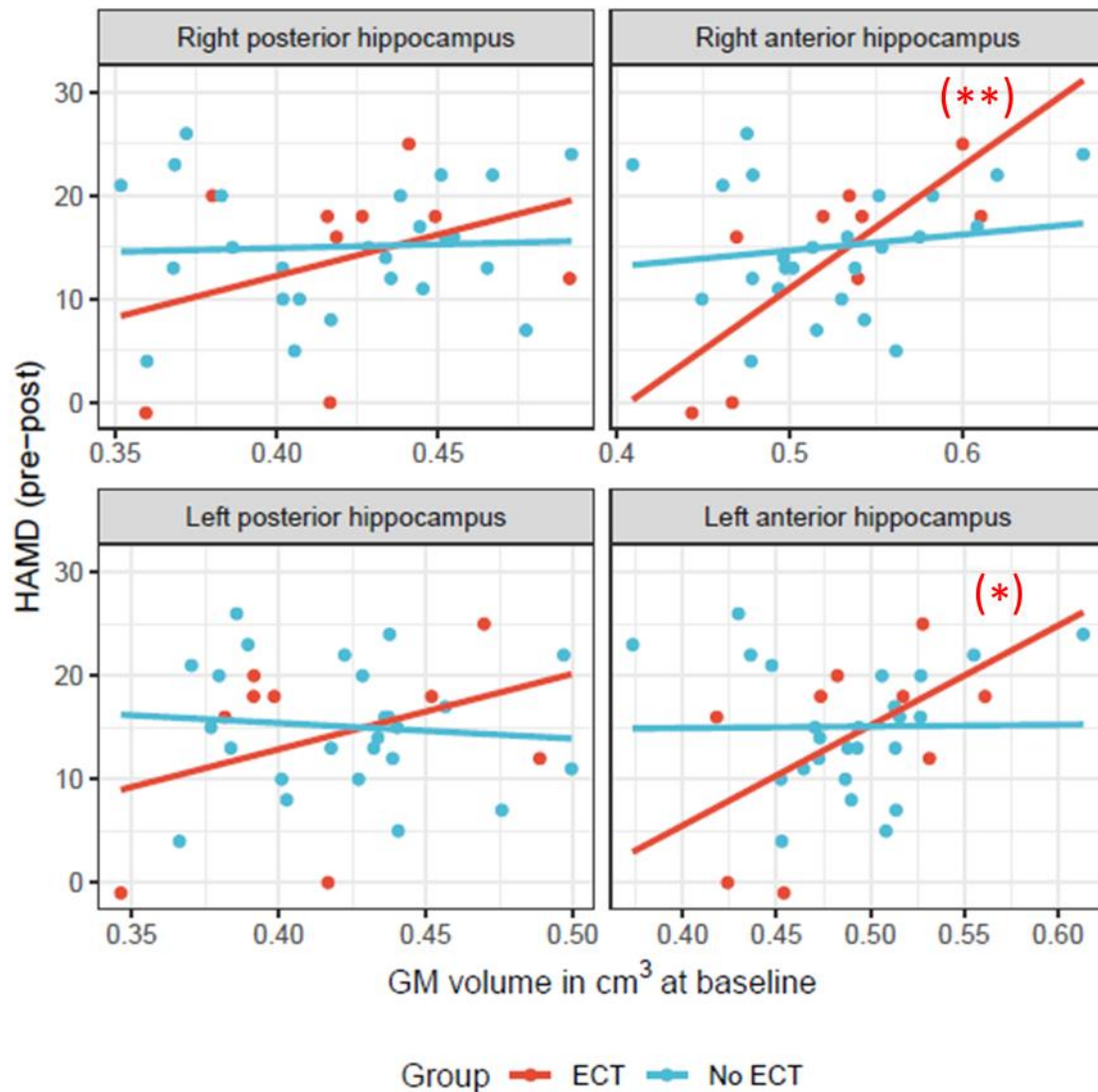


Figure 5: Scatterplots of symptom improvement assessed with the Hamilton Depression Rating Scale (HAMD) versus grey matter volume at baseline across hippocampal SUBREGIONS (anterior vs. posterior) and HEMISPHERES (left vs right) after $p_{FDR} < .05$ correction for multiple comparisons (*) across GROUPS (ECT – red, no ECT - blue). (* = $p < .05$, ** = $p < .01$).

	Group	β			lower	upper	T-ratio	p-value
		estimate	SE	df	95% CI	95% CI		
R Post	ECT	80.2	64.3	30	-51.2	211.5	1.25	0.222
	No ECT	7.3	35.8	30	-65.8	80.4	0.20	0.840
R Ant	ECT	118.4	37.3	30	42.2	194.6	3.17	0.003
	No ECT	15.4	21.3	30	-28.1	59.0	0.72	0.475
L Post	ECT	73.0	52.7	30	-34.6	180.5	1.39	0.176
	No ECT	-15.1	38.5	30	-93.6	63.5	-0.39	0.698
L Ant	ECT	96.5	46.9	30	0.8	192.3	2.06	0.048
	No ECT	1.6	29.3	30	-58.2	61.4	0.05	0.958

Table 6: Beta coefficients of the regression line presented in Figure 5 for each group and each subregion of the right (R) and left (L) hippocampus of the four models (R Post, R Ant, L Post, L Ant) testing the relationship between the grey matter volume at baseline and symptom improvement assessed with the Hamilton depression score (HAMD) between baseline and 3 months.

contrast	β				
	contrast	SE	df	T-ratio	p-value
$\beta_{ECT/R\ Post} - \beta_{NoECT/R\ Post}$	72.8	73.61	30	0.99	0.330
$\beta_{ECT/R\ Ant} - \beta_{NoECT/R\ Ant}$	103	42.98	30	2.40	0.023
$\beta_{ECT/L\ Post} - \beta_{NoECT/L\ Post}$	88.1	65.21	30	1.35	0.187
$\beta_{ECT/L\ Ant} - \beta_{NoECT/L\ Ant}$	95	55.27	30	1.72	0.096

Table 7: Group differences in each sub-region of the right (R) and left (L) hippocampus in beta coefficients of the four models testing the relationship between the GMV at baseline and symptom improvement assessed with the Hamilton depression score (HAMD) between baseline and 3 months (relative to Figure 6).

We report a negative correlation between GMV rate of change in the right anterior hippocampus and symptoms improvement assessed with the HAMD score present only in the ECT group (estimate = -44.5 ± 17 , $p < .05$). There was a trend towards a less steep slope in the ECT group as compared to the no-ECT groups for the right anterior hippocampus (estimate difference = 49.06 ± 72.85 , $p = .09$) (see Figure 6 and Tables 8 and 9).

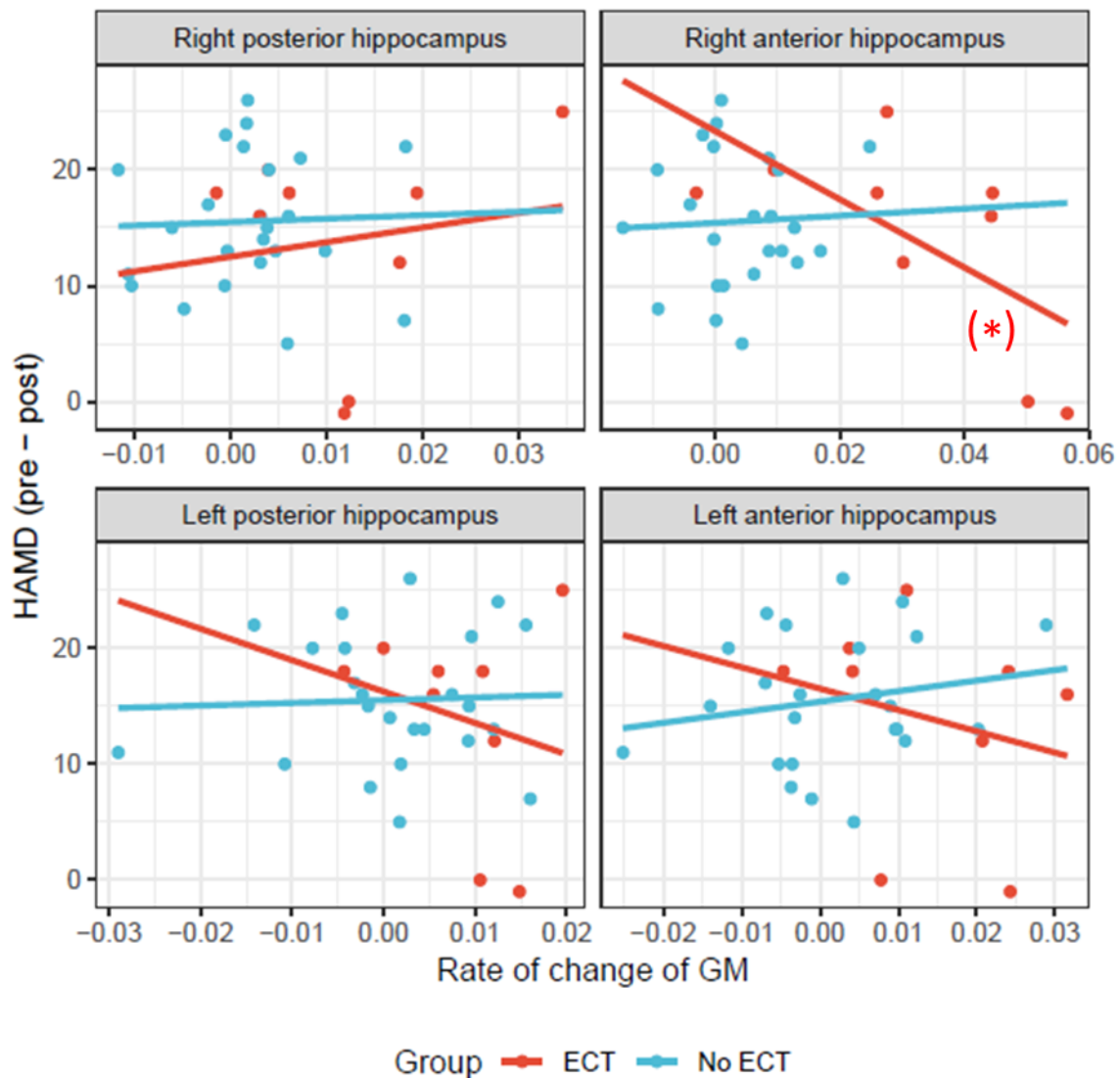


Figure 6. Scatterplots of symptom improvement assessed with the Hamilton Depression Rating Scale (HAMD) versus grey matter volume rate of change across hippocampal SUBREGIONS (anterior vs. posterior) and HEMISPHERES (left vs right) after $p_{FDR} < .05$ correction for multiple comparisons (*) across GROUPS (ECT, no-ECT).

	Group	β estimate	SE	df	lower 95% CI	upper 95% CI	T-ratio	p-value
R Post	NoECT	4.5	28.7	29	-54.2	63.2	0.16	0.877
	ECT patients	19.1	33.6	29	-49.6	87.7	0.57	0.574
R Ant	NoECT	4.6	22.0	29	-40.4	49.7	0.21	0.836
	ECT patients	-44.5	17.0	29	-79.3	-9.6	-2.61	0.014
L Post	NoECT	3.5	21.0	29	-39.5	46.5	0.17	0.868
	ECT patients	-41.0	49.3	29	-141.9	59.9	-0.83	0.413
L Ant	NoECT	13.8	18.4	29	-23.9	51.4	0.75	0.460
	ECT patients	-27.8	30.0	29	-89.1	33.5	-0.93	0.361

Table 8: Beta coefficients of the regression line presented in Figure 6 for each group and each subregion of the right (R) and left (L) hippocampus of the four models (R Post, R Ant, L Post, L Ant) testing the relationship between the grey matter volume change and symptom improvement assessed with the Hamilton depression score (HAMD) between baseline and 3 months.

contrast	β contrast	SE	df	T-ratio	p-value
$\beta_{ECT/R\ Post} - \beta_{NoECT/R\ Post}$	14.6	44.2	29	0.33	0.744
$\beta_{ECT/R\ Ant} - \beta_{NoECT/R\ Ant}$	-49.1	27.9	29	-1.76	0.089
$\beta_{ECT/L\ Post} - \beta_{NoECT/L\ Post}$	-44.5	53.6	29	-0.83	0.413
$\beta_{ECT/L\ Ant} - \beta_{NoECT/L\ Ant}$	-41.6	35.2	29	-1.18	0.247

Table 9: Group differences in each subregion of the L and R hippocampus in beta coefficients of the four models testing the relationship between the grey matter volume change and symptom improvement assessed with the Hamilton depression score (HAMD) between baseline and 3 months (relative to Figure 6)

3.3. Summary study 1

Based on previous evidence of the involvement of the anterior hippocampus in depression and in the effect of ECT, we hypothesized that the anterior hippocampus volume would be strongly affected by ECT than the posterior part. Using spatial dimensionality reduction and a special form of the linear model that enable to consider spatial correlation structure in the data, we found a gradient in the effect of ECT on hippocampal GM volume. The increase of GM volume was virtually null in the most posterior part and increased gradually when moving to the anterior part. Clinical outcome was associated with GM volume changes confined to the anterior part of the hippocampus. Together, these findings converge to the specific effect of ECT on the anterior hippocampus and on the importance of the very same region to mediate therapeutic benefit.

4. Study 2: Quantitative MRI study of the effect of ECT on brain structure

4.1. Material and methods

4.1.1. Procedure

4.1.1.1. Ethical statement

The study was approved by the local Ethics Committee. All patients gave their written informed consent prior to participation.

4.1.1.2. Participants

We recruited 9 patients (5 male/4 female, mean age = 51.46, SD = 11.39) with current diagnosis of major depressive episode (5 with major depressive disorder (2 male/3 female), 3 with bipolar disorder (2 male/1 female), 1 with schizoaffective disorder (1 male)) prepared for electroconvulsive therapy (ECT) according to best clinical practice. The diagnosis was confirmed by a board-certified psychiatrist following the criteria of the Diagnostic and Statistical Manual of Mental Disorder IV-TR (American Psychiatric Association, 2000). All patients were screened for MRI compatibility.

4.1.1.3. Study design

Data was acquired at four time points (see Figure 7) including behavioural testing, clinical evaluation and MRI scanning. The initial time point was scheduled before the start of ECT treatment (t_0), the next - during the first week of treatment after two sessions of ECT (t_1), then two months after the start of ECT treatment corresponding to the end of the therapy or to the transition to maintenance ECT (t_2), and 3 to 4 months after the end of the treatment for a follow-up evaluation (t_3).

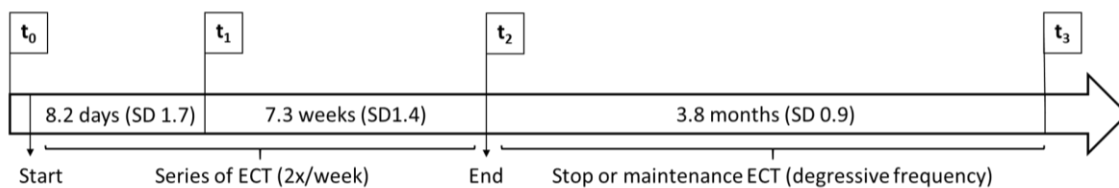


Figure 7: Timeline of the study.

4.1.1.4. ECT procedure

The very first ECT session was dedicated to the titration of electrical stimulation dose. After anaesthesia with etomidate and muscle relaxation with succinylcholine, patients received brief pulse width electrical stimulation using right unilateral electrode placement ($n = 3$) or bilateral temporal electrode placement ($n = 6$). Patients received an initial dose of 800 mA with a pulse width of 0.75 ms at 20 Hz and duration of 1 sec, representing a total delivered charge of 24 mC. Then, an incremental dosage was delivered by varying the pulse width, frequency and total duration of the electrical stimulation to achieve a total charge of twice the preceding stimulation until a seizure was triggered. Once the seizure threshold was determined, the parameters for the rest of the treatment session were defined as 6 times the total charge triggering a seizure during the titration protocol (see internal protocol in annex 3 and Kellner, 2018). In case the ECT-induced seizure lasted for more than two minutes, the seizure was interrupted by administering propofol. Following the first ECT session, patients received two ECT sessions per week, for a total number of 8 to 12 sessions during 2 months, depending on their clinical response. After 2 months, the decision about maintenance therapy vs. therapy stop was made.

4.1.2. Data acquisition and pre-processing

4.1.2.1. Clinical phenotype

At each of the four time points, patients were tested for symptom severity using the French version of the Montgomery-Asberg Depression Rating Scale (MADRS, Montgomery & Asberg, 1979). For reminder, the MADRS score tests 10 dimensions of depressive symptomatology (visible sadness, reported sadness, inner tension, reduced sleep, reduced appetite, concentration difficulties, lassitude, inability to feel, pessimistic thoughts, suicidal thoughts) and ranges from 0 (no depressive symptoms) to 60 (maximum grade in all 10 dimensions). Generally, cut-off score MADRS are: 0-6 (no depressive symptoms), 7 to 19 (mild depression), 20 to 34 (moderate depression) and more than 34 (severe depression) (Snaith, Harrop, Newby, & Teale, 1986). We defined two types of ECT outcome. First, response to ECT was related to the magnitude of symptom reduction relative to pre-treatment measures. ECT responders were thus defined as patient experiencing a decrease of more than 50 % of their MADRS score at baseline. Second, we define remission as a MADRS score below or equal to 9 (Zimmerman, Chelminski, & Posternak, 2004).

4.1.2.2. MRI data acquisition

Patients' neuroimaging data were acquired using 3 T whole-body MRI system using a 20-channel radiofrequency (RF) head and body coil for transmission (Magnetom Prisma, Siemens Medical Systems, Germany). We acquired three consecutive sequences of multi-echo fast low angle shot magnetic resonance imaging (FLASH) with T1-, Proton Density (PD) and Magnetization Transfer (MT) weighting. Repetition time (TR) and flip angle α were: $TR/\alpha = 18.7\text{ms}/20^\circ$ for T1 weighted, $TR/\alpha = 23.7\text{ms}/6^\circ$ for PD and MT weighted contrasts (Helms, Dathe, & Dechent, 2008; Helms, Dathe, Kallenberg, & Dechent, 2008; Helms, Draganski,

Frackowiak, Ashburner, & Weiskopf, 2009). The MT-weighted contrast was carried out using a Gaussian-shaped RF pulse before the excitation (duration of 4 ms, nominal flip angle of 220°, frequency offset from water resonance of 2 kHz). We acquired the multiple gradient echoes with alternating readout polarity with minimal echo time (TE) of 2.34 ms and a between-echo time of 2.34 ms. To achieve a similar timing of acquisition, 6/8/8 echoes were acquired for MT, PD, and T1-weighted contrasts respectively. The resolution of the image was 1 x 1 x 1 mm, the field of view was 256 x 240 x 176 mm and therefore matrix size was 256 x 240 x 176. In order to reduce acquisition time, we used generalized, auto-calibrating, partially parallel acquisition (GRAPPA) with an acceleration factor of 2 (Griswold et al., 2002).

We acquired maps of the local RF transmit field using a 3-D echo-planar imaging (EPI) spin-echo (SE) and stimulated echo (STE) method with different flip angles. To correct for effects of RF transmit inhomogeneities, we acquired a B1 map with a 4 mm isotropic resolution and with an acquisition duration of 3 minutes. To correct for geometric distortions of the B1 map, we also acquired a map of the static magnetic field B0 as described in Lütti et al. (2010, 2012). The total acquisition time was 27 minutes.

4.1.2.3. MRI data preprocessing

4.1.2.3.1. Maps creation (Figure 8, step 1)

The quantitative maps of PD, MT, R1 and R2* were calculated using in-house routines in the framework of SPM12 (Wellcome Trust Centre for Neuroimaging, London, UK; <https://www.fil.ion.ucl.ac.uk/spm/>) running under Matlab 2017a (Mathworks, Sherborn, MA, USA). First, the 8 volumes of PD- and T1-weighted contrasts and the 6 volumes of the MT-weighted contrasts images were averaged to increase the signal-to-noise ratio (Helms & Dechent, 2009). Then, the three averaged volumes were used to calculate the multi-

parameter maps (MPMs) of the MT saturation, the longitudinal relaxation rate $R1$ ($1/T1$), the effective transverse relaxation rate ($R2^* = 1/T2^*$) and the signal amplitude (proportional to PD) (Draganski et al., 2011; Helms, Dathe, & Dechent, 2008; Helms, Dathe, Kallenberg, et al., 2008).

4.1.2.3.2. Longitudinal data alignment (Figure 8, steps 2 and 3)

Given the quantitative nature of our MRI protocol, we slightly modified SPM12s longitudinal registration that helps avoiding asymmetric preprocessing of longitudinal data (Ashburner & Ridgway, 2013). After creating a mid-point MT average map for each subject, we co-registered to it all parameter maps across the different time points (Figure.

4.1.2.3.3. Feature extraction (Figure 8, steps 4 to 7)

Following the longitudinal data alignment, the feature extraction step for Voxel-Based-Morphometry and Voxel-Based-Quantification was performed in SPM12s framework with default settings. We performed automated tissue classification on the MT co-registered maps using the “unified segmentation” procedure of SPM12 (Ashburner & Friston, 2005) and enhanced tissue priors (Lorio et al., 2016). This was followed by estimation of spatial registration parameters to the Montreal Neurological Institute (MNI) standardized space using diffeomorphic registration (DARTEL, (Ashburner, 2007)). The individuals’ spatial registration parameters were then applied to the grey matter (GM) and quantitative maps followed by spatial smoothing with an isotropic Gaussian kernel of 8 mm full-width-at-half-maximum (FWHM). For the quantitative maps, we applied a weighted averaging procedure to ensure the preservation of the parameters total within each tissue class (Draganski et al., 2011).

4.1.2.3.4. Standardization (Figure 2, step 8)

Within each spatially normalized MRI map (GM volume, PD, MT, R1, R2*) and within each voxel, we calculated the grand mean (across subjects and time points) and standard deviation. We then subtracted the grand mean from each voxel and divided by the standard deviation. This step of within-contrasts and within-voxel standardization was implemented to ensure that the comparison of the contribution of each dependent variable (the canonical vector, see Canonical vector computation subsection in the Method section) in the multi-variate analysis was possible. Indeed, the scale of the non-standardized pre-processed data can vary with a factor of more than a 100. Therefore, all analyses were performed on the standardized data set.

4.1.2.4. Statistical analysis

4.1.2.4.1. Depression severity analysis

Change of depression score over time was tested using a linear mixed model with the fixed effect factor time (4 levels: t_0 , t_1 , t_2 , t_3) and a random intercept for each subject. Model estimation was achieved using the nlme package in R 3.6.0 and post hoc tests using the emmeans package (Pinheiro et al., 2013; Russell Lenth, 2019). Posthoc t-tests were corrected for multiple comparison using Tukey's method (Tukey, 1949).

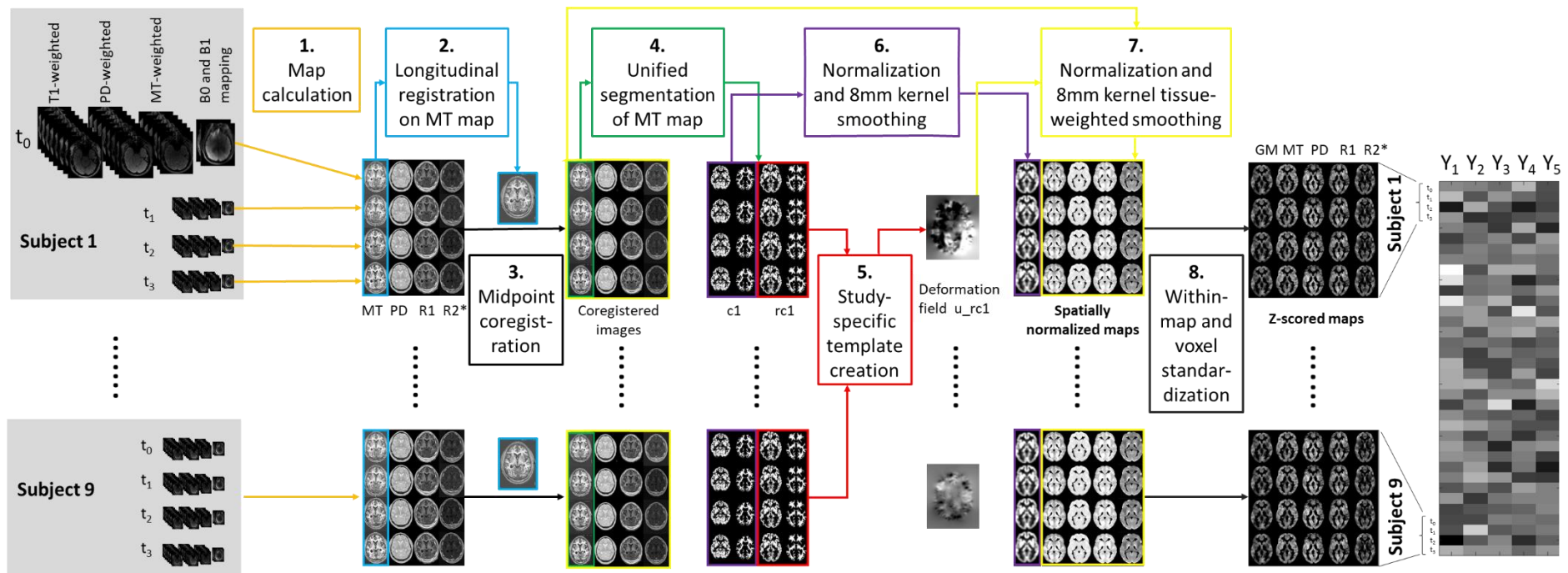


Figure 8: Overview of the preprocessing pipeline. PD = proton density, MT = magnetization transfer, R1 = relaxation rate R1, R2* = relaxation rate R2*, c1 = grey matter probability map in native space, rc1 = DARTEL imported grey matter probability map, u_rc1 = deformation field.

4.1.2.4.2. Neuroimaging analysis

Matrix of observations Y . As a result of the pre-processing (see Figure 8) we obtained 180 maps (9 subjects \times 4 time points \times 5 maps). At each voxel, we built a Y matrix of observations composed of 5 columns $\{Y_1, Y_2, Y_3, Y_4, Y_5\}$ with Y_1 the vector of voxel values coming from the GM volume map, Y_2 from PD maps, Y_3 from MT maps, Y_4 from R1 maps and Y_5 from R2* maps. Every column of Y included 36 observations organized by subjects (S) and time points (t):

$$Y_j = \{S_1t_0, S_1t_1, S_1t_2, S_1t_3, S_2t_0, S_2t_1, \dots, S_9t_3\}.$$

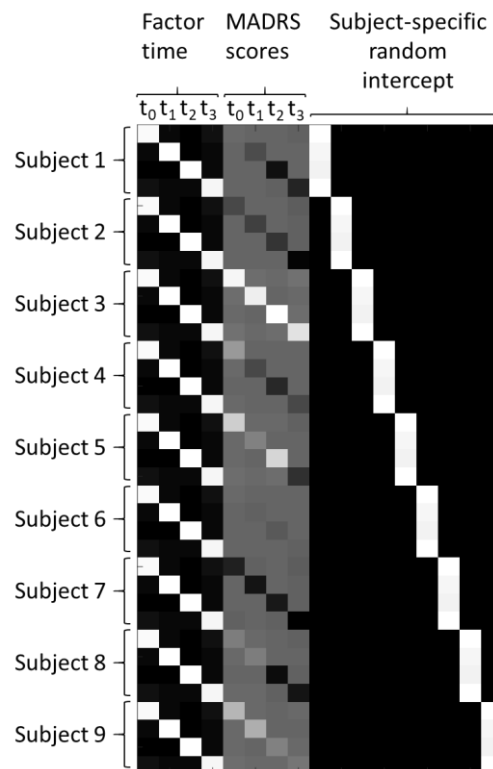


Figure 9 : Design matrix X.

4.1.2.4.3. Design matrix X.

The design matrix was constructed in order to test for the change of MRI maps over time, and to test for association between change of MRI maps and change of symptoms over time, while considering the repeated measurement design of the study. The first four columns encoded

for the four time points $t = \{t_0, t_1, t_2, t_3\}$ coded as dummy variables. The next five columns encoded a continuous variable coding the MADRS score at each time point put into interaction with the factor time. The last nine columns encoded a random intercept for each subject coded as dummy variable (see Figure 9).

4.1.2.4.4. Theory of Multivariate General Linear Model (GLM)

Multivariate GLM notation. All the analyses were conducted in the framework of the multivariate GLM as demonstrated in Fox (2015). From the multivariate general linear model equation written in matrix notation:

$$Y = XB + E \quad (1)$$

With $Y = \{Y_1, Y_2, \dots, Y_m\}$ a matrix resulting from the concatenation of m vectors of dependent variables of length N , X a $N \times p$ matrix of predictors, B a $p \times m$ matrix of regression coefficients and E a $N \times m$ matrix of residuals (see Figure 10 for the particular implementation and matrix size of the multivariate GLM estimated in this study). It has to be mentioned that in the special case where $m = 1$, the equation corresponds to the univariate GLM equation.

Assumption of multivariate GLM. The assumptions pertain to the error term and assume that each i^{th} row of the error term, denoted ε_i' has a multivariate distribution of the form:

$$\varepsilon_i' \sim N_m(0, \Sigma) \quad (2)$$

With Σ a nonsingular error-covariance matrix, constant across observations. In addition, ε_i' and $\varepsilon_{i'}$ are independent when $i \neq i'$.

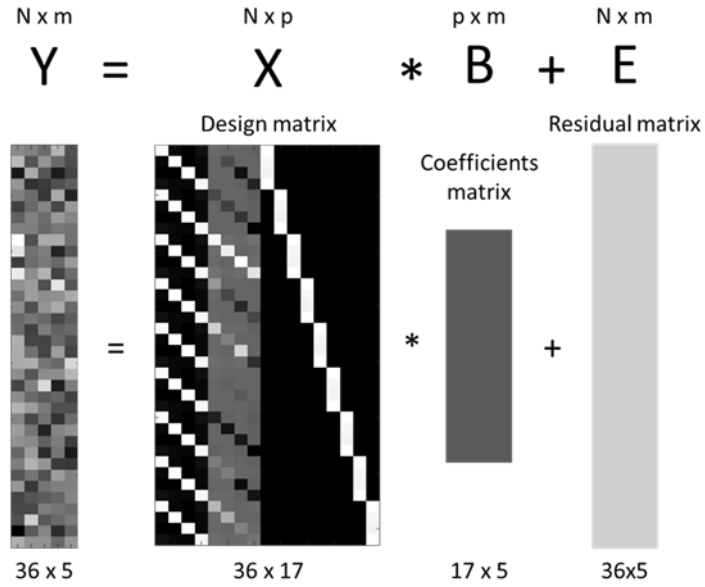


Figure 10: Overview of the particular multivariate GLM implemented in this study.

Matrices dimensions are mentioned below each matrix.

Model estimation. We estimated the matrix B of coefficients using ordinary least-square estimation:

$$B = (X'X)^{-1}X'Y \quad (3)$$

Variance partitioning. The matrix of predicted value \hat{Y} is equal to:

$$\hat{Y} = X\hat{B} \quad (4)$$

And the matrix of residual E is equal to:

$$E = Y - \hat{Y} = Y - X\hat{B} \quad (5)$$

The total sum-of-square-and-cross-product ($SSCP$) matrix of the model is:

$$SSCP_{Total} = Y'Y - N\bar{y}\bar{y}' \quad (6)$$

And can be partitioned into regression $SSCP_{Reg}$ and residual $SSCP_{Error}$:

$$\begin{aligned}
SSCP_{Total} &= SSCP_{Reg} + SSCP_{Error} \\
&= (\hat{Y}'\hat{Y} - N\bar{y}\bar{y}') + E'E
\end{aligned} \tag{7}$$

Test statistics for global significance. To estimate the global significance of the GLM, i.e. test the null hypothesis that none of the coefficients in B are different from zero, we can compute the product of $SSCP_{Reg}$ by the inverse of $SSCP_{Error}$:

$$SSCP_{Reg}SSCP_{Error}^{-1} = \frac{\hat{Y}'\hat{Y} - N\bar{y}\bar{y}'}{E'E} \tag{8}$$

And compute the eigenvalues of the resulting matrix following the general equation of eigen-decomposition with A a matrix for which we want to calculate the eigenvalues λ and eigenvectors v :

$$\begin{aligned}
Av &= \lambda v \\
Av - \lambda v &= 0 \\
(Av - \lambda I)v &= 0 \\
\det(A - \lambda I) &= 0
\end{aligned} \tag{9}$$

Then, by plugging the product of $SSCP_{Reg}$ by the inverse of $SSCP_{Error}$ into A and solving Eq. 9 we can find m eigenvalues λ :

$$\det \left(\frac{\hat{Y}'\hat{Y} - N\bar{y}\bar{y}'}{E'E} - \lambda I_m \right) = 0 \tag{10}$$

The Wilk's lambda summary statistics Λ can then be calculated as a function of the m largest eigenvalues λ (Tabachnick, Fidell, & Ullman, 2007):

$$\Lambda = \prod_{j=1}^m \frac{1}{1 + \lambda_j} \tag{11}$$

Then, statistical significance of Λ can be evaluated using an approximation to F :

$$F(df_1, df_2) = \left(\frac{1 - \Lambda^{1/s}}{\Lambda^{1/s}} \right) \left(\frac{df_2}{df_1} \right) \quad (12)$$

With

$$df_1 = lq \quad (13)$$

$$df_2 = rt - 2u$$

And with

$$l = \text{rank}(Y) \quad (14)$$

$$q = \text{rank}(X) \quad (15)$$

$$u = \frac{df_1 - 2}{4} \quad (16)$$

$$r = N - q - \frac{lq + 1}{2} \quad (17)$$

$$t = \begin{cases} \frac{l^2 q^2 - 4}{l^2 + q^2 - 5} & \text{if } l^2 + q^2 - 5 > 0 \\ 1 & \text{if } l^2 + q^2 - 5 \leq 0 \end{cases} \quad (18)$$

if $\min(l, q) \leq 2$, then the F -approximation is exact.

Test statistic for specific contrasts. The previous section presented how to test the overall significance of the multivariate GLM, i.e. to test the null hypothesis that any $\hat{\beta}$ is different from 0. Testing specific hypothesis about the relationship between all or a subset of the dependent variables and contrasts between predictors involves the following linear hypothesis (Fox, Friendly, & Weisberg, 2013):

$$H_0: CBL = \Gamma \quad (19)$$

With L a $m \times h$ hypothesis matrix on the column of B , with $h \leq m$, i.e. a combination of h dependent variables, C a $v \times p$ response transformation matrix on the rows of B , with $v \leq p$, i.e. a combination of v predictors, and the right hand-side Γ , a matrix of constant set in our case as the null matrix. The $SSCP_{Hyp}$ and $SSCP_{Error}$ can be therefore calculated as:

$$SSCP_{Hyp} = (C\hat{B}L)'[C(X'X)^{-1}C'](C\hat{B}L') \quad (20)$$

$$SSCP_{Error} = L(\hat{E}'\hat{E})L'$$

And a test statistic associated with the null hypothesis can be calculated following the same logic as in Eq. 8-11 with few modifications. First, the Wilk's Λ (Eq. 11) becomes a function of the h largest eigenvalues (previously m) and Eq. 14, 15, 17 are replaced by Eq. 21, 22 and 23, respectively:

$$l = rank(L) \quad (21)$$

$$q = rank(C) \quad (22)$$

$$r = N - rank(X) - \frac{lq + 1}{2} \quad (23)$$

Canonical vector computation. When the hypothesis matrix L involves multiple dependent variables ($q > 1$), it is of interest to extract the contribution of each dependent variable, also called canonical vector, to the test statistic Λ . This contribution corresponds to the eigenvectors of the eigendecomposition of the product of $SSCP_{Reg}$ by the inverse of $SSCP_{Error}$ (Eq. 8). This can be done by simply solving Eq. 9 for each eigenvalue $\lambda = (\lambda_1, \dots, \lambda_h)$ (Tabachnick et al., 2007). For example, the first eigenvector, or first canonical vector can be calculated by solving Eq. 8 for λ_1 . It is worth noting that in order to be able to

compare the values of the canonical vector, the columns of Y must be put on the same scale (see 3.2.2.3.4 Standardization section).

4.1.2.4.6. Planned linear contrasts

Hypotheses matrices L . To test for the joint effect on the 5 MRI maps we set the following linear $m \times h$ L contrast matrix (with m the total number of dependent variables and h the number of dependent variables involved in the contrast). In the case of the joint analysis on all maps, the contrast matrix is the 5×5 identity matrix:

$$L_{all\ maps} = \begin{bmatrix} 1 & 0 & 0 & 0 & 0 \\ 0 & 1 & 0 & 0 & 0 \\ 0 & 0 & 1 & 0 & 0 \\ 0 & 0 & 0 & 1 & 0 \\ 0 & 0 & 0 & 0 & 1 \end{bmatrix}$$

Additionally, we also set the following L contrasts to perform classical univariate analysis on each column of Y . Results of univariate analysis are reported in Supplementary Material.

$$L_{GM} = \begin{bmatrix} 1 \\ 0 \\ 0 \\ 0 \\ 0 \end{bmatrix} \quad L_{PD} = \begin{bmatrix} 0 \\ 1 \\ 0 \\ 0 \\ 0 \end{bmatrix} \quad L_{MT} = \begin{bmatrix} 0 \\ 0 \\ 1 \\ 0 \\ 0 \end{bmatrix} \quad L_{R1} = \begin{bmatrix} 0 \\ 0 \\ 0 \\ 1 \\ 0 \end{bmatrix} \quad L_{R2^*} = \begin{bmatrix} 0 \\ 0 \\ 0 \\ 0 \\ 1 \end{bmatrix}$$

Change of MRI maps over time. The following $v \times p$ C matrices of contrasts (with v the number of predictors involved in the contrast and p the total number of predictors, $p = 17$ in this case) were intended to test for:

the early effect of ECT (the effect that occur between time interval t_0 to t_1)

$$C = \begin{bmatrix} 1 & 0 & 0 & \dots & 0 \\ 0 & 1 & 0 & \dots & 0 \end{bmatrix}$$

the effect of a complete series of ECT (the effect that occur between time interval t_0 to t_2)

$$C = \begin{bmatrix} 1 & 0 & 0 & 0 & \dots & 0 \\ 0 & 0 & 1 & 0 & \dots & 0 \end{bmatrix}$$

the long-term effect of ECT (the effect that occur between time interval t_0 to t_3)

$$C = \begin{bmatrix} 1 & 0 & 0 & 0 & 0 & \dots & 0 \\ 0 & 0 & 0 & 1 & 0 & \dots & 0 \end{bmatrix}$$

the late effect of ECT (the effect that occur between between time interval t_2 to t_3)

$$C = \begin{bmatrix} 0 & 0 & 1 & 0 & 0 & \dots & 0 \\ 0 & 0 & 0 & 1 & 0 & \dots & 0 \end{bmatrix}$$

Association between change of MRI maps and change of depression severity over time.

Additionally, we also set C contrasts matrices intended to test for the association between change of MRI maps and change of MADRS score. We first set a C contrast matrix intended to test for any association between change of MRI maps and symptoms between baseline and one week of treatment (t_0 to t_1), between baseline and after the ECT series (t_0 to t_2) and between baseline and at 6 months follow-up (t_0 to t_3):

$$C = \begin{bmatrix} 0 & 0 & 0 & 0 & -1 & 1 & 0 & 0 & 0 & \dots & 0 \\ 0 & 0 & 0 & 0 & -1 & 0 & 1 & 0 & 0 & \dots & 0 \\ 0 & 0 & 0 & 0 & -1 & 0 & 0 & 1 & 0 & \dots & 0 \end{bmatrix}$$

Then in order to identify the specific time interval were association between change of MRI map and change of symptom is present, we tested the following three C contrast matrices:

$$C = [0 \ 0 \ 0 \ 0 \ -1 \ 1 \ 0 \ 0 \ 0 \ \dots \ 0]$$

$$C = [0 \ 0 \ 0 \ 0 \ -1 \ 0 \ 1 \ 0 \ 0 \ \dots \ 0]$$

$$C = [0 \ 0 \ 0 \ 0 \ -1 \ 0 \ 0 \ 1 \ 0 \ \dots \ 0]$$

4.1.2.4.7. Multiple comparisons correction.

Results were reported significant with a statistical threshold $P < .05$ at the cluster-level after family-wise error (FWE) correction for multiple comparisons over the whole volume of the GM mask using Gaussian Random Field Theory. For display purpose, the statistical map used for the figures were thresholded at $P < .001$ uncorrected for multiple comparison and a minimum

cluster size k was set to remove non-significant cluster at $P < .05$ at the cluster-level. Effects were anatomically localized according to the Neuromorphometrics atlas (Neuromorphometrics, Inc., <http://www.neuromorphometrics.com/>).

Results

4.2.1. Depression severity

4.2.1.1. Quantitative assessment.

We found a significant changes of depression score during the course of the treatment as measured by the MADRS (main effect of time $F(3, 24) = 6.84$, $p < .01$). To identify the time interval where depression score differs, we run post-hoc tests that revealed a trend towards significance for a lower MADRS score at t_2 as compared to t_0 (mean difference = 7.44, standard error (SE) = 2.72, $t = 2.7$, $p = .052$) and a significantly lower score at t_3 as compared to t_0 (mean difference = 10.89, SE = 2.7, $t = 4$, $p < .01$) (see Figure 11 A.).

4.2.1.2. Qualitative assessment.

At t_2 , one third of the patients responded to the treatment and 44% were in remission. At t_3 , two third of the patients responded and 56% were in remission. The count of patients responding to treatment can be visualized in Figure 11 B and the count of patients in remission in Figure 11 C.

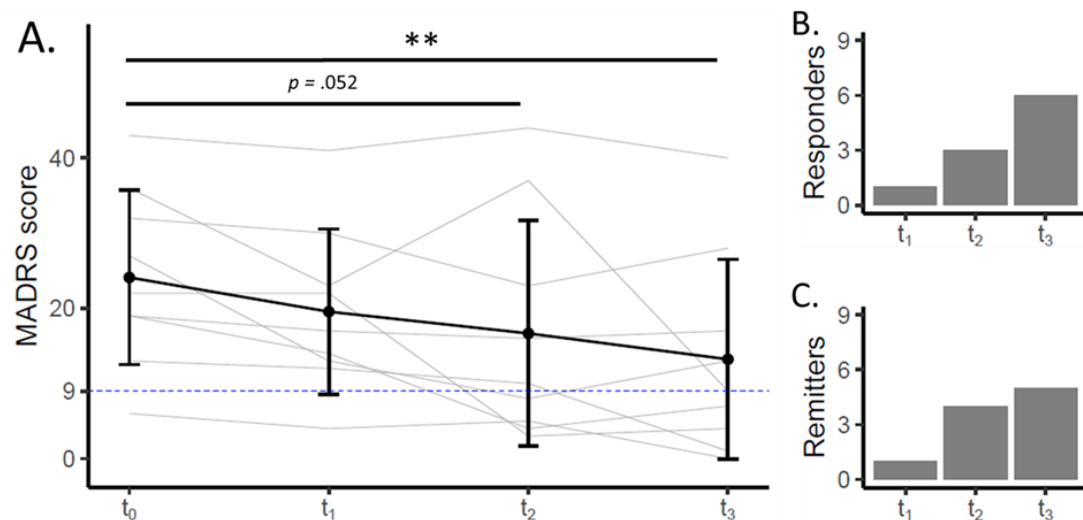


Figure 11: A. Evolution of depressive symptoms as measured by the MADRS. Black dots and error bars represent mean and standard deviation respectively. Grey lines represent individual trajectories. The blue dashed line corresponds to the remission threshold (defined as a MADRS score below or equal to 9). ** = $p < .01$ corrected for multiple comparisons using Tukey's method. **B.** Count of responder and non-responder patients at t₁, t₂ and t₃. **C.** Count of remitters and non-remitters' patients at t₁, t₂ and t₃.

4.2.2. Neuroimaging

4.2.2.1. Effect of ECT

4.2.2.1.1. Early effect of ECT.

There was no significant change between t₀ and t₁.

4.2.2.1.2. Effect of a complete series of ECT.

For t₀ to t₂, we found a significant cluster ($p_{FWE} < .05$ at the cluster level) encompassing the right hippocampus and the right para-hippocampal gyrus and a second cluster in the right anterior cingulate gyrus ($p_{FWE} < .05$ at the cluster level) (see Figure 12 and Appendix 1). The

weights attributed to each dependent variable revealed a predominant contribution of GM volume to the results.

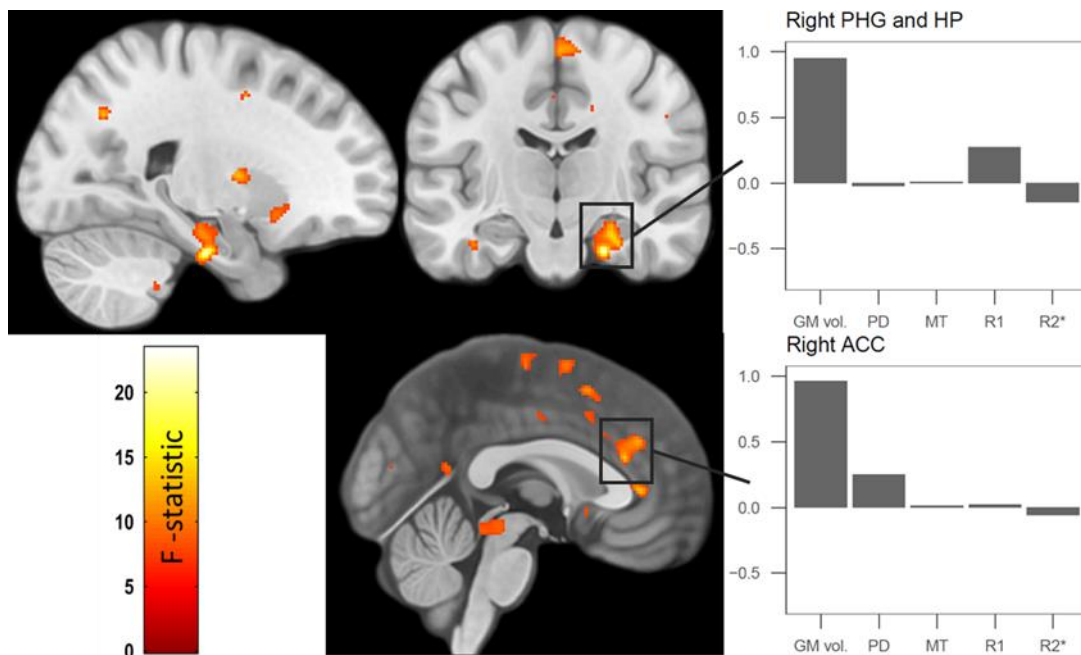


Figure 12: Statistical parametric map of multivariate analysis of the difference between t0 and t2. Displayed at $p < .001$ uncorrected. Grey bars represent the canonical vector of the data matrix Y (arbitrary unit). PHG = para-hippocampal gyrus, HP = hippocampus, ACC = anterior cingulate gyrus.

4.2.2.1.3. Long-term effect of ECT.

The result of the analysis for t0 to t3 showed a significant cluster in the left entorhinal cortex, inferior temporal gyrus and temporal pole ($p_{FWE} < .05$ at the cluster and peak levels). Like for t0 to t2 results, the main contribution to the result was found to be GM volume in the two clusters (see Figure 13 and Appendix 2).

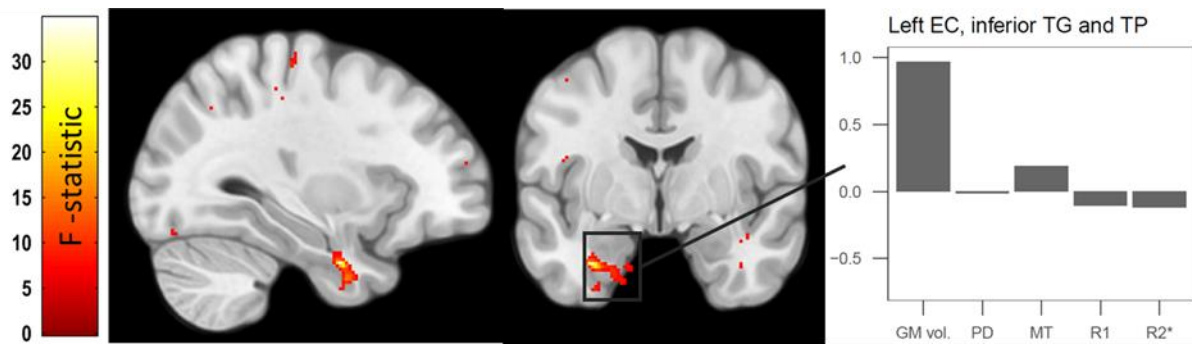


Figure 13: Statistical parametric map of multivariate analysis of the difference between t_0 and t_3 . Displayed at $p < .001$ uncorrected (unc.). Grey bars represent the canonical vector of the data matrix Y (arbitrary unit). EC = entorhinal cortex, TG = temporal gyrus, TP = temporal pole.

4.2.2.1.4. Late effect of ECT.

We found no significant effect for t_2 to t_3 .

4.2.2.2. Association with change of depression severity

Our exploratory contrast investigating any association between t_0 and t_1 , t_0 and t_2 and t_0 and t_3 revealed a widespread pattern of association with clusters significant at the peak and cluster level in the left precuneus, the hippocampal complex / amygdala, the medial PFC and the left ventral striatum (Figure 14, Appendix 4). The effect in the two first clusters were mainly driven by change in GM volume, in contrast, the effect in the two latter clusters were mainly driven by change in quantitative maps.

When investigating the association of MRI maps and change of depression severity in each time interval separately, we found that the pattern revealed in the exploratory contrast was entirely driven by the long-term association (between t_0 and t_3 , all clusters significant at the cluster level FWE) (Figure15, Appendix 5). The pattern was very similar but the effect was

bilateral in the hippocampal complex/amygdala and in the ventral striatum while it was unilateral in the exploratory contrast.

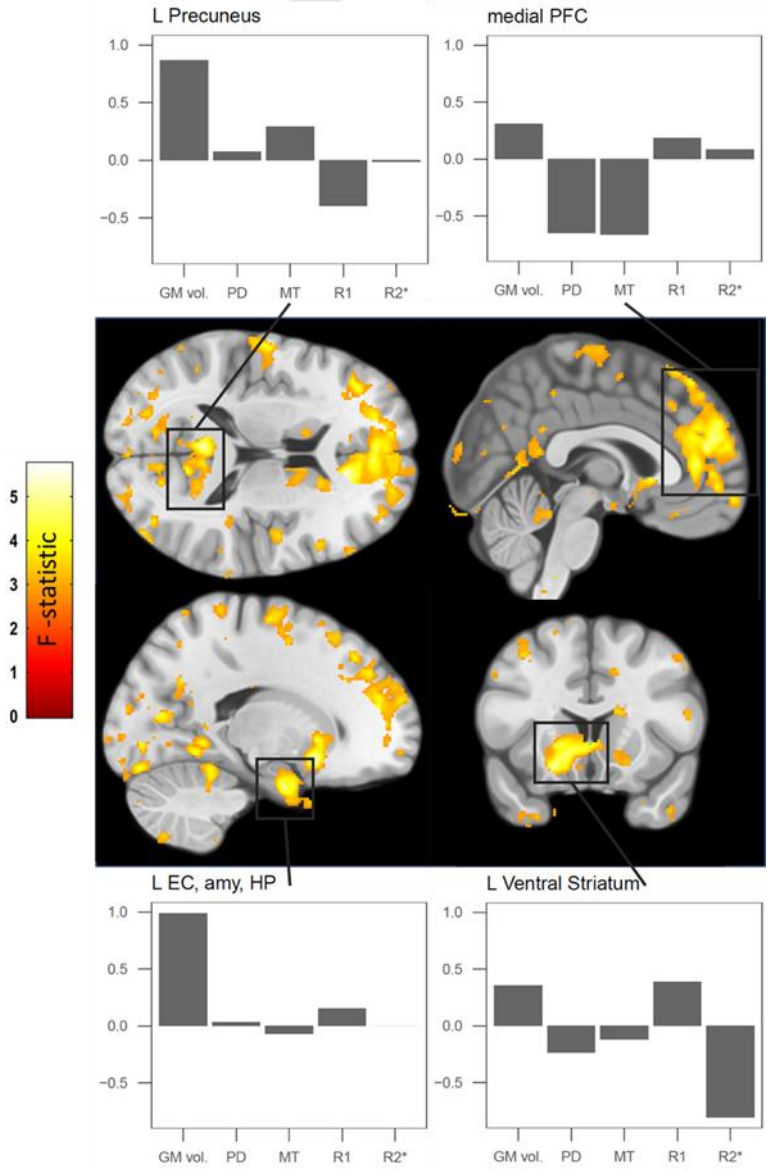


Figure 14: Statistical parametric map of multivariate association with change of depression severity between t_0 and t_1 , t_0 and t_2 and t_0 and t_3 . Displayed at $p < .001$ uncorrected (unc.). Grey bars represent the canonical vector of the data matrix Y (arbitrary unit). PFC = prefrontal cortex, EC = entorhinal cortex, amy = amygdala.

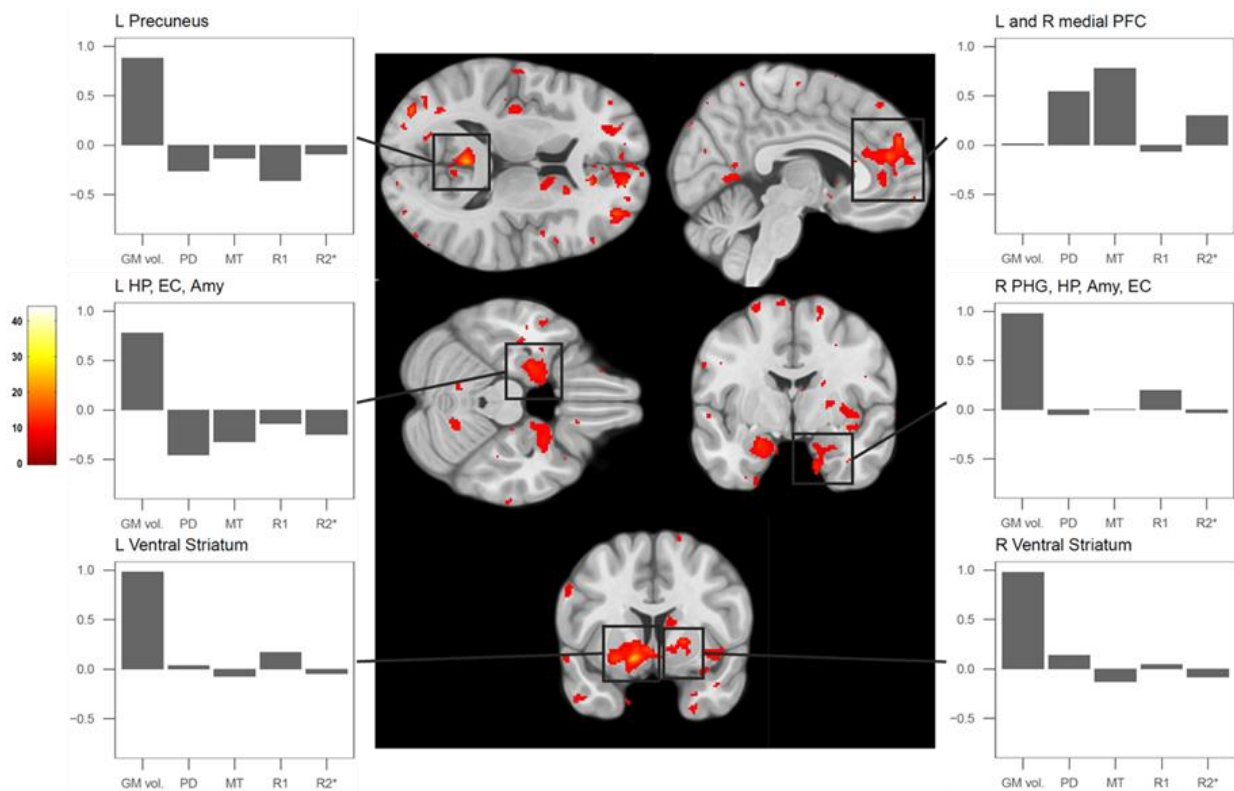


Figure 15: Statistical parametric map of multivariate association with change of depression severity between t_0 and t_3 . Displayed at $p < .001$ uncorrected (unc.). Grey bars represent the canonical vector of the data matrix Y (arbitrary unit). PFC = prefrontal cortex, EC = entorhinal cortex, amy = amygdala, HP = hippocampus, PHG = para-hippocampal gyrus.

4.3. Summary study 2

This study is the first one to investigate the effect of ECT using quantitative MRI measurements of water, myelin and iron content in addition to classical morphometric features. We found volumetric increase in the right hippocampus and anterior cingulate cortex following an ECT series with very little change in microstructural properties of brain tissue. At 6 months follow-up, we observed a volume increase in a small cluster in the left entorhinal again driven by change of GM volume. We also found that a widespread pattern of regions including the precuneus, the hippocampus, the amygdala, the medial prefrontal cortex and the ventral

striatum were related to the clinical outcome. Most of these associations were driven by GM volume, except in the medial prefrontal cortex where we found that the association involved water and myelin content rather than GM volume. This latter point put forward the advantage of qMRI over classical morphometry. Indeed, the latter technique would have been blind to this association between clinical outcome and the medial PFC.

5. Discussion

5.1. Study 1

The first study of my PhD project brings empirical evidence for a spatial gradient of ECT-induced brain anatomy changes along the longitudinal hippocampal axis. We first demonstrate that ECT increases the volume of the anterior “limbic” hippocampus. Then we link its volume at baseline and the increased rate of grey matter change during ECT treatment course to individuals’ clinical improvement. The fact that besides healthy individuals we also study an “active” control group of pharmacologically treated depressed patients reinforces our interpretation that the observed anatomical changes can be ascribed to the specific effect of ECT rather than the mere improvement of depressive symptoms.

5.1.1. ECT effect on the anterior hippocampus

The main finding of our study is that ECT-induced brain anatomy changes follow a spatial gradient along the hippocampal longitudinal axis. To support this claim, we extended the classical inference from analysis of hippocampal ROIs to data-driven topographical estimation of ECT effects along the main spatial axes whilst taking care of autocorrelation bias (Beale, Lennon, Yearsley, Brewer, & Elston, 2010). Our results go beyond previous observations of shape changes in the anterior hippocampus (Joshi et al., 2016) by adopting an iterative approach starting with whole-brain analysis that localised ECT effects to the right mesial temporal lobe followed by explicit test in a restricted search volume for differential spatial effects along the hippocampal main axes. The convergence of findings using on one hand surface-based shape analysis (Joshi et al., 2016) and on the other hand voxel-based

morphometry, makes a strong case about the regional specificity of ECT's impact on brain's anatomy.

There are several lines of neuro-biological interpretation of the observed results that converge towards the pivotal role of hippocampus in adult neurogenesis and in controlling stress responses via inhibition of the hypothalamic-pituitary-adrenal axis (HPA) (Anacker et al., 2018; Herman, Dolgas, & Carlson, 1998; Herman, Cullinan, Morano, Akil, & Watson, 1995). Stress resilience is associated with efficient neurogenesis in the ventral DG (Anacker et al., 2018) whilst depression is characterised by stress dysregulation and hippocampal atrophy (Otte, C., Gold, S. M., Penninx, B. W., Pariante, C. M., Etkin, A., Fava, M., ... & Schatzberg, 2016). ECT is thought to normalize the hyperactivity of the stress axis via seizure-induced increase in hippocampal neurogenesis and concomitant decrease of stress hormones (Burgese & Bassitt, 2015; Kunugi et al., 2006; Yuuki et al., 2005). The central role of hippocampus and particularly the differential structural and functional connectivity of its anterior and posterior portions support the involvement of the anterior hippocampus in regulation of emotion and motivation (Adnan et al., 2016; Blessing, Beissner, Schumann, Brünner, & Bär, 2016; Chase et al., 2015; Fanselow & Dong, 2010; Lambert et al., 2012), whilst the posterior part is implicated in episodic memory (Adnan et al., 2016; Blessing et al., 2016; Fanselow & Dong, 2010; Lambert et al., 2012; Wagner et al., 2016).

5.1.2. Association with clinical outcome

The correlation between clinical outcome and baseline volume estimates in anterior but not posterior hippocampus lends further support to the importance of the “limbic” sub-region for the therapeutic effects of ECT. The observation that a bigger hippocampal volume at baseline, associated with stronger symptoms reduction, corroborates the findings of a recent study

focusing on hippocampal DG (Nuninga et al., 2019), is however at odds with a previous investigation that reported the opposite pattern (Joshi et al., 2016). The apparent contradiction may stem from a number of methodological and analytical differences, the most important in our view being the reduction of a spatially dependent pattern to an average across the whole hippocampus. The correlation between clinical outcome and the dynamics of GMV rate of change confined to the anterior hippocampus lends further support to the notion of a spatial gradient of ECT effects along the hippocampal longitudinal axis. Here, the supposition of inverse relationship between the increased rate of volume change and clinical improvement contradicts the studies mentioned above (Joshi et al., 2016; Nuninga et al., 2019), but finds confirmation in recent meta- and mega-analyses (Gbyl & Videbech, 2018; Takamiya et al., 2018) that point towards an additional modulatory effect of ECT treatment duration.

5.1.3. Limitations and strength of the study

Despite the novelty of our findings on ECT effects along the longitudinal hippocampal axis, we draw attention to some limitations of our study – mainly the small sample size of the ECT group and the simplification of the hippocampal anatomical axis as a linear spatial construct. We also acknowledge the existence of more sophisticated methods for defining the main hippocampus axis (Vogel et al., 2019), however considering the shape of the hippocampus we feel confident that the linear approximation of the main longitudinal axis derived from the PCA of voxel coordinates is accurate enough to capture the actual anteroposterior axis of the hippocampus. Compared to previous reports, our approach improves the signal-to-noise ratio of the available data by averaging two MRI acquisitions per subject at each time point. The inclusion of an “active” control group of patients is an additional strong point that helps

attributing the observed effects to the ECT treatment rather than to brain anatomical changes due to symptoms improvement.

5.1.4. Conclusion study 1

In summary, we show unequivocal ECT effects on the rate of volume change in the mesial temporal lobe that follow a spatial gradient along the hippocampal longitudinal axis with strongest impact on the anterior "limbic" portion. We further highlight the importance of the notion of this spatial gradient given the correlations of the anterior hippocampus with clinical outcome. Our findings highlight the role of the anterior hippocampus for unfolding the therapeutic effects of ECT and therefore we argue that future research in this domain should consider the spatial heterogeneity not only of the hippocampus transversal axis with cytoarchitecturally well-defined borders, but also a gradient along its longitudinal axis.

5.2. Study 2

The second study of my PhD project focuses on the effect of ECT on brain structure using quantitative MRI measurements sensitive to free tissue water, myelin and iron content. I developed our own statistical methodology based on the multivariate GLM framework to appropriately model our multi-parameters and longitudinal data. After the ECT series, I observed multivariate change in regions classically reported in previous studies - the hippocampus and the anterior cingulate cortex - primarily due to change of GM volume. I also observed that a widespread pattern of brain regions encompassing the medial PFC, the anterior hippocampal complex, the ventral striatum and the precuneus were associated with the long-term clinical outcome. Interestingly, while the associations were mostly driven by GM volume in most of the regions, specifically in the medial PFC we found a strong

contribution of PD, MT and R2* indicating that microstructural reorganization rather than mere volume change was important to the recovery from depression in this cerebral region.

5.2.1. Effect of an ECT series: “true” volume change in limbic and cognitive control areas

Along ECT treatment we observed changes in the right anterior hippocampus and in the right ACC. These changes were mainly related to GM volume. Both results are confirming recent meta-analyses reviewing change of GM volume in the hippocampus (Gbyl & Videbech, 2018; Takamiya et al., 2018; Wilkinson, Sanacora, & Bloch, 2017) and many other studies that reported increase of GM volume in the anterior cingulate cortex (M. Cano et al., 2017; Marta Cano et al., 2019; Dukart et al., 2014; Gbyl & Videbech, 2018; Ota et al., 2015; Pirnia et al., 2016). With regards to the location of the effect, we found two clusters encompassing two regions involved in the processing of emotions (anterior hippocampus) on one side, and in the regulation of emotion (anterior cingulate) on the other side. According to the cognitive model of depression, the cardinal manifestations of depression are caused by a dysfunctional processing of emotion and by a reduced ability to regulate emotions (Disner et al., 2011). These specific manifestations are thought to be caused by dysfunction in the medial prefrontal network and in the limbic system (Price & Drevets, 2009). Our study provide evidence that ECT has neuro-plastic effects in crucial regions of the networks that are dysfunctional in depression.

5.2.1.1. Absence of change of water content in the hippocampus

Crucially, we do not observe change of tissue water content in the hippocampus. It has been consistently reported that, in severe form of medial temporal lobe epilepsy, an oedema as well as a parallel volume increase in the hippocampus are present shortly after a seizure (Kim

et al., 2001; R. C. Scott et al., 2002; Sokol, Demyer, Edwards-Brown, Sanders, & Garg, 2003) and that it is associated with the occurrence of long-term medial temporal lobe sclerosis (Sokol et al., 2003). Typically, ECT treatment is administered 2-3 times per week during a period of approximately 2 months. Thus, it is reasonable to assume that ECT treatment resemble epilepsy and leads alike to the same neuropathological effects, namely acute brain oedema and long-term sclerosis. Although one study reported an increase of mean diffusivity after a series of ECT (Repple et al., 2019), a measure that has been linked to the presence of an oedema, most of the recent studies using MRI measurements sensitive to water content showed a reduction of mean diffusivity in white matter tracts and in the hippocampus (Jorgensen et al., 2016; Kubicki et al., 2019; Lyden et al., 2014). These findings are not compatible with the hypothesis of an oedema. Our study, which is the first one to use Proton Density, an MRI measurement highly specific to water concentration, confirms previous finding and indicates that it is very unlikely that the process observed in epilepsy is at stake in patients undergoing ECT. In a very speculative way, we can postulate that the difference between the effect of epilepsy and ECT on the brain are due to the fact that the seizure triggered by ECT is occurring in a very controlled setting including muscle relaxation agent, monitoring of brain activity and discontinuation of the seizure if it lasted too long. In addition, the pathological process presents in epilepsy and leading to spontaneous seizure is absent in ECT patients.

5.2.2. Long-term effect of ECT

The long-term effect of ECT was manifest in a small cluster in the left entorhinal cortex, with, again, a predominant contribution of GM volume and no contribution of PD. The entorhinal cortex is the main interface between the hippocampus and the neocortex (Witter, Doan,

Jacobsen, Nilssen, & Ohara, 2017). In a recent study, Bai and colleagues (Bai et al., 2019) found that functional connectivity in the anterior hippocampus was increased after an ECT series. This was a replication of another study reporting the same observation (Abbott et al., 2014). Moreover, two other studies of the connectivity of the limbic system along the course of an ECT treatment, using structural covariance as a measure of connectivity, found that the connection of the limbic system increased after an ECT series (Wolf et al., 2016; Zeng et al., 2015). Therefore, the observed change in the entorhinal cortex might be the structural correlate of a restoration of the connectivity between the hippocampus and the cortex.

5.2.3. Association with clinical outcome

We found association between change of depressive symptoms and a widespread set of brain regions including hippocampus, amygdala, ventral striatum, medial PFC and precuneus in both hemispheres. Correlation between increase of hippocampal and amygdala volume have been already reported in several studies (M. Cano et al., 2017; Oltedal et al., 2018; Ota et al., 2015; Xu, Zhao, Luo, & Zheng, 2019). Changes of microstructural properties in these region have also been linked to clinical outcome (Kubicki et al., 2019; Yroni et al., 2019). Moreover, change of connectivity of the medial temporal lobe has been linked to reduction of depression severity in several studies using functional or structural connectivity (Abbott et al., 2014; Wolf et al., 2016; Zeng et al., 2015). In addition to limbic regions in the medial temporal lobe, the ventral striatum was also found to be linked to the clinical outcome in our study. It is in line with the report showing that an increase of volume in the ventral striatum was observed in ECT-responders (Wade et al., 2016).

We also found a complex pattern of association between change in quantitative measurement of tissue microstructural properties in the medial PFC. It has already been reported that

increase of cortical thickness in the orbitofrontal cortex after ECT was correlated with clinical improvement (Gbyl et al., 2019). Although our results point clearly towards the medial prefrontal cortex, structurally located dorsally to the orbitofrontal cortex, these data taken altogether seem to indicate that not only limbic regions are involved in the recovery of depression following ECT but that a reorganization in the ventrolateral and medial part of the PFC takes place too. The last region that was associated with clinical improvement in our study was the precuneus. This region was, to our knowledge, never reported in structural ECT studies, contrary to what is frequently reported in functional imaging ECT studies. Leaver and colleagues (2015), investigating changes of resting state following ECT with functional neuroimaging, found that the connectivity of this region was significantly affected after a series of ECT. Additionally, a recent study using perfusion MRI reported that cerebral blood flow was reduced in the precuneus after completing an ECT treatment (Leaver et al., 2019). Furthermore, a recent meta-analysis of regional brain functions following treatments of depression reported that a significant decrease of activity in central nodes of the default mode network, among which the precuneus belongs, was found after a treatment of ECT (Chau, Fogelman, Nordanskog, Drevets, & Hamilton, 2017).

As stated above, according to the cognitive model of depression, depression is caused by dysfunction in the limbic network, involved in the processing of emotion, and in the medial prefrontal cognitive control network, involved in the regulation of emotions. More specifically, dysfunctional processing of emotion is manifest in a higher reactivity to negative emotions (Gotlib & Krasnoperova, 2004) and a lower reactivity to positive emotion and reward (Heller et al., 2009). This is sometimes called a “negativity bias”. The neural correlate of the negativity bias is an increased reactivity of the amygdala to negative stimuli (Fales et al., 2008) and decreased responsiveness of the ventral striatum to positive stimuli (Heller et al., 2009;

Keedwell, Andrew, Williams, Brammer, & Phillips, 2005). The findings of association between change of depression severity and change in the bilateral amygdala and ventral striatum could indicate that the restoration of an equilibrium between the processing of negative and positive emotions is important to the recovery of depression following an ECT treatment. Not only depressed individuals are biased in emotion processing leading to an increased distressing negative emotional experience, they also poorly regulate emotion which, in interaction with the negativity bias, potentiates the distressing effect of negative affect. The fact that we found an effect of ECT in the anterior cingulate and an association with the change of depression severity in the medial PFC may indicate that this treatment is restoring the function of the brain regions involved in the control of emotion.

Based on the temporality of our findings it is difficult to distinguish what comes first: normalization of activity in the limbic network or restoration of the regulatory ability of medial prefrontal regions. Studying the course of neuro-plastic changes during the ECT treatment with a finer temporal resolution should help to better understand the sequence of events leading to therapeutic benefits, and thus, define what brain regions should be primarily targeted to alleviate depressive symptoms. Additionally, to findings in the limbic and cognitive control networks, we found that changes in the precuneus were associated with the alleviation of depression. A central manifestation observed in depression is the tendency to rumination, a maladaptive self-reflective pattern of recurrent thought about one's negative affect and its consequence. The default mode network is engaged during such process of self-reflection and its activity has been found to be increased in individuals with depression and decreased by electroconvulsive treatment (Chau et al., 2017). The precuneus is a central hub of the default mode network (Utevsky, Smith, & Huettel, 2014), thus, structural plasticity associated with symptoms improvement in this region may be part of the process of

normalization of the activity in the default mode network and therefore of the reduction of ruminations.

5.2.4. Limitations and strengths of the study

Although our results fit well with the reported neural correlate of the cognitive model of depression, our study suffers of a few, but serious, limitations, the most important being the small size of our sample of nine subjects. However, we can emphasize that the loss of statistical power due to small sample size may be compensated, in small ECT studies, by the large size effect of ECT on brain structure as reported for example by Bouckaert et al. (2016) and by Ousdal et al. (2019). Moreover, the cerebral locations of our findings are in line with previous studies giving us confidence that we were able to uncover, at least, some of the effects of ECT on the disease. Another limitation relates to the interpretation of our results by using the multivariate GLM approach. In this study, we only reported the canonical vector at the peak voxel of the clusters which may not be representative of the overall pattern in the cluster. Methodologies should be developed to summarize and assess the homogeneity or heterogeneity of the profile of the canonical vectors belonging to a cluster. In addition, the interpretation of the results is also limited by the lack of directionality given by the F-test. Application of post-hoc tests, that would enhance the interpretability of the data, should be investigated.

Another study limitation we would like to address pertains to the issue of multiple comparisons correction. Mass univariate whole-brain neuroimaging analyses involve model estimation at each voxel, typically resulting in the estimation of thousands of separate GLM. This results in a large volume of statistical values. To avoid a tremendous inflation of the type I error rate, multiple comparison correction has to be performed. However, classical solution

such as Bonferroni correction are not appropriate due to the high spatial correlation inherently present in neuroimaging data as well as due to the spatial correlation induced by the smoothing procedure implemented in the pre-processing. This problem has been addressed by using the random field theory (Brett, Penny, & Kiebel, 2003). Random field theory allows the estimation of the characteristics of a smoothed statistical map under the null hypothesis. However, this estimation requires a quantitative estimate of the smoothness of the data (Kiebel, Poline, Friston, Holmes, & Worsley, 1999). This estimation is performed on the standardized residuals of the fitted GLMs. Therefore, this estimation becomes non-trivial in the multivariate GLM as the residuals are multivariate. This aspect should be investigated in more details in the future.

Nonetheless, our study had also several methodological significant strengths. This is the first study to use quantitative MRI to examine structural effect of ECT. Classical morphometry does not allow straightforward interpretation of GM volume changes because multiple factors other than pure GM volume change are involved in the contrast. We demonstrate the usefulness of this approach by showing that increase of water content is not involved in GM volume changes due to ECT. Moreover, we believe that the multi-contrast approach and the use of multivariate method increase the sensitivity to detect wide structural effects. This is shown in the analysis testing the association with the clinical outcome that reveal a wider range of brain area than what was observed in other studies. Moreover, we found an association between clinical outcome and the medial prefrontal cortex that was entirely due to water and myelin content. Therefore, classical morphometry would be blind to such effect. Finally, the multivariate approach as compared to the classical multiple univariate models' approach reduces the probability of committing a type I error because only one model is estimated and the change in all the maps are jointly tested within a single contrast.

5.2.5. Conclusion study 2

In conclusion, we presented here the first study using quantitative MRI and multivariate statistics with the goal to understand the neuro-plastic effect of ECT on the brain. We provide strong evidence against the hypothesis that an oedema is the cause of increase of GM volume in the hippocampus. We also reported that a wide range of regions involved in emotional processing, cognitive control and self-referential processes are modulated by ECT and associated with clinical outcome.

6. General conclusion

The two studies of my PhD project focus on understanding the effect of electroconvulsive therapy on brain structure. In the first one I sought to test the hypothesis that the effect of electroconvulsive therapy on grey matter volume in the hippocampus was predominant on the anterior as compared to the posterior part of this structure. To this purpose, I developed my own methodology using spatial dimensionality reduction to approximate the longitudinal axis of the hippocampus and generalized least squares linear coefficient estimation to fit a regression model with highly spatially autocorrelated data. I found that the effect of ECT on GM becomes stronger when moving towards the anterior part of the hippocampus. Baseline GMV in the anterior part of the hippocampus was predictive of symptoms improvement while the posterior part was not. Furthermore, the change of GMV in the anterior hippocampus on the side of the stimulation was related to symptoms improvement while nor the contralateral anterior hippocampus and nor the posterior parts of the hippocampus were related to symptoms improvement. These three findings converge to indicate that ECT is preferentially modulating the anterior part of the hippocampus and that the very same part of the hippocampus is involved in mediating the therapeutic effect of ECT.

The second study of my project was aimed to go beyond volumetric analysis of the effect of ECT using T1-weighted imaging, which has limited interpretation, and assess how microstructural properties of the brain tissue is affected by ECT. To this aim, I acquired quantitative MRI measurements specific to water, myelin and iron concentration of the brain tissue. I also developed a multivariate statistical approach to model multi-contrast and longitudinal data appropriately. I found that ECT induces volume changes in the hippocampus and in the anterior cingulate without significant contributions of microstructure property

changes. I did not find change of tissue free water content in the hippocampus which indicates that GM volume increase in the hippocampus is not related to an oedema, thus contradicting assumptions based on clinical observations in patients with status epilepticus.

I also report that the long-term effect of ECT is manifest in the entorhinal cortex and this result may be linked to other studies reporting an increase of connectivity between the hippocampus and the rest of the brain. In addition, we found that a vast set of regions involved in emotion processing, in cognitive control and in self-referential processes were associated with the clinical outcome. Therefore, we speculate that although the ECT has focal effect on the brain the clinical outcome is associated with a widespread cortical and subcortical reorganization.

7. References

- Abbott, C. C., Jones, T., Lemke, N. T., Gallegos, P., McClintock, S. M., Mayer, A. R., ... Calhoun, V. D. (2014). Hippocampal structural and functional changes associated with electroconvulsive therapy response. *Translational Psychiatry*, 4(11), e483.
- Adnan, A., Barnett, A., Moayed, M., McCormick, C., Cohn, M., & McAndrews, M. P. (2016). Distinct hippocampal functional networks revealed by tractography-based parcellation. *Brain Structure and Function*, 221(6), 2999–3012.
- Akber, S. F. (1996). NMR relaxation data of water proton in normal tissues. *Physiological Chemistry and Physics and Medical NMR*, 28, 205–238.
- American Psychiatric Association. (2000). *Diagnostic and Statistical Manual of Mental Disorders: {DSM-IV-TR}* (4th ed., t). Washington, DC: Autor.
- American Psychiatric Association. (2013). *Diagnostic and statistical manual of mental disorders: {DSM-5}* (5th ed.). Washington, DC: Autor.
- Anacker, C., Luna, V. M., Stevens, G. S., Millette, A., Shores, R., Jimenez, J. C., ... Hen, R. (2018). Hippocampal neurogenesis confers stress resilience by inhibiting the ventral dentate gyrus. *Nature*, 1.
- Armstrong, C. (2011). APA releases guideline on treatment of patients with major depressive disorder. *American Family Physician*, 83(10), 1224–1226.
- Aruta, A. (2011). Shocking Waves at the Museum: The Bini--Cerletti Electro-shock Apparatus. *Medical History*, 55(3), 407–412.
- Ashburner, J. (2007). A fast diffeomorphic image registration algorithm. *NeuroImage*, 38(1), 95–113.
- Ashburner, J., & Friston, K. J. (2005). Unified segmentation. *NeuroImage*, 26(3), 839–851.
- Ashburner, J., & Ridgway, G. R. (2013). Symmetric diffeomorphic modeling of longitudinal structural MRI. *Frontiers in Neuroscience*, 6, 197.
- Bai, T., Wei, Q., Xie, W., Wang, A., Wang, J., Ji, G. J., ... Tian, Y. (2019). Hippocampal-subregion functional alterations associated with antidepressant effects and cognitive impairments of electroconvulsive therapy. *Psychological Medicine*, 49(8), 1357–1364.
- Barbier, J. M., Serra, G., Loas, G., & Breathnach, C. S. (1999). Constance Pascal: pioneer of French psychiatry. *History of Psychiatry*, 10(40), 425–437.
- Beale, C. M., Lennon, J. J., Yearsley, J. M., Brewer, M. J., & Elston, D. A. (2010). Regression analysis of spatial data. *Ecology Letters*, 13(2), 246–264.
- Beck, A. T. (1979). *Cognitive therapy of depression*. Guilford press.
- Beck, A. T. (2008). The Evolution of the Cognitive Model of Depression and Its Neurobiological Correlates. *Am J Psychiatry*, 1658.

- Beck, A. T., & Bredemeier, K. (2016). A unified model of depression: Integrating clinical, cognitive, biological, and evolutionary perspectives. *Clinical Psychological Science*, 4(4), 596–619.
- Beevers, C. G., Clasen, P., Stice, E., & Schnyer, D. (2010). Depression symptoms and cognitive control of emotion cues: A functional magnetic resonance imaging study. *Neuroscience*, 167(1), 97–103.
- Blessing, E. M., Beissner, F., Schumann, A., Br nner, F., & B r, K. J. (2016). A data-driven approach to mapping cortical and subcortical intrinsic functional connectivity along the longitudinal hippocampal axis. *Human Brain Mapping*, 37(2), 462–476.
- Boldrini, M., Fulmore, C. A., Tartt, A. N., Simeon, L. R., Pavlova, I., Poposka, V., ... Mann, J. J. (2018). Human Hippocampal Neurogenesis Persists throughout Aging. *Cell Stem Cell*, 589–599.
- Boldrini, M., Galfalvy, H., Dwork, A. J., Rosoklija, G. B., Trencevska-Ivanovska, I., Pavlovski, G., ... Mann, J. J. (2019a). Resilience is associated with larger dentate gyrus, while suicide decedents with major depressive disorder have fewer granule neurons. *Biological Psychiatry*, 85(10), 850–862.
- Boldrini, M., Galfalvy, H., Dwork, A. J., Rosoklija, G. B., Trencevska-Ivanovska, I., Pavlovski, G., ... Mann, J. J. (2019b). Resilience Is Associated with Larger Dentate Gyrus while Suicide Decedents with Major Depressive Disorder have Fewer Granule Neurons. In *Biological Psychiatry*. Society of Biological Psychiatry.
- Boldrini, M., Hen, R., Underwood, M. D., Rosoklija, G. B., Dwork, A. J., Mann, J. J., & Arango, V. (2012). Hippocampal angiogenesis and progenitor cell proliferation are increased with antidepressant use in major depression. *Biological Psychiatry*, 72(7), 562–571.
- Boldrini, M., Santiago, A. N., Hen, R., Dwork, A. J., Rosoklija, G. B., Tamir, H., ... Mann, J. J. (2013). Hippocampal granule neuron number and dentate gyrus volume in antidepressant-treated and untreated major depression. *Neuropsychopharmacology*, 38(6), 1068–1077.
- Boldrini, M., Underwood, M. D., Hen, R., Rosoklija, G. B., Dwork, A. J., John Mann, J., & Arango, V. (2009). Antidepressants increase neural progenitor cells in the human hippocampus. *Neuropsychopharmacology*, 34(11), 2376–2389.
- Bouckaert, F., De Winter, F.-L., Emsell, L., Dols, A., Rhebergen, D., Wampers, M., ... Vandenbulcke, M. (2016). Grey matter volume increase following electroconvulsive therapy in patients with late life depression: a longitudinal MRI study. *Journal of Psychiatry & Neuroscience : JPN*, 41(2), 105–114.
- Brett, M., Penny, W., & Kiebel, S. (2003). Introduction to random field theory. *Human Brain Function*, 2.
- Bromet, E., Andrade, L., Hwang, I., Sampson, N. A., Alonso, J., de Girolamo, G., ... Cho, M. (2011). Cross-national epidemiology of DSM-IV major depressive episode. *BMC Medicine*, 9(1), 90.
- Brosch, T., Scherer, K. R., Grandjean, D., & Sander, D. (2013). *The impact of emotion on perception, attention, memory, and decision-making*. (May), 1–10.

- Brun, V. H., Solstad, T., Kjelstrup, K. B., Fyhn, M., Witter, M. P., Moser, E. I., & Moser, M. B. (2008). Progressive increase in grid scale from dorsal to ventral medial entorhinal cortex. *Hippocampus*, *18*(12), 1200–1212.
- Burgese, D. F., & Bassitt, D. P. (2015). Variation of plasma cortisol levels in patients with depression after treatment with bilateral electroconvulsive therapy. *Trends in Psychiatry and Psychotherapy*, *37*(1), 27–36.
- Bush, G., Luu, P., & Posner, M. I. (2000). Cognitive and emotional influences in anterior cingulate cortex. *Trends in Cognitive Sciences*, *4*(6), 215–222.
- Cano, M., Martínez-Zalacaín, I., Bernabéu-Sanz, Contreras-Rodríguez, O., Hernández-Ribas, R., Via, E., ... Soriano-Mas, C. (2017). Brain volumetric and metabolic correlates of electroconvulsive therapy for treatment-resistant depression: A longitudinal neuroimaging study. *Translational Psychiatry*, *7*(2), e1023-8.
- Cano, Marta, Lee, E., Cardoner, N., Martínez-Zalacaín, I., Pujol, J., Makris, N., ... Camprodon, J. A. (2019). Brain volumetric correlates of right unilateral versus bitemporal electroconvulsive therapy for treatment-resistant depression. *Journal of Neuropsychiatry and Clinical Neurosciences*, *31*(2), 152–158.
- Cao, B., Luo, Q., Fu, Y., Du, L., Qiu, T., Yang, X., ... Qiu, H. (2018). Predicting individual responses to the electroconvulsive therapy with hippocampal subfield volumes in major depression disorder. *Scientific Reports*, *8*(1), 1–8.
- Chase, H. W., Clos, M., Dibble, S., Fox, P., Grace, A. A., Phillips, M. L., & Eickhoff, S. B. (2015). Evidence for an anterior-posterior differentiation in the human hippocampal formation revealed by meta-analytic parcellation of fMRI coordinate maps: Focus on the subiculum. *NeuroImage*, *113*, 44–60.
- Chau, D. T., Fogelman, P., Nordanskog, P., Drevets, W. C., & Hamilton, J. P. (2017). Distinct neural-functional effects of treatments with selective serotonin reuptake inhibitors, electroconvulsive therapy, and transcranial magnetic stimulation and their relations to regional brain function in major depression: a meta-analysis. *Biological Psychiatry: Cognitive Neuroscience and Neuroimaging*, *2*(4), 318–326.
- Chen, A. C., & Etkin, A. (2013). Hippocampal network connectivity and activation differentiates post-traumatic stress disorder from generalized anxiety disorder. *Neuropsychopharmacology*, *38*(10), 1889–1898.
- Conus, P., Despland, J. N., Herrera, F., Chanachev, A., Eap, C. B., Mall, J. F., ... others. (2013). Psychiatry. *Revue Médicale Suisse*, *9*(368), 76–79.
- Conway, C. R., George, M. S., & Sackeim, H. A. (2017). Toward an evidence-based, operational definition of treatment-resistant depression: When Enough is enough. *JAMA Psychiatry*, *74*(1), 9–10.
- Costafreda, S. G., Brammer, M. J., David, A. S., & Fu, C. H. Y. (2008). Predictors of amygdala activation during the processing of emotional stimuli: A meta-analysis of 385 PET and fMRI studies. *Brain Research Reviews*, *58*(1), 57–70.

- Cuijpers, P., Vogelzangs, N., Twisk, J., Kleiboer, A., Li, J., & Penninx, B. W. (2014). Comprehensive meta-analysis of excess mortality in depression in the general community versus patients with specific illnesses. *American Journal of Psychiatry*, *171*(4), 453–462.
- Dalton, M. A., McCormick, C., & Maguire, E. A. (2018). Differences in functional connectivity along the anterior-posterior axis of human hippocampal subfields. *NeuroImage*, *192*(February), 410720.
- Davidson, R. J. (2000). Affective style, psychopathology, and resilience: brain mechanisms and plasticity. *American Psychologist*, *55*(11), 1196.
- Del Arco, A., & Mora, F. (2008). Prefrontal cortex--nucleus accumbens interaction: in vivo modulation by dopamine and glutamate in the prefrontal cortex. *Pharmacology Biochemistry and Behavior*, *90*(2), 226–235.
- Disner, S. G., Beevers, C. G., Haigh, E. A. P., & Beck, A. T. (2011). Neural mechanisms of the cognitive model of depression. *Nature Reviews Neuroscience*, *12*(8), 467–477.
- Draganski, B., Ashburner, J., Hutton, C., Kherif, F., Frackowiak, R. S. J., Helms, G., & Weiskopf, N. (2011). Regional specificity of MRI contrast parameter changes in normal ageing revealed by voxel-based quantification (VBQ). *NeuroImage*, *55*(4), 1423–1434.
- Drevets, W. C. (2001). Neuroimaging and neuropathological studies of depression: Implications for the cognitive-emotional features of mood disorders. *Current Opinion in Neurobiology*, *11*(2), 240–249.
- Dukart, J., Regen, F., Kherif, F., Colla, M., Bajbouj, M., Heuser, I., ... Draganski, B. (2014). Electroconvulsive therapy-induced brain plasticity determines therapeutic outcome in mood disorders. *Proceedings of the National Academy of Sciences of the United States of America*, *111*(3), 1156–1161.
- Eaton, W. W., Anthony, J. C., Gallo, J., Cai, G., Tien, A., Romanoski, A., ... Chen, L. (2014). *Natural History of Diagnostic Interview Schedule/DSM-IV Major Depression*.
- Endler, N. S. (1988). The origins of electroconvulsive therapy (ECT). *Convulsive Therapy*.
- Epstein, J., Pan, H., Kocsis, J. H., Yang, Y., Butler, T., Chusid, J., ... Silbersweig, D. A. (2006). Lack of ventral striatal response to positive stimuli in depressed versus normal subjects. *American Journal of Psychiatry*, *163*(10), 1784–1790.
- Eriksson, P. S., Perfilieva, E., Björk-Eriksson, T., Alborn, a M., Nordborg, C., Peterson, D. a, & Gage, F. H. (1998). Neurogenesis in the adult human hippocampus. *Nature Medicine*, *4*(11), 1313–1317.
- Fabbri, C., Kasper, S., Kautzky, A., Bartova, L., Dold, M., Zohar, J., ... Serretti, A. (2018). Genome-wide association study of treatment-resistance in depression and meta-analysis of three independent samples. *The British Journal of Psychiatry*, 1–6.
- Fales, C. L., Barch, D. M., Rundle, M. M., Mintun, M. A., Snyder, A. Z., Cohen, J. D., ... Sheline, Y. I. (2008). Altered Emotional Interference Processing in Affective and Cognitive-Control Brain Circuitry in Major Depression. *Biological Psychiatry*, *63*(4), 377–384.

- Fanselow, M. S., & Dong, H. W. (2010). Are the Dorsal and Ventral Hippocampus Functionally Distinct Structures? *Neuron*, *65*(1), 7–19.
- Folkerts, H. W., Michael, N., Tölle, R., Schonauer, K., Mücke, S., & Schulze-Mönking, H. (1997). Electroconvulsive therapy vs. paroxetine in treatment-resistant depression - A randomized study. *Acta Psychiatrica Scandinavica*, *96*(5), 334–342.
- Fox, J. (2015). *Applied regression analysis and generalized linear models*. Sage Publications.
- Fox, J., Friendly, M., & Weisberg, S. (2013). Hypothesis tests for multivariate linear models using the car package. *R Journal*, *5*(1), 39–52.
- Gartlehner, G., Wagner, G., Matyas, N., Titscher, V., Greimel, J., Lux, L., ... Lohr, K. N. (2017). Pharmacological and non-pharmacological treatments for major depressive disorder: Review of systematic reviews. *BMJ Open*, *7*(6), 1–13.
- Gbyl, K., Rostrup, E., Raghava, J. M., Carlsen, J. F., Schmidt, L. S., Lindberg, U., ... Videbech, P. (2019). Cortical thickness following electroconvulsive therapy in patients with depression – a longitudinal MRI study . *Acta Psychiatrica Scandinavica*, 205–216.
- Gbyl, K., & Videbech, P. (2018). Electroconvulsive therapy increases brain volume in major depression: a systematic review and meta-analysis. *Acta Psychiatrica Scandinavica*, *138*(3), 180–195.
- Gotlib, I. H., & Krasnoperova, E. (2004). Attentional Biases for Negative Interpersonal Stimuli in Clinical Depression. *Journal of Abnormal Psychology*, *113*(1), 127–135.
- Gracien, R.-M., Maiworm, M., Brüche, N., Shrestha, M., Nöth, U., Hattingen, E., ... Deichmann, R. (2019). How stable is quantitative MRI? – Assessment of intra- and inter-scanner-model reproducibility using identical acquisition sequences and data analysis programs. *NeuroImage*, (November), 116364.
- Griswold, M. A., Jakob, P. M., Heidemann, R. M., Nittka, M., Jellus, V., Wang, J., ... Haase, A. (2002). Generalized autocalibrating partially parallel acquisitions (GRAPPA). *Magnetic Resonance in Medicine*, *47*(6), 1202–1210.
- Grözinger, M., Conca, A., Nickl-Jockschat, T., & Di Pauli, J. (2013). *Elektrokonvulsionstherapie kompakt*. Springer.
- Heller, A. S., Johnstone, T., Shackman, A. J., Light, S. N., Peterson, M. J., Kolden, G. G., ... Davidson, R. J. (2009). Reduced capacity to sustain positive emotion in major depression reflects diminished maintenance of fronto-striatal brain activation. *Proceedings of the National Academy of Sciences of the United States of America*, *106*(52), 22445–22450.
- Hellsten, J., West, M. J., Arvidsson, A., Ekstrand, J., Jansson, L., Wennström, M., & Tingström, A. (2005). Electroconvulsive seizures induce angiogenesis in adult rat hippocampus. *Biological Psychiatry*, *58*(11), 871–878.
- Helms, G., Dathe, H., & Dechent, P. (2008). Quantitative FLASH MRI at 3T using a rational approximation of the Ernst equation. *Magnetic Resonance in Medicine*, *59*(3), 667–672.

- Helms, G., Dathe, H., Kallenberg, K., & Dechent, P. (2008). High-resolution maps of magnetization transfer with inherent correction for RF inhomogeneity and T1 relaxation obtained from 3D FLASH MRI. *Magnetic Resonance in Medicine*, *60*(6), 1396–1407.
- Helms, G., & Dechent, P. (2009). Increased SNR and reduced distortions by averaging multiple gradient echo signals in 3D FLASH imaging of the human brain at 3T. *Journal of Magnetic Resonance Imaging*, *29*(1), 198–204.
- Helms, G., Draganski, B., Frackowiak, R., Ashburner, J., & Weiskopf, N. (2009). Improved segmentation of deep brain grey matter structures using magnetization transfer (MT) parameter maps. *NeuroImage*, *47*(1), 194–198.
- Herman, J P, Dolgas, C. M., & Carlson, S. L. (1998). Ventral subiculum regulates hypothalamo-pituitary--adrenocortical and behavioural responses to cognitive stressors. *Neuroscience*, *86*(2), 449–459.
- Herman, James P, Cullinan, W. E., Morano, M. I., Akil, H., & Watson, S. J. (1995). Contribution of the ventral subiculum to inhibitory regulation of the hypothalamo-pituitary-adrenocortical axis. *Journal of Neuroendocrinology*, *7*(6), 475–482.
- Herzallah, M. M., Moustafa, A. A., Natsheh, J. Y., Abdellatif, S. M., Taha, M. B., Tayem, Y. I., ... Gluck, M. A. (2013). Learning from negative feedback in patients with major depressive disorder is attenuated by SSRI antidepressants. *Frontiers in Integrative Neuroscience*, *7*(SEP), 1–9.
- Huys, Q. J., Pizzagalli, D. A., Bogdan, R., & Dayan, P. (2013). Mapping anhedonia onto reinforcement learning: a behavioural meta-analysis. *Biology of Mood & Anxiety Disorders*, *3*(1).
- Jain, M. K., & Singh, R. (2010). Relevance of Modified ECT in Managing Psychiatric Patients. *Delhi Psychiatry Journal*, *13*(247–253).
- Jansson, L., Wennström, M., Johanson, A., & Tingström, A. (2009). Glial cell activation in response to electroconvulsive seizures. *Progress in Neuro-Psychopharmacology and Biological Psychiatry*, *33*(7), 1119–1128.
- Jorgensen, A., Magnusson, P., Hanson, L. G., Kirkegaard, T., Benveniste, H., Lee, H., ... others. (2016). Regional brain volumes, diffusivity, and metabolite changes after electroconvulsive therapy for severe depression. *Acta Psychiatrica Scandinavica*, *133*(2), 154–164.
- Joshi, S. H., Espinoza, R. T., Pirnia, T., Shi, J., Wang, Y., Ayers, B., ... Narr, K. L. (2016). Structural plasticity of the hippocampus and amygdala induced by electroconvulsive therapy in major depression. *Biological Psychiatry*, *79*(4), 282–292.
- Keedwell, P. A., Andrew, C., Williams, S. C. R., Brammer, M. J., & Phillips, M. L. (2005). The neural correlates of anhedonia in major depressive disorder. *Biological Psychiatry*, *58*(11), 843–853.
- Kellner, C. H., Greenberg, R. M., Murrrough, J. W., Bryson, E. O., Briggs, M. C., & Pasculli, R. M. (2012). ECT in treatment-resistant depression. *American Journal of Psychiatry*, *169*(12), 1238–1244.

- Kellough, J. L., Beevers, C. G., Ellis, A. J., & Wells, T. T. (2008). Time course of selective attention in clinically depressed young adults: An eye tracking study. *Behaviour Research and Therapy*, *46*(11), 1238–1243.
- Kennedy, S. H., Milev, R., Giacobbe, P., Ramasubbu, R., Lam, R. W., Parikh, S. V., ... Ravindran, A. V. (2009). Canadian Network for Mood and Anxiety Treatments (CANMAT) Clinical guidelines for the management of major depressive disorder in adults.: IV. Neurostimulation therapies. *Journal of Affective Disorders*, *117*, S44–S53.
- Kessler, R. C., Berglund, P., Demler, O., Jin, R., Koretz, D., Merikangas, K. R., ... Wang, P. S. (2003). The Epidemiology of Major. *Jama*, *289*(23), 3095–3105.
- Kho, K. H., van Vreeswijk, M. F., Simpson, S., & Zwinderman, A. H. (2003). A Meta-Analysis of Electroconvulsive Therapy Efficacy in Depression. *The Journal of ECT*, *19*(3), 139–147.
- Kiebel, S. J., Poline, J. B., Friston, K. J., Holmes, A. P., & Worsley, K. J. (1999). Robust smoothness estimation in statistical parametric maps using standardized residuals from the general linear model. *NeuroImage*, *10*(6), 756–766.
- Kim, J. A., Chung, J., Pyeong Ho Yoon, Dong Ik Kim, Chung, T. S., Kim, E. J., & Jeong, E. K. (2001). Transient MR signal changes in patients with generalized tonicoclonic seizure or status epilepticus: Periictal diffusion-weighted imaging. *American Journal of Neuroradiology*, *22*(6), 1149–1160.
- Krishnamoorthy, E. S., & Trimble, M. R. (1999). *Forced Normalization : Clinical and Therapeutic Relevance*. 57–64.
- Kubicki, A., Leaver, A. M., Vasavada, M., Njau, S., Wade, B., Joshi, S. H., ... Narr, K. L. (2019). Variations in Hippocampal White Matter Diffusivity Differentiate Response to Electroconvulsive Therapy in Major Depression. *Biological Psychiatry: Cognitive Neuroscience and Neuroimaging*, *4*(3), 300–309.
- Kunigiri, G., Jayakumar, P. N., Janakiramaiah, N., & Gangadhar, B. N. (2007). MRI T2 relaxometry of brain regions and cognitive dysfunction following electroconvulsive therapy. *Indian Journal of Psychiatry*, *49*(3), 195.
- Kunugi, H., Ida, I., Ohashi, T., Kimura, M., Inoue, Y., Nakagawa, S., ... Mikuni, M. (2006). Assessment of the dexamethasone/CRH test as a state-dependent marker for hypothalamic-pituitary-adrenal (HPA) axis abnormalities in major depressive episode: A multicenter study. *Neuropsychopharmacology*, *31*(1), 212–220.
- Lambert, C., Zrinzo, L., Nagy, Z., Lutti, A., Hariz, M., Foltynie, T., ... Frackowiak, R. (2012). Confirmation of functional zones within the human subthalamic nucleus: Patterns of connectivity and sub-parcellation using diffusion weighted imaging. *NeuroImage*, *60*(1), 83–94.
- Landolt, H. (1958). Serial EEG investigations during psychotic episodes in epileptic patients and during schizophrenic attacks. *Lectures on Epilepsy*.
- Leaver, A. M., Espinoza, R., Pirnia, T., Joshi, S. H., Woods, R. P., & Narr, K. L. (2015). Modulation of Intrinsic Brain Activity by Electroconvulsive Therapy in Major Depression. *Biological Psychiatry: Cognitive Neuroscience and Neuroimaging*, *1*(1), 77–86.

- Leaver, A. M., Vasavada, M., Joshi, S. H., Wade, B., Woods, R. P., Espinoza, R., & Narr, K. L. (2019). Mechanisms of Antidepressant Response to Electroconvulsive Therapy Studied With Perfusion Magnetic Resonance Imaging. *Biological Psychiatry*, *85*(6), 466–476.
- Lépine, J.-P., & Briley, M. (2011). The increasing burden of depression. *Neuropsychiatric Disease and Treatment*, *7*(Suppl 1), 3.
- Lorio, S., Fresard, S., Adaszewski, S., Kherif, F., Chowdhury, R., Frackowiak, R. S., ... Draganski, B. (2016). New tissue priors for improved automated classification of subcortical brain structures on MRI. *NeuroImage*, *130*, 157–166.
- Lorio, S., Lutti, A., Kherif, F., Ruef, A., Dukart, J., Chowdhury, R., ... Draganski, B. (2014). Disentangling in vivo the effects of iron content and atrophy on the ageing human brain. *NeuroImage*, *103*, 280–289.
- Lyden, H., Espinoza, R. T., Pirnia, T., Clark, K., Joshi, S. H., Leaver, A. M., ... Narr, K. L. (2014). Electroconvulsive therapy mediates neuroplasticity of white matter microstructure in major depression. *Translational Psychiatry*, *4*(4), e380-8.
- Madsen, T. M., Treschow, A., Bengzon, J., Bolwig, T. G., Lindvall, O., & Tingström, A. (2000). Increased neurogenesis in a model of electroconvulsive therapy. *Biological Psychiatry*, *47*(12), 1043–1049.
- Malberg, J. E., Eisch, A. J., Nestler, E. J., & Duman, R. S. (2000). Chronic antidepressant treatment increases neurogenesis in adult rat hippocampus. *The Journal of Neuroscience : The Official Journal of the Society for Neuroscience*, *20*(24), 9104–9110.
- Mander, A. J., Whitfield, A., Kean, D. M., Smith, M. A., Douglas, R. H., & Kendell, R. E. (1987). Cerebral and brain stem changes after ECT revealed by nuclear magnetic resonance imaging. *The British Journal of Psychiatry : The Journal of Mental Science*, *151*, 69–71.
- Mathews, A., & Macleod, C. (2005). COGNITIVE VULNERABILITY TO EMOTIONAL DISORDERS. *October*, (1), 167–195.
- McCall, W. V. (2019). Handbook of ECT: A Guide to Electroconvulsive Therapy for Practitioners. In *The Journal of ECT* (Cambridge).
- McClintock, S. M., Choi, J., Deng, Z. De, Appelbaum, L. G., Krystal, A. D., & Lisanby, S. H. (2014). Multifactorial determinants of the neurocognitive effects of electroconvulsive therapy. *Journal of ECT*, *30*(2), 165–176.
- McCrone, P., Rost, F., Koeser, L., Koutoufa, I., Stephanou, S., Knapp, M., ... Fonagy, P. (2018). The economic cost of treatment-resistant depression in patients referred to a specialist service. *Journal of Mental Health*, *27*(6), 567–573.
- McFarquhar, M., McKie, S., Emsley, R., Suckling, J., Elliott, R., & Williams, S. (2016). Multivariate and repeated measures (MRM): A new toolbox for dependent and multimodal group-level neuroimaging data. *NeuroImage*, *132*, 373–389.
- Metastasio, A., & Dodwell, D. (2013). A translation of " L'Elettroshock" by Cerletti & Bini, with an introduction. *The European Journal of Psychiatry*, *27*(4), 231–239.
- Miller, B. R., & Hen, R. (2015). The current state of the neurogenic theory of depression and anxiety. *Current Opinion in Neurobiology*, *30*, 51–58.

- Montgomery, S. A., & Asberg, M. (1979). A New Depression Scale Designed to be Sensitive to Change. *Brit. J. Psychiat.*, *134*(9), 382–389.
- Moreno-jiménez, E. P., Flor-garcía, M., Terreros-roncal, J., Rábano, A., Cafini, F., Pallas-bazarra, N., ... Llorens-martín, M. (2019). Adult hippocampal neurogenesis is abundant in neurologically healthy subjects and drops sharply in patients with Alzheimer ' s disease. *Nature Medecine*.
- Nolen-hoeksema, S. (2000). *The Role of Rumination in Depressive Disorders and Mixed Anxiety / Depressive Symptoms*. *109*(3), 504–511.
- Nuninga, J. O., Claessens, T. F. I., Somers, M., Mandl, R., Nieuwdorp, W., Boks, M. P., ... Sommer, I. E. C. (2018). Immediate and long-term effects of bilateral electroconvulsive therapy on cognitive functioning in patients with a depressive disorder. *Journal of Affective Disorders*, *238*(April), 659–665.
- Nuninga, J. O., Mandl, R. C. W., Boks, M. P., Bakker, S., Somers, M., Heringa, S. M., ... Sommer, I. E. C. (2019). Volume increase in the dentate gyrus after electroconvulsive therapy in depressed patients as measured with 7T. *Molecular Psychiatry*, *i*, 11–14.
- Oltedal, L., Narr, K. L., Abbott, C., Anand, A., Argyelan, M., Bartsch, H., ... Dale, A. M. (2018). Volume of the Human Hippocampus and Clinical Response Following Electroconvulsive Therapy. *Biological Psychiatry*, *84*(8), 574–581.
- Ota, M., Noda, T., Sato, N., Okazaki, M., Ishikawa, M., Hattori, K., ... Kunugi, H. (2015). Effect of electroconvulsive therapy on gray matter volume in major depressive disorder. *Journal of Affective Disorders*, *186*, 186–191.
- Otte, C., Gold, S. M., Penninx, B. W., Pariante, C. M., Etkin, A., Fava, M., ... & Schatzberg, A. F. (2016). Major depressive disorder. *Nature Reviews Disease Primers*, *2*, 79–90.
- Ousdal, Argyelan, M., Narr, K., Abbott, C., Wade, B., Vandenbulcke, M., ... Oltedal, L. (2019). *Archival Report Brain Changes Induced by Electroconvulsive Therapy Are Broadly Distributed*. 1–11.
- Ousdal, O. T., Argyelan, M., Narr, K. L., Abbott, C., Wade, B., Vandenbulcke, M., ... others. (2019). Brain changes induced by electroconvulsive therapy are broadly distributed. *Biological Psychiatry*.
- Peckham, A. D., McHugh, R. K., & Otto, M. W. (2010). A meta-analysis of the magnitude of biased attention in depression. *Depression and Anxiety*, *27*(12), 1135–1142.
- Penninx, B. W. J. H., Milaneschi, Y., Lamers, F., & Vogelzangs, N. (2013). Understanding the somatic consequences of depression: biological mechanisms and the role of depression symptom profile. *BMC Medicine*, *11*(1), 129.
- Perera, T. D., Coplan, J. D., Lisanby, S. H., Lipira, C. M., Arif, M., Carpio, C., ... Dwork, A. J. (2007). *Antidepressant-Induced Neurogenesis in the Hippocampus of Adult Nonhuman Primates*. *27*(18), 4894–4901.
- Phelps, E. A., & LeDoux, J. E. (2005). Contributions of the amygdala to emotion processing: From animal models to human behavior. *Neuron*, *48*(2), 175–187.

- Pine, D. S., Cohen, P., Johnson, J. G., & Brook, J. S. (2002). Adolescent life events as predictors of adult depression. *Journal of Affective Disorders, 68*(1), 49–57.
- Pinheiro, J. C., Bates, D. M., DebRoy, S., Sarkar, D., & The R Development Core Team. (2013). *nlme: Linear and Nonlinear Mixed Effects Models*. 1–336.
- Pirnia, T., Joshi, S. H., Leaver, A. M., Vasavada, M., Njau, S., Woods, R. P., ... Narr, K. L. (2016). Electroconvulsive therapy and structural neuroplasticity in neocortical, limbic and paralimbic cortex. *Translational Psychiatry, 6*(6), e832-8.
- Pizzagalli, D. A., Iosifescu, D., Hallett, L. A., Ratner, K. G., & Fava, M. (2008). Reduced hedonic capacity in major depressive disorder: Evidence from a probabilistic reward task. *Journal of Psychiatric Research, 43*(1), 76–87.
- Price, J. L., & Drevets, W. C. (2009). Neurocircuitry of Mood Disorders. *Neuropsychopharmacology, 35*(1), 192–216.
- Repple, J., Meinert, S., Bollettini, I., Grotegerd, D., Redlich, R., Zaremba, D., ... Dannlowski, U. (2019). Influence of electroconvulsive therapy on white matter structure in a diffusion tensor imaging study. *Psychological Medicine*.
- Righini, A., Pierpaoli, C., Alger, J. R., & Di Chiro, G. (1994). Brain parenchyma apparent diffusion coefficient alterations associated with experimental complex partial status epilepticus. *Magnetic Resonance Imaging, 12*(6), 865–871.
- Rush, A. J., Trivedi, M. H., Wisniewski, S. R., Nierenberg, A. A., Stewart, J. W., Warden, D., ... others. (2006). Acute and longer-term outcomes in depressed outpatients requiring one or several treatment steps: a STAR* D report. *American Journal of Psychiatry, 163*(11), 1905–1917.
- Russell, L. (2018). Emmeans: estimated marginal means, aka least-squares means. *R Package Version, 1*(2).
- Russell Lenth. (2019). *emmeans: Estimated Marginal Means, aka Least-Squares Means*.
- Sabbatini, R. M. E. (1997). The history of shock therapy in psychiatry. *Brain & Mind Magazine, 2003*.
- Santarelli, L. (2003). Requirement of Hippocampal Neurogenesis for the Behavioral Effects of Antidepressants. *Science, 301*(5634), 805–809.
- Satpute, A. B., Mumford, J. A., Naliboff, B. D., & Poldrack, R. A. (2012). Human anterior and posterior hippocampus respond distinctly to state and trait anxiety. *Emotion, 12*(1), 58–68.
- Schmaal, L., Hibar, D. P., Sämann, P. G., Hall, G. B., Baune, B. T., Jahanshad, N., ... Veltman, D. J. (2017). Cortical abnormalities in adults and adolescents with major depression based on brain scans from 20 cohorts worldwide in the ENIGMA Major Depressive Disorder Working Group. *Molecular Psychiatry, 22*(6), 900–909.
- Schmaal, L., Veltman, D. J., van Erp, T. G. M., Sämann, P. G., Frodl, T., Jahanshad, N., ... Hibar, D. P. (2016). Subcortical brain alterations in major depressive disorder: findings from the ENIGMA Major Depressive Disorder working group. *Molecular Psychiatry, 21*(6), 806–812.

- Scott, A. I. F., Douglas, R. H. B., Whitfield, A., & Kendell, R. E. (1990). Time course of cerebral magnetic resonance changes after electroconvulsive therapy. *British Journal of Psychiatry*, *156*(APR.), 551–553.
- Scott, R. C., Gadian, D. G., King, M. D., Chong, W. K., Cox, T. C., Neville, B. G. R., & Connelly, A. (2002). Magnetic resonance imaging findings within 5 days of status epilepticus in childhood. *Brain*, *125*(9), 1951–1959.
- Seedat, S., Scott, K. M., Angermeyer, M. C., Berglund, P., Bromet, E. J., Brugha, T. S., ... others. (2009). Cross-national associations between gender and mental disorders in the World Health Organization World Mental Health Surveys. *Archives of General Psychiatry*, *66*(7), 785–795.
- Shafritz, K. M., Collins, S. H., & Blumberg, H. P. (2006). The interaction of emotional and cognitive neural systems in emotionally guided response inhibition. *NeuroImage*, *31*(1), 468–475.
- Siegle, G. J., Steinhauer, S. R., Thase, M. E., Stenger, V. A., & Carter, C. S. (2002). Can't shake that feeling: Event-related fMRI assessment of sustained amygdala activity in response to emotional information in depressed individuals. *Biological Psychiatry*, *51*(9), 693–707.
- Snaith, R. P., Harrop, F. M., Newby, D. A., & Teale, C. (1986). Grade Scores of the Montgomery—Åsberg Depression and the Clinical Anxiety Scales. *The British Journal of Psychiatry*, *148*(5), 599–601.
- Sokol, D. K., Demyer, W. E., Edwards-Brown, M., Sanders, S., & Garg, B. (2003). From swelling to sclerosis: acute change in mesial hippocampus after prolonged febrile seizure. *Seizure*, *12*(4), 237–240.
- Sorrells, S. F., Paredes, M. F., Cebrian-Silla, A., Sandoval, K., Qi, D., Kelley, K. W., ... Alvarez-Buylla, A. (2018). Human hippocampal neurogenesis drops sharply in children to undetectable levels in adults. *Nature*.
- Spalding, K. L., Bergmann, O., Alkass, K., Bernard, S., Salehpour, M., Huttner, H. B., ... Frisén, J. (2013). Dynamics of Hippocampal Neurogenesis in Adult Humans. *Cell*, *153*(6), 1219–1227.
- Spijker, J., Graaf, R., Bijl, R., & Beekman, A. (2002). Duration of MDD episodes in the general population. *British Journal of Psychiatry*, *181*(Cidi), 208–213.
- Stefani, A., Mitterling, T., Heidbreder, A., Steiger, R., Kremser, C., Frauscher, B., ... Scherfler, C. (2019). Multimodal Magnetic Resonance Imaging reveals alterations of sensorimotor circuits in restless legs syndrome. *Sleep*.
- Strange, B. a, Witter, M. P., Lein, E. S., & Moser, E. I. (2014). Functional organization of the hippocampal longitudinal axis. *Nature Publishing Group*, *15*(10), 655–669.
- Szabo, K., Hirsch, J. G., Krause, M., Ende, G., Henn, F. A., Sartorius, A., & Gass, A. (2007). Diffusion weighted MRI in the early phase after electroconvulsive therapy. *Neurological Research*, *29*(3), 256–259.

- Szabo, K., Poepel, A., Pohlmann-Eden, B., Hirsch, J., Back, T., Sedlaczek, O., ... Gass, A. (2005). Diffusion-weighted and perfusion MRI demonstrates parenchymal changes in complex partial status epilepticus. *Brain*, *128*(6), 1369–1376.
- Tabachnick, B. G., Fidell, L. S., & Ullman, J. B. (2007). *Using multivariate statistics* (Vol. 5). Pearson Boston, MA.
- Takamiya, A., Chung, J. K., Liang, K. C., Graff-Guerrero, A., Mimura, M., & Kishimoto, T. (2018). Effect of electroconvulsive therapy on hippocampal and amygdala volumes: Systematic review and meta-analysis. *British Journal of Psychiatry*, *212*(1), 19–26.
- Tanti, A., & Belzung, C. (2013). Hippocampal neurogenesis: a biomarker for depression or antidepressant effects? Methodological considerations and perspectives for future research. *Cell and Tissue Research*, *354*(1), 203–219.
- Tendolkar, I., van Beek, M., van Oostrom, I., Mulder, M., Janzing, J., Voshaar, R. O., & van Eijndhoven, P. (2013). Electroconvulsive therapy increases hippocampal and amygdala volume in therapy refractory depression: A longitudinal pilot study. *Psychiatry Research: Neuroimaging*, *214*(3), 197–203.
- The UK ECT Review Group. (2003). Efficacy and safety of electroconvulsive therapy in depressive disorders: a systematic review and meta-analysis. *Lancet*, *361*, 799–808.
- Thom, M. (2014). Review: Hippocampal sclerosis in epilepsy: A neuropathology review. *Neuropathology and Applied Neurobiology*, *40*(5), 520–543.
- Tofts, P. S. (2004). PD: Proton Density of Tissue Water. *Quantitative MRI of the Brain*, 83–109.
- Tørring, N., Sanghani, S. N., Petrides, G., Kellner, C. H., & Østergaard, S. D. (2017). The mortality rate of electroconvulsive therapy: a systematic review and pooled analysis. *Acta Psychiatrica Scandinavica*, *135*(5), 388–397.
- Tsay, C. J. (2013). Julius Wagner-Jauregg and the legacy of malarial therapy for the treatment of general paresis of the insane. *The Yale Journal of Biology and Medicine*, *86*(2), 245.
- Tukey, J. (1949). Comparing Individual Means in the Analysis of Variance. *Biometrics*, *5*(2), 99–114.
- Ueno, M., Sugimoto, M., Ohtsubo, K., Sakai, N., Endo, A., Shikano, K., ... Segi-Nishida, E. (2019). The effect of electroconvulsive seizure on survival, neuronal differentiation, and expression of the maturation marker in the adult mouse hippocampus. *Journal of Neurochemistry*, *149*(4), 488–498.
- Utevsky, A. V, Smith, D. V, & Huettel, S. A. (2014). *Precuneus Is a Functional Core of the Default-Mode Network*. *34*(3), 932–940.
- Vogel, J. W., La, R., & Grothe, M. J. (2019). *A molecular gradient along the longitudinal axis of the human hippocampus informs large-scale behavioral systems*.
- Vos, T., Allen, C., Arora, M., Barber, R. M., Brown, A., Carter, A., ... Zuhlke, L. J. (2016). Global, regional, and national incidence, prevalence, and years lived with disability for 310 diseases and injuries, 1990–2015: a systematic analysis for the Global Burden of Disease Study 2015. *The Lancet*, *388*(10053), 1545–1602.

- Wade, B. S. C., Joshi, S. H., Njau, S., Leaver, A. M., Vasavada, M., Woods, R. P., ... Narr, K. L. (2016). Effect of Electroconvulsive Therapy on Striatal Morphometry in Major Depressive Disorder. *Neuropsychopharmacology*, *41*(10), 2481–2491.
- Wager, T. D., Davidson, M. L., Hughes, B. L., Lindquist, M. A., & Ochsner, K. N. (2008). Prefrontal-Subcortical Pathways Mediating Successful Emotion Regulation. *Neuron*, *59*(6), 1037–1050.
- Wagner-Jauregg, J. (1887). *Ueber die Einwirkung, fieberhafter Erkrankungen auf Psychosen*. Toeplitz & Deuticke.
- Wagner, G., Gussew, A., Köhler, S., de la Cruz, F., Smesny, S., Reichenbach, J. R., & Bär, K. J. (2016). Resting state functional connectivity of the hippocampus along the anterior-posterior axis and its association with glutamatergic metabolism. *Cortex*, *81*, 104–117.
- Walker, E. R., McGee, R. E., & Druss, B. G. (2015). Mortality in mental disorders and global disease burden implications a systematic review and meta-analysis. *JAMA Psychiatry*, *72*(4), 334–341.
- Wang, G., Milne, B., Rooney, R., & Saha, T. (2014). Modified electroconvulsive therapy in a patient with gastric adenocarcinoma and metastases to bone and liver. *Case Reports in Psychiatry*, 2014.
- Weiskopf, N., Mohammadi, S., Lutti, A., & Callaghan, M. F. (2015). Advances in MRI-based computational neuroanatomy: from morphometry to in-vivo histology. *Current Opinion in Neurology*, *28*(4), 313–322.
- Weiskopf, N., Suckling, J., Williams, G., Correia M., M. M., Inkster, B., Tait, R., ... Lutti, A. (2013). Quantitative multi-parameter mapping of R1, PD*, MT, and R2* at 3T: A multi-center validation. *Frontiers in Neuroscience*.
- Whitfield-Gabrieli, S., & Ford, J. M. (2012). Default mode network activity and connectivity in psychopathology. *Annual Review of Clinical Psychology*, *8*, 49–76.
- Wilkinson, S. T., Sanacora, G., & Bloch, M. H. (2017). Hippocampal Volume Changes Following Electroconvulsive Therapy: A Systematic Review and Meta-analysis. *Biological Psychiatry: Cognitive Neuroscience and Neuroimaging*, *2*(4), 327–335.
- Witter, M. P., Doan, T. P., Jacobsen, B., Nilssen, E. S., & Ohara, S. (2017). *Architecture of the Entorhinal Cortex A Review of Entorhinal Anatomy in Rodents with Some Comparative Notes*. *11*(June), 1–12.
- Wolf, R. C., Nolte, H. M., Hirjak, D., Hofer, S., Seidl, U., Depping, M. S., ... Thomann, P. A. (2016). Structural network changes in patients with major depression and schizophrenia treated with electroconvulsive therapy. *European Neuropsychopharmacology*, *26*(9), 1465–1474.
- Wright, M. D., & Bruce, A. (1990). An historical review of electroconvulsive therapy. *Jefferson Journal of Psychiatry*, *8*(2), 10.
- Wu, M. V., & Hen, R. (2014). Functional dissociation of adult-born neurons along the dorsoventral axis of the dentate gyrus. *Hippocampus*, *24*(7), 751–761.

- Xu, H., Zhao, T., Luo, F., & Zheng, Y. (2019). Dissociative changes in gray matter volume following electroconvulsive therapy in major depressive disorder: a longitudinal structural magnetic resonance imaging study. *Neuroradiology*, *61*(11), 1297–1308.
- Yroni, A., Nemmi, F., Billoux, S., Giron, A., Sporer, M., Taib, S., ... others. (2019). Significant decrease in hippocampus and amygdala mean diffusivity in treatment resistant depression patients who respond to electroconvulsive therapy. *Frontiers in Psychiatry*, *10*, 694.
- Yuuki, N., Ida, I., Oshima, A., Kumano, H., Takahashi, K., Fukuda, M., ... Mikuni, M. (2005). HPA axis normalization, estimated by DEX/CRH test, but less alteration on cerebral glucose metabolism in depressed patients receiving ECT after medication treatment failures. *Acta Psychiatrica Scandinavica*, *112*(4), 257–265.
- Zaremba, D., Enneking, V., Meinert, S., Förster, K., Bürger, C., Dohm, K., ... Dannlowski, U. (2018). Effects of cumulative illness severity on hippocampal gray matter volume in major depression: A voxel-based morphometry study. *Psychological Medicine*, *48*(14), 2391–2398.
- Zeng, J., Luo, Q., Du, L., Liao, W., Li, Y., Liu, H., ... Meng, H. (2015). Reorganization of anatomical connectome following electroconvulsive therapy in major depressive disorder. *Neural Plasticity*, *2015*.
- Zhao, C., Warner-Schmidt, J., Duman, R. S., & Gage, F. H. (2012). Electroconvulsive seizure promotes spine maturation in newborn dentate granule cells in adult rat. *Developmental Neurobiology*, *72*(6), 937–942.
- Zhao, L., Jiang, Y., & Zhang, H. (2016). Effects of modified electroconvulsive therapy on the electroencephalogram of schizophrenia patients. *SpringerPlus*, *5*(1), 1063.
- Ziegler, G., Ridgway, G. R., Blakemore, S. J., Ashburner, J., & Penny, W. (2017). Multivariate dynamical modelling of structural change during development. *NeuroImage*, *147*(June 2016), 746–762.
- Zimmerman, M., Chelminski, I., & Posternak, M. (2004). A review of studies of the Montgomery-Asberg Depression Rating Scale in controls: Implications for the definition of remission in treatment studies of depression. *International Clinical Psychopharmacology*, *19*(1), 1–7.

8. Appendices

8.1.1. Appendix 1

Statistical table for the effect of a complete series of ECT (Study 2).

Set-level		Cluster-level				Peak-level					Coordinates [mm]		
p	c	p _{FWE-corr}	p _{FDR-corr}	k _E	p _{uncorr}	p _{FWE-corr}	p _{FDR-corr}	F	Z _{equiv}	p _{uncorr}	x	y	z
0.000	4	0.007	0.023	582	0.000	0.014	0.199	23.4	5.2	0.000	22.5	-16.5	-28.5
						1.000	0.894	7.7	3.4	0.000	18	-18	-15
						1.000	0.925	6.9	3.2	0.001	27	-9	-18
		0.038	0.100	397	0.002	0.093	0.336	17.4	4.7	0.000	42	-10.5	16.5
						0.988	0.726	8.8	3.6	0.000	39	0	15
		0.003	0.018	656	0.000	0.367	0.454	13.5	4.3	0.000	-12	-33	-10.5
						0.492	0.454	12.6	4.2	0.000	7.5	-27	-12
						1.000	0.914	7.4	3.3	0.000	19.5	-25.5	-13.5
		0.000	0.000	1357	0.000	0.428	0.454	13.0	4.3	0.000	0	30	21
						0.441	0.454	12.9	4.2	0.000	7.5	34.5	22.5
						0.577	0.463	12.1	4.1	0.000	0	36	28.5

8.1.2. Appendix 2

Statistical table for the long-term effect of ECT (Study 2)

Set-level		Cluster-level				Peak-level					Coordinates [mm]		
p	c	p _{FWE-corr}	p _{FDR-corr}	k _E	p _{uncorr}	p _{FWE-corr}	p _{FDR-corr}	F	Z _{equiv}	p _{uncorr}	x	y	z
0.008	1	0.005	0.028	557	0.000	0.009	0.073	35.9	5.4	0.000	-31.5	-3	-31.5
						0.506	0.983	16.0	4.3	0.000	-31.5	0	-39
						0.993	0.983	10.4	3.6	0.000	-43.5	6	-37.5

8.1.3. Appendix 3

Statistical table for the association with symptoms (omnibus test) (Study 2)

Set-level		Cluster-level				Peak-level					Coordinates [mm]		
p	c	p _{FWE-corr}	p _{FDR-corr}	k _E	p _{uncorr}	p _{FWE-corr}	p _{FDR-corr}	F	Z _{equiv}	p _{uncorr}	x	y	z
0.000	7	0.000	0.000	3630	0.000	0.000	0.011	5.7	5.7	0.000	-12	12	-6
						0.001	0.016	5.4	5.5	0.000	-19.5	13.5	-13.5
						0.007	0.046	4.9	5.1	0.000	-37.5	33	-7.5
		0.000	0.000	11505	0.000	0.000	0.011	5.7	5.7	0.000	12	33	13.5
						0.001	0.016	5.4	5.5	0.000	4.5	46.5	18
						0.002	0.024	5.2	5.4	0.000	4.5	54	21
		0.000	0.000	3199	0.000	0.001	0.016	5.4	5.5	0.000	-3	-48	13.5
						0.042	0.076	4.4	4.7	0.000	-6	-52.5	34.5
						0.054	0.080	4.3	4.7	0.000	10.5	-58.5	16.5
		0.000	0.000	1758	0.000	0.009	0.046	4.9	5.1	0.000	21	-91.5	21
						0.012	0.053	4.8	5.0	0.000	36	-78	22.5
						0.044	0.076	4.4	4.7	0.000	13.5	-85.5	24
		0.000	0.000	4071	0.000	0.019	0.065	4.6	4.9	0.000	-36	-85.5	12
						0.025	0.069	4.6	4.9	0.000	-24	-87	18
						0.033	0.076	4.5	4.8	0.000	-36	-64.5	9
		0.000	0.000	1526	0.000	0.037	0.076	4.5	4.8	0.000	-16.5	-12	67.5
						0.149	0.125	4.1	4.4	0.000	-1.5	-6	69
						0.337	0.174	3.8	4.2	0.000	-19.5	-1.5	54
		0.000	0.001	1384	0.000	0.038	0.076	4.5	4.8	0.000	-25.5	-43.5	-28.5
						0.074	0.099	4.3	4.6	0.000	-21	-45	-21
						0.146	0.125	4.1	4.4	0.000	-16.5	-55.5	-7.5

8.1.4. Appendix 4

Statistical table for the association with symptoms between baseline and the at the 6 months follow-up (Study 2)

Set-level		Cluster-level				Peak-level					Coordinates [mm]		
p	c	P _{FWE-corr}	P _{FDR-corr}	k _E	P _{uncorr}	P _{FWE-corr}	P _{FDR-corr}	F	Z _{equiv}	P _{uncorr}	x	y	z
0.000	10	0.000	0.001	854	0.000	0.003	0.083	43.8	5.6	0.000	36	-78	22.5
						0.563	0.490	15.4	4.2	0.000	33	-85.5	27
						0.896	0.645	12.5	3.9	0.000	22.5	-93	22.5
		0.000	0.000	1183	0.000	0.072	0.404	24.7	4.9	0.000	-13.5	7.5	-9
						0.422	0.484	16.8	4.3	0.000	-4.5	6	-4.5
						0.710	0.530	14.2	4.1	0.000	-25.5	7.5	-10.5
		0.000	0.000	1268	0.000	0.076	0.404	24.4	4.9	0.000	21	-18	-28.5
						0.203	0.423	20.0	4.6	0.000	16.5	0	-40.5
						0.701	0.530	14.3	4.1	0.000	16.5	-6	-33
		0.002	0.005	656	0.000	0.088	0.404	23.7	4.8	0.000	-1.5	-61.5	3
						0.091	0.404	23.6	4.8	0.000	-1.5	-48	12
						0.775	0.533	13.6	4.0	0.000	10.5	-58.5	16.5
		0.000	0.000	2917	0.000	0.090	0.404	23.6	4.8	0.000	31.5	45	3
						0.101	0.404	23.1	4.8	0.000	33	51	10.5
						0.121	0.404	22.2	4.7	0.000	12	33	13.5
		0.032	0.058	371	0.002	0.206	0.423	19.9	4.6	0.000	19.5	4.5	1.5
						0.954	0.676	11.6	3.8	0.000	9	6	-3
						0.967	0.682	11.3	3.8	0.000	15	12	-9
		0.001	0.003	729	0.000	0.212	0.423	19.8	4.6	0.000	-15	52.5	28.5
						0.467	0.484	16.3	4.3	0.000	-16.5	60	19.5
						0.619	0.522	14.9	4.2	0.000	-9	43.5	39
		0.003	0.007	592	0.000	0.236	0.423	19.3	4.5	0.000	-21	-6	-19.5
						0.953	0.676	11.6	3.8	0.000	-18	0	-27
						0.964	0.676	11.4	3.8	0.000	-24	-13.5	-21
		0.042	0.068	349	0.002	0.527	0.486	15.8	4.2	0.000	-12	30	58.5
						0.555	0.488	15.5	4.2	0.000	-4.5	27	60
						0.935	0.654	11.9	3.8	0.000	0	24	54
		0.029	0.058	382	0.001	0.840	0.602	13.0	4.0	0.000	-9	-63	34.5
						0.906	0.645	12.3	3.9	0.000	-24	-66	24
						0.921	0.645	12.1	3.9	0.000	-19.5	-63	31.5